COMBUSTION STRESS IN COMPRESSION-IGNITION ENGINES

ANDREW BRUCE TAYLOR

Submitted in partial fulfilment of the
requirements for the degree of
Ph.D.

Department of Agricultural Engineering
University of Natal
1989

ABSTRACT

South Africa produces alternative fuels from a number of different sources. The properties of a fuel are known to affect the nature of combustion in compression-ignition engines significantly, and have occasionally resulted in engine failures. Combustion analyses have been conducted on a wide range of fuels and combustion has been thoroughly quantified. However, the role played by the different combustion variables in failures was not known. The result was that it was not possible to predict the implications of variations in the nature of combustion. There was thus a need to investigate the relative role of combustion variables in the failure of engines.

The mechanisms of combustion and engine failure were studied. All the variables required to determine combustion and engine durability were measured simultaneously. This research required the development of a complete engine research facility as well as specialized transducers. Fast response surface thermocouples were designed and constructed in order to monitor transient surface temperatures. Heat transfer rates were then calculated with the aid of Fourier analysis. Dynamic stresses were monitored by strain-gauges applied to the engine. A special high speed data acquisition system was developed. An existing heat release model was modified and used to calculate combustion rates. A comprehensive finite element model was developed to calculate piston temperatures and stresses. The role of each combustion variable in stress and durability was investigated by statistical analysis.

The results successfully identified the causes of combustion related engine failures. The primary cause of engine failure was

found to be thermal loading. The principal cause of any variation in thermal loading and thus engine durability was maximum cylinder pressure. The life of the engine was proved to be determined almost entirely by peak cylinder pressure. The role of the rate of pressure rise was proved to be insignificant.

All the implications of variations in the nature of combustion can now be determined accurately. It will thus be possible to optimise engine modifications and fuel properties before validation by durability testing.

I wish to certify that the work reported in this thesis is my own original and unaided work except where specific acknowledgement is made. In addition I wish to declare that the thesis has not been submitted for a degree in any other University.

Signed .....

A.B. TAYLOR

ACKNOWLEDGEMENTS

The author wishes to record his sincere appreciation for the assistance given by the following :-

Prof. P. Meiring, Head of the Department of Agricultural Engineering, University of Natal, who supervised the work.

Mr. A.C. Hansen and Mr. P.W.L. Lyne, Lecturers, Department of Agricultural Engineering, University of Natal, for their advice and assistance during the course of the project.

Mr. P.B. Crookes, Mr. R.P. North and Mr. C. Tredrea who provided the technical expertise required for this project.

Mrs K. Temple and Miss J. Whyte for their assistance in preparing this document.

Mr. T. Bruton, who assisted in the construction of the gold foil thermocouples.

Sastech, Research and Development, Sasolburg, who provided financial support.

The Council for Scientific and Industrial Research, Pretoria, who provided financial support.

The National Energy Council, Pretoria, who provided financial support.

My wife, Mathilda, for her patience and encouragement throughout the project.

TABLE OF CONTENTS

LIST OF TABLES

LIST OF FIGURES

1. INTRODUCTION

More than half the liquid fuel presently consumed in South Africa is possibly synthetic fuel derived from coal. In addition, a significant amount of fuel will be produced synthetically from natural gas. The production of ethanol from sugarcane as a by-product, is already in progress. Large scale ethanol production, for use in vehicles, is being considered carefully. Minimizing South Africa's dependence on imported crude-oil is of vital importance to the stability of Southern Africa. The production and application of methanol from coal is thus also being researched extensively. Conventional fuel derived from imported crude oil merely supplements the fuel manufactured within the country. South Africa clearly utilizes a unique and diverse range of fuels.

In order to optimize production processes and additive formulations to produce economical fuels of the highest quality, it is necessary to conduct extensive combustion research. The cetane scale has been used traditionally to quantify fuel quality. The cetane scale has, however, been proved to be incapable of consistently quantifying the quality of many alternative fuels. Considerable work has been done on the quantification of combustion in compression-ignition engines (Hansen, Taylor, Lyne and Meiring, 1987 and Taylor, 1987). All aspects of combustion behaviour have, in fact, been quantified for many years. This has, however, been of little practical value since the implications of variations in combustion behaviour have not been known. It has thus been impossible to interpret the results of combustion analyses conclusively. For example, in the work conducted by Taylor (1987) it was found that some fuels had higher rates of pressure rise than conventional diesel fuel while the maximum pressures were lower. Although it was known that these fuels were responsible for

increased engine noise, their effect on engine life could not be predicted from the results.

Engine durability is undoubtedly the most important variable when considering engine modifications or the quality of alternative fuels. The determination of the effect of an alternative fuel or of engine modifications on the life of an engine is a difficult and expensive process. Conclusive durability testing requires numerous engines to be run to destruction over long periods of time. Engine failures unrelated to the test can cause total loss of data and even the entire test. It was therefore imperative that a reliable method of predicting the implications of fuel changes or engine modifications on the life of the engine be found. Unsuitable fuels could thus be improved or discarded before durability testing commenced. Durability testing would merely be conducted to validate the laboratory findings. This capability is considered to be of vital importance in the development of alternative fuels.

The objective of the research programme was to ascertain the relationship between the variables normally determined from laboratory engine tests, and the resulting engine life. This was done by first identifying the causes and mechanisms of engine failure. All the combustion variables which could contribute to engine failure were measured. Such information allowed the life of engine components to be predicted. The relationships between engine life and variables which quantify combustion behaviour were then investigated. The final objective was to gather adequate information to predict the effect of a fuel on engine life immediately after completing simple laboratory tests. This information would allow fuels to be rated in terms of their actual combustive quality. These results constituted the first step towards replacing the cetane scale with appropriate parameters which relate directly to the behaviour of fuels in modern engines.

2. COMBUSTION QUALITY OF COMPRESSION-IGNITION FUELS

There are numerous aspects relating to the quality of a compression-ignition fuel. These aspects include;

(i) ignition quality,
(ii) combustion behaviour,
(iii) engine durability,
(iv) storage stability,
(v) ease of handling,
(vi) corrosivity and materials compatibility,
(vii) lubricity and viscosity, and
(viii) toxicity.

If a fuel is considered economically viable then ignition quality and combustion behaviour are normally the first parameters to be evaluated. The reason for this is that if these aspects of the fuel are found to be unsatisfactory, they are the most difficult to rectify. If the ignition quality and combustion behaviour are considered satisfactory then the other factors are investigated. This work has concentrated on those aspects of fuel quality which determine engine durability. Namely, ignition quality and combustion behaviour.

2.1 Ignition Quality

Ignition quality has for more than fifty years been quantified by the cetane scale. The cetane number of a fuel is based on the ignition delay in a standard Co-operative Fuel Research (CFR) engine. A fuel with a low cetane number would be expected to have a long ignition delay in practice and would thus be considered of lower quality. Since the compression-ignition engine relies entirely on the ability of the fuel to ignite spontaneously, it is

important that the ignition process be clearly understood.

The ignition delay is the result of two different delay mechanisms, the physical delay and the chemical delay. Due to the fact that the combustion chamber contents are in a heterogeneous state during the ignition delay, the physical and chemical delay periods run concurrently at different points (Ryan, 1985). The physical delay period involves the following processes ;

(i) atomization of the fuel,
(ii) heating of the fuel droplets,
(iii) evaporation from the fuel droplets, and
(iv) mixing of the evaporated fuel with air (Benson and Whitehouse, 1983).

Where there is contact between fuel vapor and air, precombustion reactions commence. The chemical delay is the time required for these reactions to reach completion. The precombustion reactions involve certain molecular chain breaking or decomposition processes which yield the various radicals that are required to initiate combustion (Bacon, Bacon, Moncrieff and Walker, 1980 and Saeed and Henein, 1984). The physical and chemical precombustion processes are known collectively as preparation.

In the case of a steady state premixed burner such as a bunsen burner, fuel preparation is greatly assisted by the transfer of chemically active species from the combustion zone to the precombustion zone. Due to the absence of these chemically active species, the activation energies of the precombustion reactions in a compression-ignition engine are between 25 and 30 times greater than those of a premixed burner (Edwards, 1977).

When both physical and chemical precombustion processes are complete the fuel is said to be fully prepared. The prepared fuel will, however, not ignite unless a number of criteria are

satisfied. The mixture ratio of the prepared fuel must be between the rich and lean limits for combustion and the temperature must be above the spontaneous ignition temperature of the mixture. The volume of this prepared mixture must be large enough for it not to be diluted by turbulence (Bacon et al., 1980).

The precombustion processes are influenced both in rate and duration by a number of variables. Increased air temperature caused by a higher compression ratio will result in reduced ignition delay and increased rate of fuel preparation (Hardenberg and Hase, 1979). The design of the fuel injection equipment determines injection spray pattern, droplet size and the rate of fuel injection. Engine design controls the nature of the turbulence in the combustion chamber. These factors will not only affect the duration of the ignition delay, but will also influence the amount of prepared fuel at the end of the ignition delay.

Chan, Moncrieff and Pettitt (1982) indicated that the chemical properties of the fuel have a dominant effect on ignition delay. It can also be deduced from the work of Leone, Danieli and Canonaco (1979) that the duration of the chemical delay far exceeds that of the physical delay. Physical properties of a fuel will thus have a dominant effect on the amount of fuel prepared during the ignition delay. The duration of the ignition delay is, however, determined largely by the chemical properties.

It is possible that in some cases only a certain fraction of the evaporated fuel will be involved in precombustion reactions. It is difficult to determine which fractions of the fuel are available for precombustion reactions during the ignition delay since it can be assumed that the lighter fractions will boil off first, causing droplets to become richer in heavier fuel. Whether or not the heavy fractions become available for precombustion reactions before ignition will depend on air temperature, droplet size, turbulence

and the boiling curve.

When blending fuels it is possible to add fuel with a low boiling range, high latent heat of evaporation and low ignition quality, to one which has good ignition quality. The evaporation of the volatile fuel from the droplet may delay the evaporation of that fraction of the good fuel which best undergoes precombustion reactions. An unexpectedly long ignition delay could thus result. This would explain why the cetane number for ethanol, derived by Hardenberg and Ehnert (1981) from a range of ethanol-diesel blends, was lower than expected.

The advantage of the cetane scale is that given a range of similar fuels, it will accurately quantify their ignition quality (Taylor, 1987). Traditionally the majority of liquid fuel used has been derived from crude-oil and thus the cetane scale has been adequate for purposes of comparison. The cetane scale has also correlated well with the combustion behaviour and engine durability.

In recent years fuels derived from other sources have been analysed and put into production. These fuels include coal derived fuels, alcohols, vegetable oils and, more recently, fuels derived from natural gas. The result is a range of fuels which differ considerably in both physical and chemical properties. It is thus possible that a fuel which displays high ignition quality in one engine will display low quality in a different type of engine. When tested in a Perkins 3.152 engine, a blend of ethanol and ignition improver displayed ignition quality superior to a large range of fuels (Hansen, Taylor, Lyne and Meiring, 1987 and Taylor, 1987). This fuel when tested in an Atlantis Diesel Engines (ADE) 4.236 engine displayed ignition quality vastly inferior to the same range of fuels. The significant difference between these engines is the compression ratio.

It is also possible to have two different fuels which have identical ignition delay, but different preparation rates. This would result in different amounts of prepared fuel at ignition which would lead to differences in combustion behaviour. Based on the cetane scale, however, these fuels would be considered to be of the same quality. It is thus evident that fuel quality can no longer be determined from ignition delay alone. In order to determine fuel quality in future it will be necessary to study the combustion behaviour in conjunction with the ignition delay. Ignition delay should be used to a greater extent to determine ease of starting and engine roughness and to a lesser extent to describe combustion behaviour. Ignition quality should also be evaluated in engines representative of those in production and not the standard CFR engine which no longer resembles the engines in use. Understanding and interpreting the combustion process and the effect of combustion on engine durability is thus of ever increasing importance.

2.2 Combustion Behaviour

During the ignition delay a significant amount of fuel becomes fully prepared, while additional evaporated fuel is still involved in precombustion reactions. All this fuel is said to be premixed. Ignition at any location may be followed by simultaneous ignition at other points. The combustion of this fully prepared fuel will accelerate the preparation and ignition of the remaining premixed fuel. The result is that a large amount of energy is released in a short space of time, causing rapid increases in pressure and temperature. The extent of these increases is determined by the amount of premixed fuel in the combustion chamber which in turn is influenced by the preparation rate and the ignition delay (Timoney, 1987b). This process is known as premixed combustion.

The nature of premixed combustion is controlled almost entirely by the preparation processes during the ignition delay. The duration of premixed combustion appears to be relatively independent of any engine or fuel variables (Taylor, 1987). By studying the nature of premixed combustion with the aid of heat release analysis, it is possible to gain information about the processes occurring in the ignition delay. Premixed combustion is also important since it influences pressure and temperature rise to a significant extent which in turn affect engine stresses.

From the moment of ignition there are fuel droplets which are surrounded by flame. The bulk of the fuel in these droplets and the fuel still being injected will undergo diffusion combustion. In diffusion combustion the fuel and oxidant are introduced to the flame zone prior to mixing. Fuel evaporates from the surface of the droplet and undergoes precombustion reactions in the absence of oxygen. These reactions are known as pyrolitic precombustion reactions and under certain conditions are responsible for particulate emission. The fuel then enters the flame zone from the droplet surface while the oxygen enters from the outside and mixing occurs within the flame zone (Edwards, 1977).

The time required for the combustion of prepared fuel is minimal when compared to the time required for evaporation and mixing. Diffusion combustion rate is thus controlled by the rates of evaporation and mixing (Whitehouse and Way, 1971). It can be assumed that early in combustion, when oxygen is plentiful, combustion rate is controlled by evaporation rate. Later when temperatures are greater and oxygen becomes scarce, combustion rate is controlled by the rate of mixing.

Lighter fractions of a fuel will evaporate from the droplet first, causing the concentration of the heavy fractions to increase. This progressive increase in the concentration of heavy fractions along

with the decrease in oxygen leads to an increase in soot formation towards the end of combustion (Edwards, 1977). The duration of diffusion combustion and the amount of soot formed will thus depend on both engine and fuel variables. A short combustion duration is desirable in order to achieve high thermal efficiency and minimal smoke emission. The consequences of reducing combustion duration are, however, an increase in heat release rate and in peak pressures which could affect engine durability.

2.3 Durability Considerations

It is evident that fuel properties have a dominant effect on the manner in which heat is released in the engine. Heat release in turn determines the development of gas temperature and pressure. Although it is well known that these factors result in stresses in combustion chamber components, only tentative guesses have been made about the effect of combustion variations on component life. Experience has shown that undesirable combustion behaviour caused either by poor fuel quality or by maladjustment of engine variables, can result in cracking or erosion of the piston, cylinder liner and cylinder head. Failure often occurs in conditions associated with rapid pressure rise. The results of Sarsten (1979) show that piston temperatures can vary by as much as 50°C as a result of differences between fuels. This could have a dramatic effect on engine durability.

Pressure and temperature result in two forms of component loading. Firstly, gas pressure causes mechanical forces within the components. Secondly, heat transfer from the hot gasses produces temperature gradients in the components which leads to thermal stress. The components are exposed to the combined effect of these stresses. Neither the effects of the rate of application of these loads nor their relative magnitudes are understood or documented to any useful extent. In the work of Taylor (1987) difficulty was

experienced with the interpretation of heat release results. Some of the alternative fuels analysed displayed higher rates of heat release and pressure than conventional fuels while they resulted in lower peak pressures. A conclusion could not be reached on whether or not these fuels would have a detrimental effect on engine life.

Hardenberg (1986) stated that combustion induced pressure rise prior to top dead centre (TDC) resulted in excessive thermal loading on the piston crown and should be avoided. He also stated that to achieve acceptable engine noise the rate of pressure rise would need to be below a value which is normally well within the limits of engine durability. These were, however, subjective observations based on experience and no exact theories were available.

Wotherspoon (1988) stated that, from his experience, if the rate of pressure rise in a particular engine exceeded a certain limit, either due to timing advance or an inferior fuel, then piston cracking and erosion could occur. Wacker and Coelingh (1984) stated that mechanical fatigue cracks occurred in the combustion bowl edge. They attributed these cracks to "mechanical overloading as a result of high firing pressures and/or steep pressure rises". Other engine and fuel researchers were questioned on the subject and although all agreed that engine failure would result from certain combustion behaviour, none could offer exact theories on the relationships between failure and combustion.

Unlike the measurement of other aspects of fuel quality, the determination of the effect of a fuel on engine life can be extremely expensive and requires long periods of time. Conclusive durability testing requires that a large number of engines be worked to destruction in a wide range of applications. The process could be influenced by factors other than the fuel, such as

incorrect engine timing which could require the test to be repeated. It would thus be beneficial to determine the relationship between combustion and engine stresses in such a way that engine life could be predicted from the results of heat release analysis. This would allow variables such as engine timing and the proportion of ignition improver, to be optimized before conducting durability tests.

Accurate information may even render durability testing unnecessary or at least reduce the amount of testing required to reach a conclusion. By measuring combustion behaviour and factors indicative of engine stress simultaneously, it is possible to draw conclusions on the relationship between these parameters. This, however, requires considerable knowledge of the mechanisms by means of which the components undergo stress.

3. ENGINE STRESS

By studying engine stress it is possible to understand the manner in which combustion contributes to failure. Such knowledge would allow measures to be taken in order to minimize failures. Emphasis is thus placed on the stresses in those components which experience combustion related forces. Forces such as acceleration which are unrelated to the fuel are not discussed.

An effort has been made to gather information about stresses in engines by analysing the components which have failed in practice in South Africa. The investigation has been concentrated on ADE engines which will soon comprise the majority of engines in South Africa. These engines all make use of the same deep bowl, direct injection combustion system. Information has also been gained from service and repair organizations, particularly regarding the relative vulnerability of components and the frequency and cause of their failure. The discussion and analysis in the project has been concentrated on those components which are considered to be most likely to fail as a result of abnormal combustion behaviour.

It is evident that by far the most common failure which can be related to combustion, is cracking of the piston crown around the combustion bowl. This is often accompanied by cracking of the cylinder liners and, less frequently, by cracking of the cylinder head (Smith, Angus and Lamb, 1971). These failures normally occur in applications which frequently involve rapid load variations. In most cases of cracking, stresses have not exceeded the yield point of the material, indicating that the failure is fatigue related. The stresses in the components surrounding the combustion chamber are the result of the combined effect of both pressure loading and thermal loading (Sander and Schoeckle, 1979 and Munro,

Griffiths, Allen, Travailli and Bolton, 1986).

The mechanisms by means of which the nature of combustion of a fuel may affect the life of an engine are displayed graphically in figure 1.

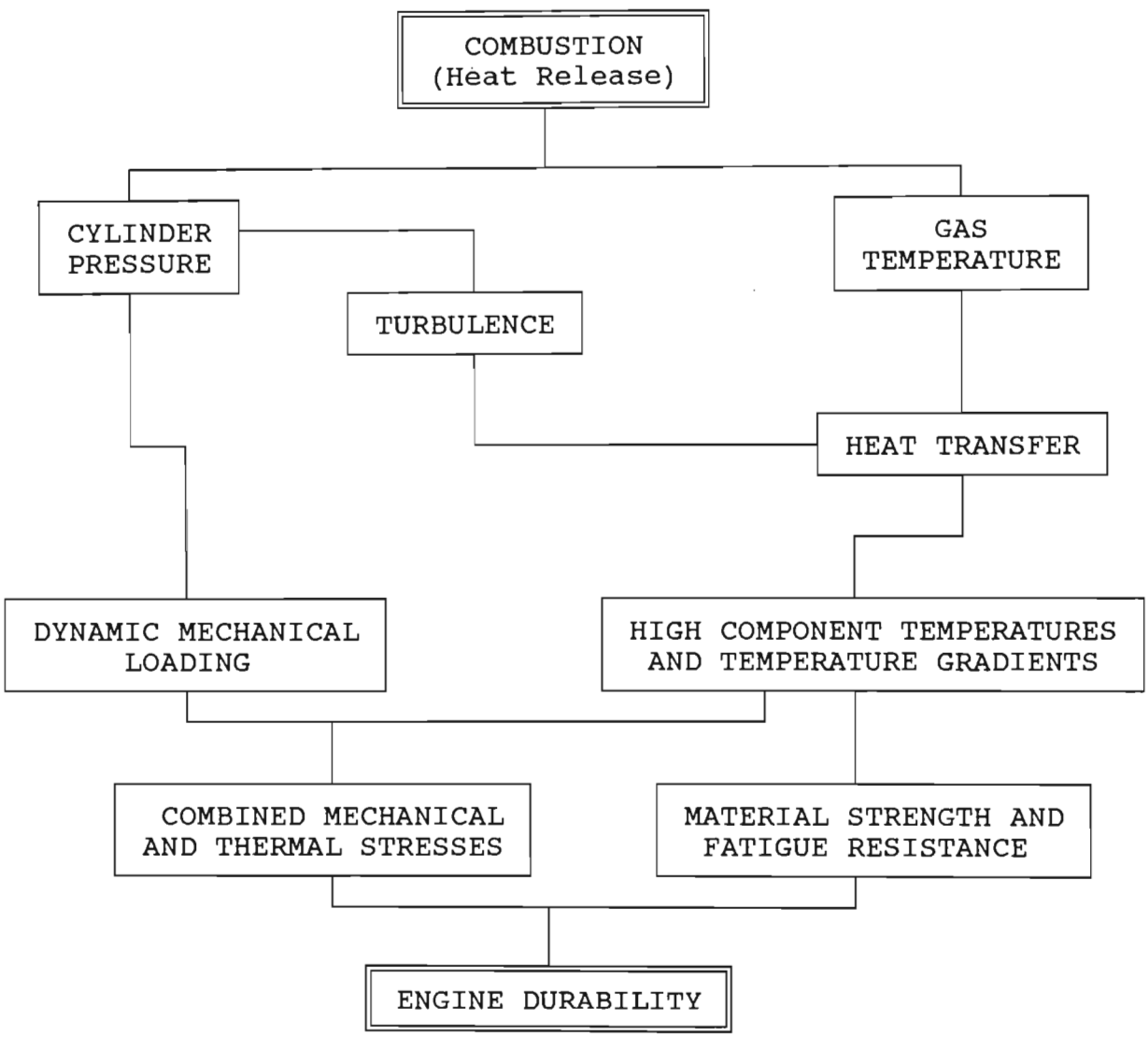

Figure 1. Mechanisms by means of which the nature of combustion of a fuel influences the durability of a compression-ignition engine.

It can be seen that cylinder pressure and gas temperature are determined by the nature of combustion. By creating turbulence and high gas velocities the rate and timing of pressure rise could influence the heat transfer coefficients between the gasses and the engine components. The resulting heat transfer coefficients and gas temperatures determine the rate at which heat is transferred to the combustion chamber components. Cylinder pressure is responsible for exerting mechanical forces on the engine components. Temperature gradients which are determined by the rate of heat transfer, are responsible for thermal stresses. Stresses in the components are the result of the combined effect of the mechanical and thermal loadings. These combined component stresses along with the material temperatures determine the life of the components.

Both the pressure forces and the thermal loading are of a cyclic nature. The frequency of the pressure loading is equal to half engine speed. This is referred to as high cycle loading. Thermal loading varies primarily at the rate at which engine load is changed and is considered to be low cycle loading (Blech, 1982). Thermal loading also varies to some extent at the high cycle rate. Although the high and low cycle loadings both contribute to combined component stress their mechanisms are different and should be discussed separately.

3.1 High Cycle Loading

High cycle loading is the result of fluctuation in cylinder pressure and surface temperature. The role of rapid fluctuations in surface temperature during the engine cycle is at present not established clearly. These fluctuations are the result of rapidly changing gas temperature and heat transfer in the combustion chamber. Although little evidence is available most researchers

consider the role of high cycle thermal loading to be insignificant and have not included its effects in their investigations (Roehrle, 1978; Blech, 1982 and Assanis and Badillo, 1988). Assanis and Badillo (1988) and Morel, Keribar and Blumberg (1988) did, however, prove that the effects of high cycle thermal loading are far more significant in ceramic components than in aluminium components. Due to lower heat capacity and lower thermal conductivity, the temperature swing in a ceramic surface would be over 100°C as a result of conditions which would cause a swing of less than 20°C in aluminium.

Hansen, Lyne and Meiring (1984) reported piston erosion in an engine running on an ethanol diesel blend. Pitting was observed at the points where the injected fuel spray impinged on the combustion bowl walls. Failure was attributed to highly localised pressures caused by impinging fuel which resulted in surface fatigue. The problem was, however, solved by adding a small amount of ignition improver to the fuel. This would not have had any influence on the spray pattern and impingement forces, thus indicating that other failure mechanisms were involved in the pitting. Subsequent investigation of these pistons and other pistons showed that combustion bowl lip cracking had also occurred along with piston erosion. Different pistons which were cracked in a similar nature had not experienced pitting, thus indicating that piston erosion may only occur in material which has already experienced thermal and mechanical fatigue.

The fact that pitting occurs in the vicinity of the fuel sprays indicates that high cycle loading other than pressure loading definitely contributes to failure. The fuel spray could cause increased high cycle thermal loading at these locations by impinging and evaporating. Unnaturally high heat loss would thus result. Ignition which occurs in the same vicinity would then result in above average heating as a result of increased heat

transfer coefficients and gas temperatures. It is thus probable that the temperature swing and subsequent thermal loading at these locations of the piston is considerably greater than that of the rest of the combustion chamber wall. High cycle thermal loading should thus not be disregarded and further investigations into the subject are justified. Fuel impingement which is a high cycle mechanical load may also contribute to failure by means of a mechanism similar to cavitation erosion.

It is well understood that any increase in peak cylinder pressure will lead to increased stresses in components such as the pistons, cylinder liners, cylinder head, connecting rod and crank shaft. Munro et al. (1986) stated that piston pin boss cracking is the most likely failure particularly at high operating temperatures. Cyclic pressure induced stress is superimposed on thermal stress and makes a significant contribution to the failure in areas such as the combustion bowl lip and the piston ring groove (Francis, Griffiths, Gazzard and Avezou, 1986). This is supported by the observations of Munro (1979) who reported that crown cracking often coincided with maximum mechanical stress due to cylinder pressure. Partial damage due to different forces calculated by Sander and Schoeckle (1979) indicate that firing pressure is the main cause of fatigue failure in internally cooled pistons. Blech (1982), however, stated that neither high cycle thermal stresses nor pressure forces contributed significantly to the failure of cylinder heads.

The role of the rate of pressure rise in component failure is not clearly understood by researchers and appears to be misinterpreted. Browne, Partridge and Greeves (1986) observed a correlation between piston erosion and cetane number, and attributed this to high rates of pressure rise. Wacker and Coelingh (1984) stated that high rates of pressure rise could cause piston failure by cracking. They stated that failure occurred due to increased mechanical

stresses in the piston bowl lip as a result of steep pressure rise.

Hardenberg (1986) indicated that, in order to achieve permissible engine noise, rates of pressure rise were kept at levels well below those which would cause failure. From the results of Miyamoto, Murayama and Gotoh (1980) it can be seen that peak crank shaft strain varied by as much as 37,5% as a result of variations in the rate of pressure rise while the peak pressure remained unchanged. The variation was only 19,2% for cylinder head displacement and the deflection of the valves was independent of rate of pressure rise.

If a load is rapidly applied the instantaneous maximum stress can approach a value double the steady state value, depending on the rate of application. The phenomenon is affected by the relative magnitudes of the rate of application of the force, stiffness, inertia and damping of the structure. Clearly the crank shaft and cylinder head structures are such that the rates of pressure rise in the engine are fast enough to influence their peak stresses significantly. The valves on the other hand are adequately stiff to be insensitive to the rate of pressure rise and their stresses are thus directly proportional to pressure.

Combustion related failure does not, however, occur in the crank shaft and cylinder head bolts, but does occur in the pistons, cylinder liners and cylinder head. Whether or not these components are of such a stiffness as to be affected by the rate of pressure application, requires investigation. A successful investigation would indicate whether the high cycle mechanical stresses should be determined from peak pressure values alone or whether rate of pressure rise should be included in the calculations.

Combustion behaviour determines the rate of heat release and it is the rate of heat release which controls the pressure development.

Peak pressure in an engine, at a particular load and speed, can vary by as much as 23,3% as a result of different fuels (Taylor, 1987). The pressure induced stress would probably vary by a similar order, but the resulting component life would be far more sensitive to these changes. The results of Sander and Schoeckle (1979) indicate that a stress increase of 25% can reduce component life to one fifth of the original value. The implications of differences in high cycle loading, as a result of fuel differences and design changes, should thus be investigated and documented.

3.2 Low Cycle Loading

Heat transfer from the hot combustion gasses to the coolant results in temperature gradients in the components surrounding the combustion chamber. Due to differences in expansion these temperature gradients result in thermal stress in the components (Blech, 1982). Component failures are most often witnessed in engines which undergo rapid and frequent load variations. The resulting variations in thermal stress lead to thermal fatigue (Munro, 1979; Blech, 1982; Francis et al., 1986 and Munro et al., 1986). Munro (1979) and Francis et al. (1986) indicate that step changes between low and high load can result in momentary peaks in thermal stress. They indicated that these transient stresses are far greater than the stresses occurring during steady state running. The resulting stress range can be seven times the difference between the steady state stresses at high and low load.

There are two theories on the mechanisms of thermal fatigue. Smith et al. (1971) and Blech (1982) indicate that prolonged operation under conditions of high temperature and compressive stress results in plastic flow or compressive creep. Creep serves to relieve the compressive stresses, but results in residual tensile stresses when the component cools, which finally leads to cracking. The stress

range between high and low steady state load calculated by Munro (1979) was small while the momentary stresses were extremely high. The stress levels and available time were thus inadequate to have resulted in compressive creep. Failure in this instance would simply have been due to repeated cycling through a large stress range.

Investigation of cracked components revealed that in some instances, particularly in cylinder heads and pistons, the cracks had opened by a significant amount. This indicated that plastic compressive creep or simply plastic compression, had occurred at high temperatures. It is thus evident that both mechanisms may occur in components, depending on the nature of both the component and the load cycle. It is thus not possible to define one engine load cycle which is universally valid (Saugerud and Sandsmark, 1980). The combined role of cyclic thermal stresses acting on material which is considerably weakened by high temperatures is clearly significant in the failure of components. Smith et al. (1971) and Roehrle (1978) indicated that cracking would not occur unless critical temperature limits were exceeded.

The nature of failures occurring in practice as a result of low cycle thermal loading are as follows:

(i) Piston cracking and erosion, particularly around the combustion bowl lip. This problem is most prevalent in pistons with either small bowl edge radius or re-entrant bowl form (Roehrle, 1978; Adams, Revello, van Ruiten and Travailli, 1986; Munro et al. 1986). The piston bowl lip is clearly the region in the combustion chamber which is the most sensitive to combustion behaviour (Hansen et al., 1984).

(ii) Cylinder head cracking mainly in the flame plate between the valves also occurs, although less frequently (Smith et al., 1971 and Blech, 1982).

(iii) Cylinder liner cracking is occasionally observed in conditions which have also resulted in piston crown cracking. This indicates that the failure is also related to low cycle thermal loading.

By raising metal temperatures the maximum thermal loading results in the components being far more sensitive to the high cycle forces. The thermal loading can thus have an effect on failures such as pin boss cracking and piston ring wear (Munro et al., 1986).

Roehrle (1978) suggested that crown cracking was related to bowl configuration because the form of the combustion bowl determines the speed at which the combustion gasses leave the combustion bowl. Being in the region of rapid gas flow and having a large heated surface area and a small area for conducting the heat away, the bowl lip reaches higher temperatures. The theory is supported by the fact that increasing bowl lip radius reduces the occurrence of crown cracking (Munro et al., 1986). It is thus evident that any factor which affects the rate at which the gasses leave the combustion bowl will affect the thermal loading. The rate of pressure rise and the time at which it occurs could thus, along with gas temperature, influence the temperature of the piston crown. Information relating thermal loading to those variables which quantify combustion behaviour would clarify the matter. Such information would be extremely valuable when interpreting test results.

3.3 Resultant Stress and Durability

Engine stresses are the result of the interaction of a number of different forms of loading. Possibly the most significant engine loadings are as follows:

(i) High cycle pressure load, which could be influenced by the rate of pressure rise as well as the amplitude.

(ii) High cycle thermal load.

(iii) Low cycle thermal load.

The manner and extent to which these loadings are affected by combustion is, however, not known. There is thus a need to investigate the relationships between each of these loadings and combustion behaviour. This would involve determining which combustion variables significantly influence the different forms of loading.

Information is also required on the relative contribution to failure of the different forms of loading. This would allow the relative significance of the loads and combustion variables to be evaluated. It is imperative that the sensitivity of engine life to variations in loading and thus variations in combustion, be investigated. The implications of combustion variations could thus be fully interpreted immediately after conducting laboratory tests.

Clearly, the nature of combustion plays a major role in the stressing of engine components. Engine life is thus affected by the properties of the fuel used as well as the nature of the duty cycle. Traditionally, researchers have attempted to maintain thermal loading within levels previously measured. The criterion used has been exhaust temperature (Sarsten, 1979). Peak pressures, injection timing and rates of pressure rise have been kept within known values in the hope that failures will not occur (Hansen et al., 1984). Better information describing the relationship between combustion and stresses would allow more accurate solutions to be achieved. Information about the role played by each aspect of combustion in failure will allow fuels and engines to be optimized exactly.

It is thus necessary to conduct tests in which combustion and stress are simultaneously determined. In this manner it will be possible to investigate the effect of changes in combustion parameters on engine life. Even subjective information about the relationship would improve the ability of researchers to develop new fuels and improve engines. The results could possibly have an effect on the criteria presently used for rating fuel quality.

4. RESEARCH PROCEDURE

In order to ascertain the relationship between combustion and engine stress it is necessary that both engine stress and combustion behaviour be determined. Neither of these two criteria can, however, be measured directly. They must be calculated from related information. The research procedure was thus to measure all those variables which were required for the calculation of combustion rates and engine stresses. Combustion rates and engine stresses were then calculated and the relationships between them were investigated.

The factors resulting from combustion, which determine component stress can be seen in figure 2. This figure indicates which variables were measured and which were calculated. Measured cylinder pressure was used as the basis for the calculation of combustion rate, mechanical stresses and gas temperatures. Transient surface temperature was recorded in order to allow the calculation of heat transfer rate. There was thus no need to determine turbulence. Heat transfer rate was used in both the calculation of combustion rate and thermal loading.

Combustion is quantified by variables determined from heat release analyses. Heat release analyses require a number of engine variables to be measured. Accurate cylinder pressure data are imperative, while data describing variables such as needle lift, speed, torque and fuel flow are often used. The results of heat release analyses involve considerable amounts of data which are best displayed graphically. These data are often summarized and represented by a few discrete values which describe the nature of the combustion. These values can then be used in graphical and statistical comparisons between combustion and other variables (Hansen et al., 1987).

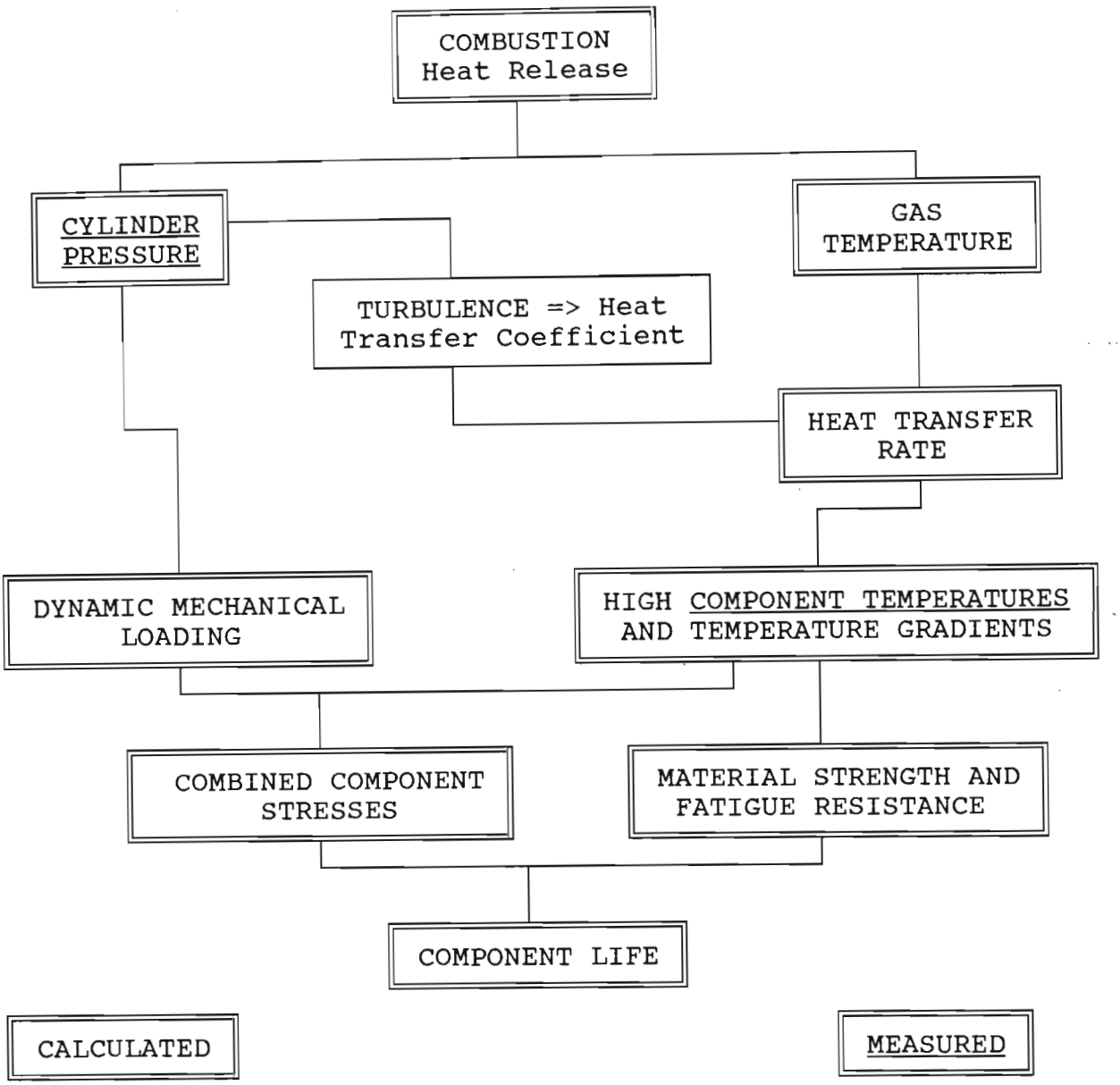

Figure 2. Factors relating combustion to component stress and durability. These factors were determined either by measurement or by calculation.

Engine stress was calculated from measured data which described both the thermal and mechanical loading. Mechanical loading can be determined from cylinder pressure data. Whether or not the rate

of pressure rise plays a significant role in the stresses in components is uncertain. Relevant information can be gained by measuring and calculating the strain of selected components as a function of time. The dynamic strain of a cylinder head bolt was measured and compared to measured pressure. This investigation was conducted to examine the effect of the rate of pressure rise on component stresses.

Thermal stresses are normally deduced by measuring temperature at different points in the engine. Temperature measurements at selected locations can be used to calculate surface heat transfer rates (Sihling and Woschni, 1977). Measured cylinder pressure and exhaust, oil and water temperatures were also used in the calculation of heat transfer in the engine. Temperature distribution and thermal stress were then calculated from heat transfer rate.

Both combustion behaviour and engine stress were determined for a representative range of fuels. Relationships between relevant variables describing these two criteria were then determined statistically. The objective was to investigate the relative effects of combustion variations on engine stress and durability. Detailed results of the type needed by engine designers were thus not required for the objectives of the project. Considerable additional effort and expense would have been required in order to achieve absolute detail. This was, however, not justified because such results would only apply to one engine model and could only be used on a relative basis when other engine designs are studied. There would thus have been no benefit from attempting to achieve extremely detailed results. However, an effort was made to ensure that measurements and calculations were accurate and consistent at all times.

5. INSTRUMENTATION AND DATA ACQUISITION

Despite their different origins the differences between the fuels marketed in South Africa are relatively small. Even the behaviour of many of the alternative fuels being considered does not differ dramatically from that of the conventional fuels. Accurate and consistent measurements of all relevant variables should thus be made at all times. Clearly, it is vitally important that all the instruments are sensitive and extremely consistent. In this manner even the smallest differences between fuels would be detected and quantified.

Measurement of the variables required to determine combustion rate and heat transfer rate requires a particularly high standard of accuracy and repeatability. A considerable effort was thus made to maintain consistency in all measurements and calculations. All the implications of simplifications and assumptions were studied and understood. In all cases any errors introduced were independent of the fuel used and would thus not affect the relative comparisons.

Most of the test apparatus used was developed and built during the duration of the project. The advantage of this was that the overall objectives and requirements were considered during the development of each aspect of the test apparatus. The same applied to the development of the measurement and calibration techniques. It was thus possible to maintain a high standard of sensitivity, accuracy and consistency throughout the project. These factors played an important role in the successful quantification of combustion and engine durability.

5.1 Engine and Standard Instrumentation

All testing was carried out on an ADE 4.236 engine. This engine is used in the majority of agricultural tractors and in numerous light transport applications. It is possibly the most widely used diesel engine in South Africa. This engine is similar to the Perkins 4.248 used by Hansen *et al.* (1984) which was sensitive to combustion quality. The ADE 4.236 engine has a deep bowl combustion chamber and relies considerably on squish flow to assist air/fuel mixing. The combustion system is similar to those used in the majority of engines manufactured in South Africa. The ADE 4.236 is thus the engine most suitable for carrying out research into engine stress related to combustion. A conventional water to air heat exchanger and fan system was used for engine cooling. The size of all elements was as recommended by the engine manufacturer.

The dynamometer used was an AW model NEB400 manufactured by AW Dynamometer Inc. which operated on the pony brake principle. In order to avoid destructive torsional vibration on start-up and shutdown, a clutch was fitted to the engine. This also allowed zero load to be achieved. Both the engine and dynamometer used were mounted on an engine test bed designed and built for the project. The dynamometer was originally designed to operate at low speeds and at torque values as high as 2500 Nm. The engine torque output of less than 250 Nm necessitated dynamometer modification in order to achieve stable operation. This involved lowering the cooling water level such that the brake drum protruded into the water by approximately 40 mm. The speed of the pump which supplied hydraulic fluid for control purposes was reduced in order to reduce the supply pressure. These modifications permitted stable operation at low torque values and high speeds. The test engine and dynamometer are illustrated in figure 3.

Relevant temperatures in the engine were measured with K type thermocouple probes. Oil temperature was measured in the engine sump and water temperature was measured in the top of the heat exchanger. Exhaust temperature was measured in the manifold at a point 60 mm from the junction of the different ports in a straight section of pipe. Intake air temperature was measured at the inlet valve. A thermocouple junction was placed in the airflow of the inlet port within 10 mm of the inlet valve stem.

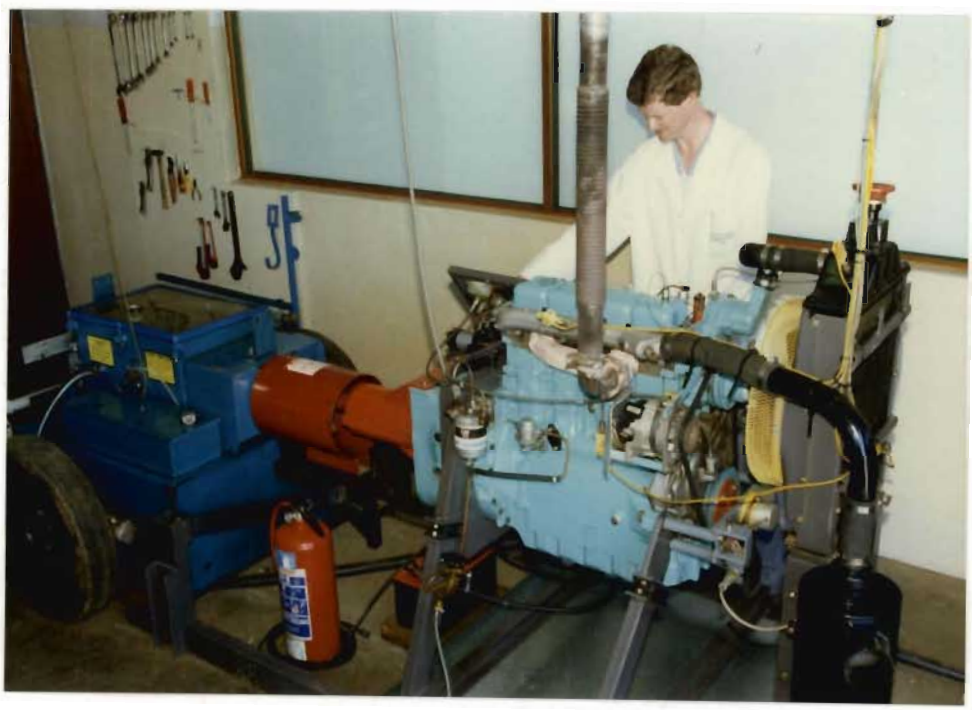

Figure 3. The layout of the ADE 4.236 engine and dynamometer.

Engine torque was recorded with the aid of a strain gauge load cell, manufactured by AW Dynamometers Inc.. The load cell measures the reaction force exerted on the brake device of the dynamometer, which is mounted on a balance. Some difficulty was experienced in maintaining a consistent zero point. This was due to the stiffness of the piping between the balance and the dynamometer body which is required to carry cooling water. The problem was overcome by pre-loading the balance in the positive torque direction with an

adjustable spring device. This reduced movement effectively to the extent of load cell strain and solved the problem.

Fuel consumption rate was measured with a batch fuel flow device which was initially developed by Meiring, Haestier and North (1972). This device used optic sensors to detect the meniscus of fuel flowing out of a calibrated flask. The sensors start and stop a timer which records the time required for the fuel in the flask to be consumed. The system was calibrated by using a mass balance to measure the mass of fuel contained in the flask. The device was fully automated and on demand re-routed fuel flow to the engine, from the fuel reservoir to the flask. When the second sensor detected that the flask was empty, the fuel flow path was returned to the reservoir and the flask was recharged.

Air flow through the engine was measured with the aid of a parabolic orifice at the air inlet. Static pressure in the orifice was measured with the aid of an inclined water manometer. It was found that the flow fluctuations caused by the engine were not dampened sufficiently by the paper element air cleaner unit and the related piping. The pressure recorded in a parabolic orifice is proportional to the square of air flow rate. If the average orifice pressure is used to calculate the average air flow rate, then the calculated value will exceed the actual value. This is due to the non-linear relationship between airflow and orifice pressure. The extent of the discrepancy is determined by the magnitude of the flow variations.

It was thus necessary to reduce the flow velocity variations to an insignificant level. This was done by separating the orifice from the engine with two 210 l damping chambers. The elasticity of the air resulted in an adequate reduction in airflow variations at the orifice. Volumetric efficiency was calculated at different engine speeds and loads. The test was carried out with two orifices of

different diameter. On investigation these results compared favorably and any differences in volumetric efficiency were attributable to small measurement errors. The values and trends of volumetric efficiency compared favorably with those reported by Taylor (1979) and Taylor (1987).

Cylinder pressure was detected by a Kistler 6121 pressure transducer. This transducer was equipped with a thermal shield which protected the diaphragm and piezoelectric crystal from the effects of direct flame. Water cooling of the transducer was not required. The transducer signal was processed by a Kistler type 5007 charge amplifier. The location of the transducer in the combustion chamber can have a marked effect on the quality of the resulting signal (Timoney, 1987a). Significant resonance has been witnessed in signals from transducers which are located above the piston in the squish zone and at the end of access passages. At ignition the rapid flow of gas into any confined crevice or passage results in rapid pressure fluctuations which are superimposed on the measured cylinder pressure. Pressure oscillations at the natural frequency of the combustion chamber are also responsible for signal distortion, but are less significant.

It was thus decided that the pressure transducer should be mounted flush with the cylinder head directly over the combustion bowl in the piston. Access to this region is, however, limited. A location was required which was over the combustion bowl, but which did not coincide with either the injector or the valves. The only suitable location was at the perimeter of the bowl between the exhaust and inlet ports as indicated in figure 4.

A hole was machined through the cylinder head and was tapered with a taper pin reamer. A tapered sleeve was manufactured and inserted into the hole from the inside outwards as illustrated in figure 5. On the outside of the cylinder head the sleeve was threaded and a

nut was used to pull the sleeve outwards. The metal contact on the taper provided an adequate seal between the combustion chamber and the water jacket. The seal between the water jacket and the camshaft housing on the outside was provided by an "O" ring which was clamped between the cylinder head and the sleeve by a nut. A second sleeve was screwed on to the end of the first sleeve and protruded through the timing cover. This provided an access to the combustion bowl from the outside and also prevented the coolant, combustion gasses and engine oil from leaking or coming into contact with one another.

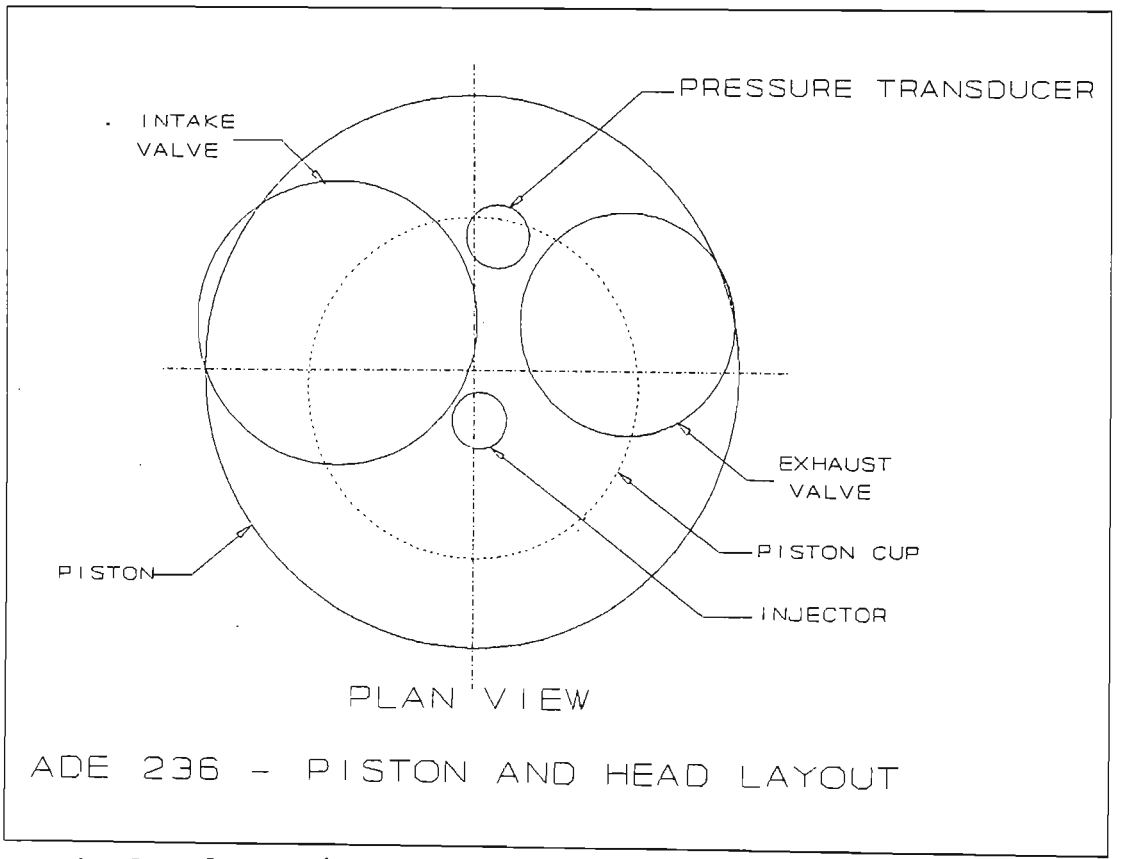

Figure 4. A plan view showing the position of the pressure transducer in relation to the cylinder head, valves and piston bowl.

The transducer was screwed into the end of a third sleeve which could be inserted into the cylinder and clamped against the transducer seat by an external nut. This system proved to be

highly effective and avoided some of the problems which had been experienced previously (Taylor, 1987). One of the problems which had been overcome was the difficulty experienced in extracting the transducer from a blind hole. The external clamp nut was made in such a way that it could pull the transducer and sleeve out in a controlled manner. The only disadvantage of the system was that the transducer operated in the proximity of the exhaust port. The result was that the transducer operated at high temperatures which could have had a detrimental effect on the performance (Koeberl and Wurzinger, 1986).

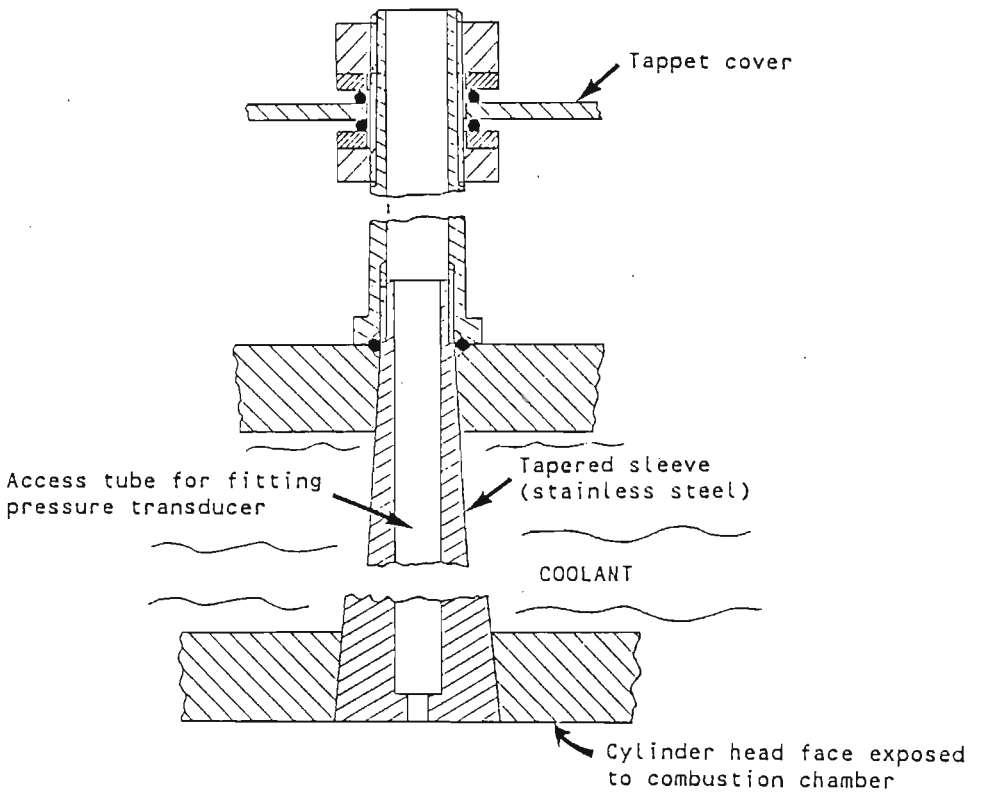

Figure 5. A simplified cross-section of the cylinder head showing the tapered sleeve for accessing the combustion chamber.

Injection timing was determined from needle lift. A needle lift transducer was designed and built into an extended injector cap. The transducer was an inductive device and when correctly calibrated it had a linear response. This is because the range of

operation was a small fraction of its measuring range. If the range of operation was adjusted to be in the region of maximum gain, then the change in gain across the range of operation was negligible. This design proved to be effective and compact. Some difficulty was however experienced when some of the ethanol based fuels attacked the material insulating the coil. The problem was, however, overcome by sealing the coil with silicon room temperature vulcanising.

To ensure that data are recorded at specific points in the engine cycle an accurate crank shaft reference is required. A BEI Electronics model L25G-F3-SB-720-ABZC-7404-SC36 optical shaft encoder was thus fitted to the crank shaft. This device which is illustrated in figure 6 generated two sets of pulses every half degree of crank shaft rotation. These pulses were one quarter of a degree wide and offset by one eighth of a degree, thus allowing pulses to be generated as often as eight times a degree. An additional channel provided a single pulse per revolution which is used as a top dead centre reference. The pulses from the shaft encoder were also used to determine engine speed.

In order to avoid the effects of crank shaft twisting, the shaft encoder was fitted at the front end of the engine. This was adjacent to the number one cylinder which was fitted with the pressure transducer and needle lift sensor. The portion of the crank shaft which lay between the number one cylinder and the shaft encoder experienced no torsional forces other than those which were required to drive the timing gear, fuel injection pump, water pump and alternator. In this manner it was ensured that the encoder displayed the actual position of the relevant crank regardless of crankshaft flexing.

The apparatus described above was designed, assembled, tested and used between commencement and completion of the project. This

process alone required considerable time and effort. The quality of the data recorded from the test apparatus was comparable with data reported by other successful researchers. This was despite the fact that the total development cost was a small fraction of that of similar commercial test apparatus.

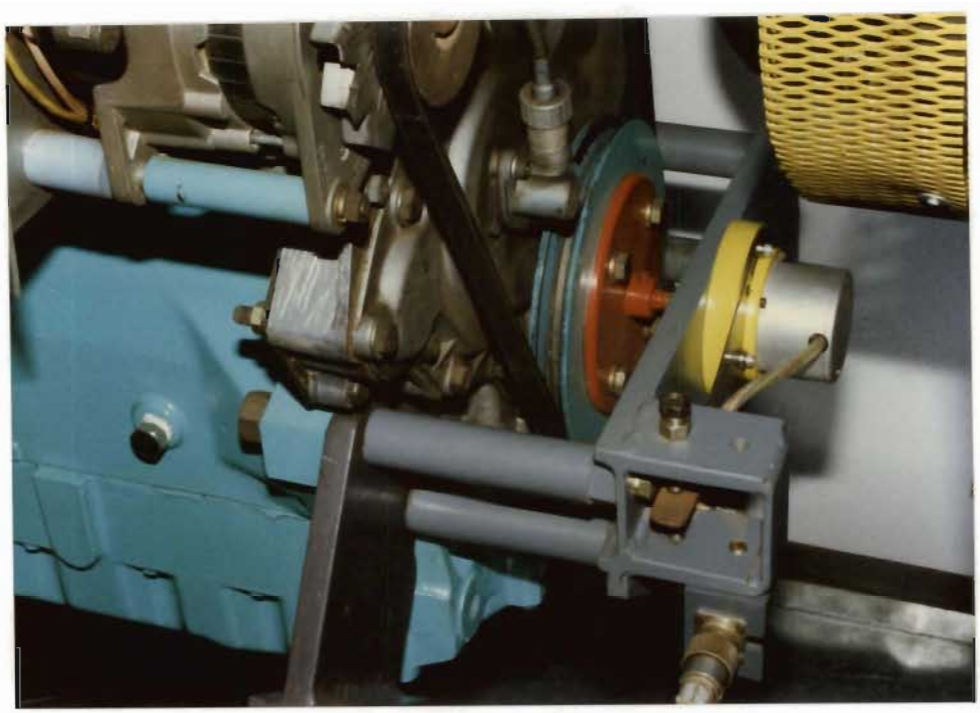

Figure 6. The crank shaft position encoder.

5.2 Cylinder Head Displacement Transducer

By measuring stresses in components which are loaded predominantly by cylinder pressure, it is possible to investigate the relationship between pressure development and the resulting mechanical stress. Miyamoto et al. (1980) measured the strain of a number of components, namely, the valves, the crankshaft and the cylinder head bolt. Not only is the cylinder head bolt the most accessible component, but the resulting stresses indicated that dynamic stress was not simply proportional to absolute pressure. The results of Miyamoto et al. (1980) indicated that peak stress

was determined by peak pressure and the rate of pressure rise in some cases. The strain of the cylinder head bolt can be easily and cheaply measured with the aid of strain gauges.

It was for these reasons that a cylinder head displacement transducer was designed and built. This device which is illustrated in figure 7 was fitted in place of one of the cylinder head bolts in the region of the number one cylinder. A location was sought which would yield maximum displacement in order to maximize the signal. The transducer was made in the form of a stud, being threaded at both ends. A short portion of the stud was machined down to a small rectangular section while the remaining dimensions were kept as large as possible. Strain gauges were adhered to the rectangular section. The strain gauges were then wired in such a way as to compensate for torsion, bending and temperature.

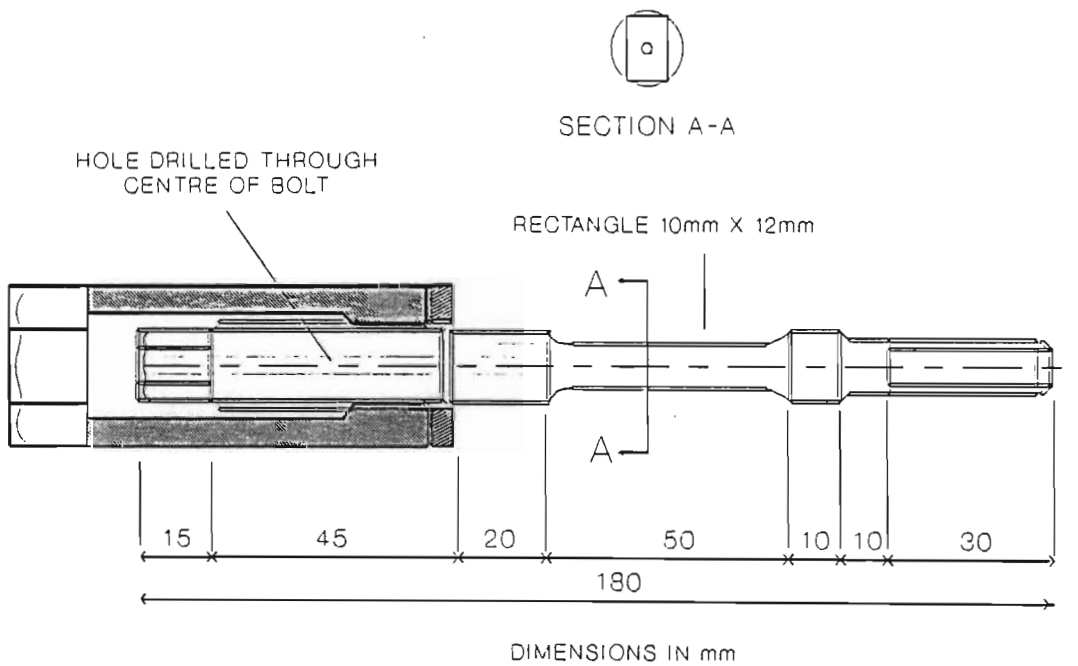

Figure 7. A schematic diagram of the cylinder head displacement transducer.

The length of the transducer between the attachment points was kept as short as possible. This factor, in conjunction with the fact that the sectional area at the point of measurement was kept as small as possible, ensured that the measured strain was maximized. The largest possible voltage output from the strain gauge bridge was thus achieved. The conductors were brought out from the strain gauges through the hollow centre of the bolt.

The temperature at the strain gauges was expected to exceed 100°C. Both strain gauges and adhesive were thus selected to withstand temperatures of up to 200°C. The strain gauges used were HBM (Hottinger Baldwin Messtechnik) type 3/120XY11 and the adhesive was HBM type EP310. The adhesive, was cured at a range of gradually increasing temperatures. The maximum curing temperature exceeded the maximum expected working temperature.

The exact tensile yield point of the steel used for the transducer was measured with a tensiometer. The area of the measurement section could thus be minimized in order to maximize the strain and resulting output voltage. The yield strength was found to be 773 MPa. The objective was to operate the transducer as close to the yield point as possible without exceeding the yield point. The transducer loading is the combined effect of cylinder head pre-load and the gas pressure force. The pre-load force was calculated on the basis of the specified pre-load torque and the dimensions of the thread. The cyclic pressure force was calculated on the basis of expected maximum cylinder pressure. A minimal factor of safety was used.

It was discovered that the force resulting from the pressure loading was less than 2% of the magnitude of the cylinder head pre-load. The cylinder head pre-load resulted in a strain gauge signal which exceeded 15 mV. The range of the signal resulting from cylinder pressure was approximately 0,2 mV and was superimposed on

the pre-load signal.

This posed unusual demands on the signal processing apparatus since accurate measurements of the pressure induced stresses were required. An amplifier was required which could compensate for a large voltage offset while operating at an exceptionally high gain. A Tecktronix model 5A22N differential amplifier was found to be suitable. The unit formed part of a Tecktronix model 5223 digitising oscilloscope system and the amplified signal was available as an output from the oscilloscope. The signal was then passed through a second stage of amplification before being recorded.

Due to different expansion rates of the various components the offset of the strain signal was found to drift with engine temperature. This did not, however, pose a problem since the range of the pressure induced signal was the only information required. The signal, being very small, was highly susceptible to noise. The problem was aggravated by the fact that long conductors were required between the strain gauges and the amplifiers. As was the case with the cylinder pressure and needle lift signals, the strain signal also displayed cycle to cycle variation. Averaging of multiple cycles was thus necessary. The signal noise, being out of phase with the engine cycle, was largely eliminated by the averaging process. This is because, by averaging, any single disturbance of the signal is divided by the number of cycles being averaged. The sum of the reduced noise, which is out of phase from cycle to cycle, tends to approach zero as the number of cycles being averaged increases.

5.3 Surface Temperature and Heat Flux Probe

Thermal stresses in any component are dependent on the temperature distribution of the material within that component. It is thus

evident that in order to calculate thermal stress, the temperature distribution must first be calculated. The temperature of a component is determined by the rate of heat transfer within the component. Knowledge of the rates of heat transfer is thus required in order to calculate the thermal stresses in an engine (Sarsten, 1979).

The rate of heat transfer can be determined from measured temperature gradients or from a measured time history of surface temperature. It was decided that any device designed to determine surface heat transfer rate should measure both these variables. It was also assumed that any variation in heat transfer rate, resulting from fuel property differences, would be proportionally similar at all points in the combustion chamber. Heat transfer rate was thus measured at a single location in the combustion chamber. The assumption satisfied the objectives of the project, which were to compare fuels on a relative basis.

The housing constructed for the pressure transducer is located above the piston just within the combustion bowl lip. This location is in the region of maximum gas velocity during combustion and thus experiences extreme heat transfer rates (Hardenberg and Daudel, 1981). A probe mounted at the location would thus be most sensitive to changes in heat transfer brought about by fuel properties. A probe was thus built to fit into the pressure transducer housing such that the face was flush with the cylinder head surface. The probe used is illustrated in figure 8. A fast response surface thermocouple was built on the face of the probe while a second junction was fitted within 2.5 mm of the face.

To ensure that the rate of heat transfer through the probe was similar to that through the surrounding cylinder head, it was machined out of cast iron. Before designing the surface thermocouple a study of those used by other researchers was

conducted. It was concluded that with the available facilities, the design used by Hohenberg (1979) would be the easiest to manufacture. The design was also well suited to the relatively limited diameter of the probe. The construction involved drilling through the length of the probe and bonding a commercial K type thermocouple in the hole with the end protruding beyond the face of the probe.

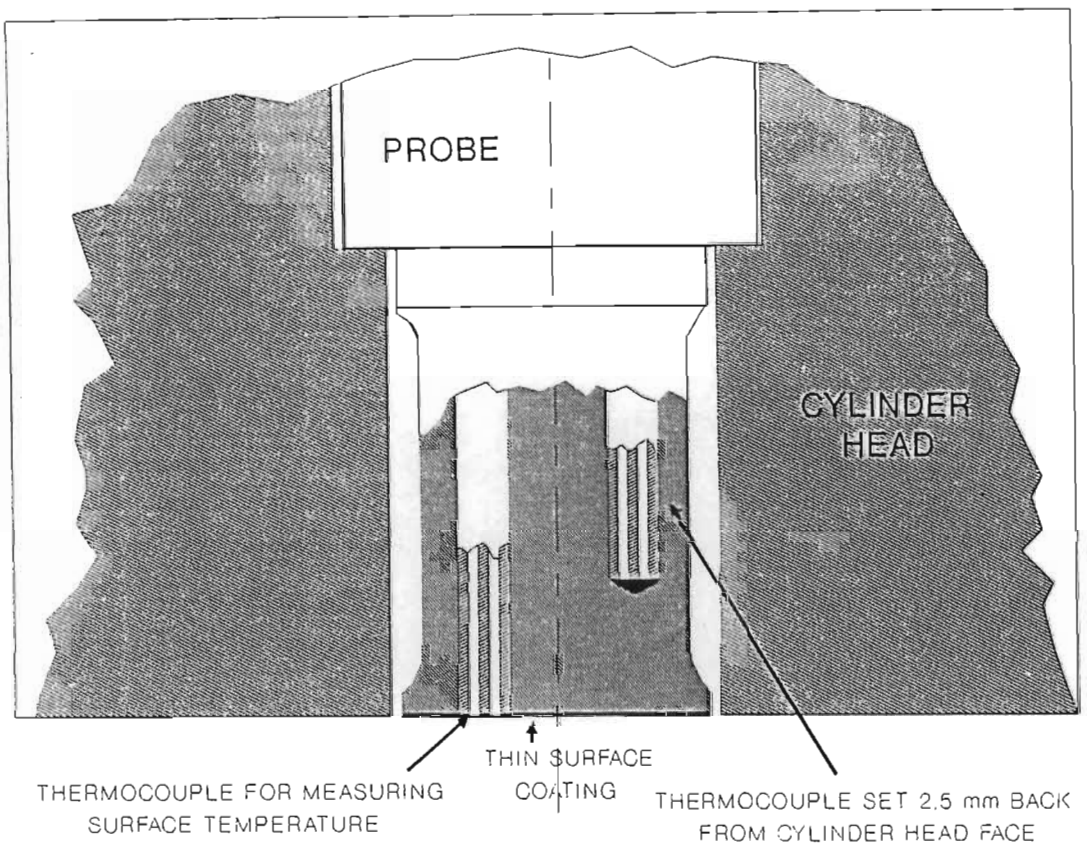

Figure 8. A cross section of the surface temperature and heat flux probe.

The commercial thermocouple unit was made of a 1,5 mm stainless steel tube with two 0,25 mm conductors within. The conductors were insulated by ceramic magnesium oxide powder inside the tube. The thermocouple was machined away at the face of the probe and the ceramic powder was removed to a depth of approximately 1 mm. The powder was replaced by a ceramic cement which was capable of

resisting cylinder pressure forces at the high temperatures which exist in the engine. The ceramic cement used for both the face of the probe and to bond the thermocouple into the probe was Kyowa HC-25A high temperature strain gauge cement.

After the thermocouple had been machined away, a situation existed where the chromel and alumel wires had been brought through to what would be the surface of the combustion chamber. These wires, which normally formed the thermocouple junction, were insulated, supported and sealed by the ceramic cement. The face of the probe was then coated with a thin vapor deposited gold layer. This process was carried out in a vacuum chamber at extremely low pressure.

The gold coating formed two thermocouple junctions by contacting the chromel and the alumel simultaneously. The two junctions being chromel-gold and gold-alumel. As long as the temperature of the two junctions was identical the presence of the gold would not have played any role in the voltage between chromel and alumel. The junction would thus respond as a chromel-alumel junction. The thickness of the gold was estimated to be less than 5 μm. The result was that the junctions were within 5 μm of the surface and had negligible thermal capacitance. The output voltage, measured between the chromel and alumel conductors, would thus have responded rapidly to changes in surface temperature.

The gold film played a second important role in that it served to ground both the chromel and alumel conductors. The effect of signal noise in the conductors, which were unscreened over a length of approximately 20m, was thus reduced. This was in fact so effective that failure of the junction between the gold film and the probe, resulted in the signal being obscured by noise. A second commercial thermocouple junction was placed within the probe at a point approximately 2.5 mm from the face of the probe.

Temperature gradient was calculated from the difference between the temperatures at the two junctions.

The calculation of heat transfer rate from both transient surface temperature and temperature gradient relies on the assumption of single dimensional heat flux. In order to encourage single dimensional heat flux, an effort was made to thermally insulate the probe in the transverse direction. This was done by creating an air gap between the probe and the surrounding cylinder head. From within 1 mm of the probe face to a point well beyond the second junction, the diameter of the probe was slightly reduced. The clearance between the probe and the cylinder head at the face of the probe was minimal. This created a seal reducing the flow of combustion gasses into the air gap between the probe and the cylinder head. The insulation properties of an air gap are eleven times better than a ceramic layer of equivalent thickness (Hohenberg, 1979). It was thus reasonable to assume that heat flux within the probe approached being single dimensional.

The calculation of heat transfer rate requires an accurate knowledge of the thermal properties of the materials within the probe. Even if the material properties are known, construction variables such as contact resistance can result in uncertainty of the probe properties (Hohenberg, 1979 and Morel, Wahiduzzaman and Fort, 1988). The fact that the probe supplied two signals which could be used to calculate heat transfer rate was used to overcome the problem. The probe was calibrated by correlating the results calculated from these signals with each other and other variables which were measured. The emphasis was again focussed on achieving absolute consistency and sensitivity. The pressure transducer, heat flux probe, needle lift transducer and cylinder head displacement transducer can be seen in figure 9.

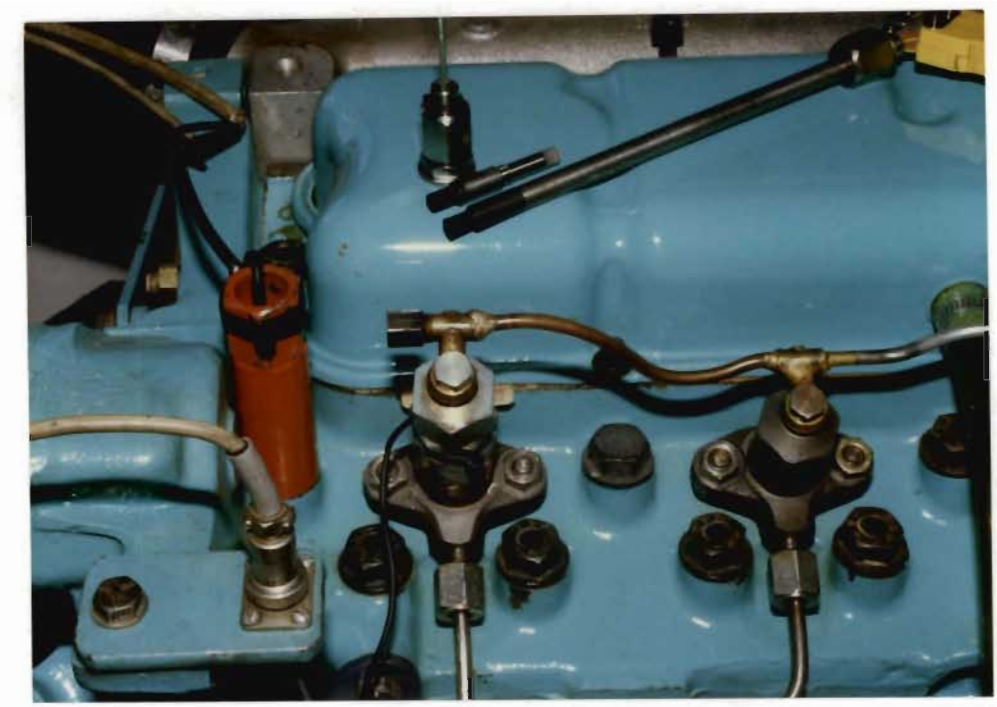

Figure 9. The pressure transducer, heat flux probe, needle lift transducer and cylinder head displacement transducer.

5.4 Data Acquisition System

In order to monitor and record the signals emanating from the numerous transducers a multichannel data acquisition system was required. The system would need to record both high speed and steady state variables simultaneously. Although systems for recording both high speed and steady state data were available, none of these systems were capable of recording both forms of data simultaneously. Even the most expensive commercially available systems were not suitable for the requirements of the project. At the time of commencement of the project a highly effective data acquisition system based on a Sinclair Spectrum computer was available (Taylor, 1987). The system was, however, inadequate for the requirements of the project because it was limited to single channel data acquisition. It was thus necessary to develop a

better system in order to achieve the objectives of the project.

A statistical analysis of the cycle to cycle variation in cylinder pressure can be carried out to determine the minimum number of cycles which must be recorded in order to achieve an acceptable average. Averaging more than 30 cycles of cylinder pressure will normally yield an average within 1% of the true average with a 99% level of confidence. The variation in the rate of pressure rise is, however, far greater and more than 1000 cycles should be recorded to get an average of the same accuracy (Taylor, 1987). Cycle to cycle variation in surface temperature is also such that many cycles must be recorded in order to achieve an acceptable average (Sihling and Woschni, 1977). The variation in the rate of change of surface temperature could thus be even greater. The calculated rates of heat release and heat transfer are highly sensitive to the rates of pressure and temperature rise respectively. It is thus of major importance that representative averages be determined. Unfortunately, few data acquisition systems are capable of recording the large number of cycles which are required for this purpose. The result is a situation of compromise in which as many cycles as practically possible are recorded.

Experience with the development and use of the Sinclair Spectrum computer based system provided valuable information required to develop a better system. The success of any system is largely determined by the speed and precision with which it can digitise the incoming signals and store data in memory. A wide range of data acquisition cards designed to plug into computer expansion slots are commercially available.

After a thorough study of the possibilities it was decided that a Data Translation DT2821-F-16SE data acquisition card was best suited to the application. The device is capable of carrying out

analogue to digital (A/D) conversions on 16 single ended input channels. The conversions can be carried out in any order under control of either an external trigger or a programmable timer clock. The maximum rate at which A/D conversions can take place approaches 150 000 per second, depending on the type of application. The fact that incoming signals can be amplified by software selectable gains of 1, 2, 4 or 8 before being digitised at a resolution of 12 bits, results in high levels of precision. Two 8 bit input output (I/O) channels are available as well as two 12 bit digital to analogue (D/A) channels.

High speed data should be digitised at known crankshaft angles and thus the A/D converter should be controlled by an encoder on the crankshaft. This eliminates the effects of crankshaft deceleration and acceleration during the cycle. While the data acquisition board acted as an interface between the instruments and the computer, an interface was required between the crankshaft encoder and the data acquisition board. This allowed for some conditioning of the shaft encoder signals in order to generate trigger signals to control A/D conversions. A digital interface was thus designed and built.

The computer used was an IBM PC/AT compatible and the software was written in Borland Turbo Pascal. The reason for using the PC/AT was that a machine was required which had a sixteen bit data bus and two sixteen bit direct memory access (DMA) channels. Apart from other reasons which include speed and ease of application, Turbo Pascal was used because it was capable of communicating with I/O ports using sixteen bit words. An advantage of having a system based on a fast computer running under a powerful computer language is that a considerable amount of data processing can be carried out during data acquisition. Such a system should not be dedicated to any particular test, but instead, it should be capable of accommodating a wide variety of test formats. This can be achieved

by ensuring that all system functions are software controlled. The software should in turn be controlled from a system of menus. Operators who are unfamiliar with the hardware and the computer language can thus use the system.

The system which was finally achieved, included a single executable program which was entirely menu driven, a DT2821-F-16SE board and a cabinet. The cabinet was connected to the board which was housed within the computer. All the signals emanating from the various instruments were connected to the cabinet by a range of appropriate sockets. The digital interface was contained within the cabinet and the analogue voltages, trigger signals and digital I/O lines were carried from the cabinet to the data acquisition board by a platted ribbon cable. The system had three basic modes of operation, the setup mode, the data acquisition mode and the data processing mode.

On execution, after displaying an introductory banner, the program entered the setup mode. It was at this point that the desired test configuration was selected. The relevant information was entered through a setup editor. Initially the test title was entered. The title was used as the basis for all data file names. All relevant information describing the engine geometry such as compression ratio was then entered. The number of steady state channels required was selected and information about these channels was inputed. The information included the channel name, the signal voltage range, the point on the cabinet at which the signal was connected and the gain and offset of the signals. The program could thus convert the incoming signal to real scientific units immediately.

The number of high speed channels was then selected. Again the information necessary to calculate real scientific units was input. With the aid of the digital interface the system was capable of

isolating any portion of the engine cycle and only recording the high speed channels in that portion. The start and end points of the portion required were entered relative to the TDC between the exhaust and intake strokes. These points could be selected with a resolution of four crank angle degrees. This facility was achieved by using the two eight bit I/O channels to communicate with the digital interface.

The digital interface had counters which begin counting four degree pulses starting immediately after top dead centre. The trigger pulses to the A/D converter which were disabled initially were enabled when the first counter reached the value selected in the setup editor. The selected high speed channels were digitised until the second counter reached a value equal to the end value selected in the setup editor. The trigger signal was then disabled until the start point in the following cycle was reached. In this manner only the data relevant to the test was recorded. This portion was referred to as the window. The resolution at which data were digitised could be selected in the setup editor from a range of possibilities. The range included 1/8, ¼, ½, 1, 2 and 4°CA resolutions.

Since there were two TDC pulses per engine cycle some method of discriminating between them was required. The choice of two different methods was offered by the digital interface. The most simple method was based on a flip-flop device which inhibited every alternate TDC pulse. A switch on the digital interface allowed the system to be alternated if the TDC pulse being inhibited was actually the one required as a zero reference for the test. The system allowed tests to be referenced from either of the two TDC pulses, thus enabling a detailed study of the intake and exhaust strokes if it were required. A second method for inhibiting the TDC pulse relied on the fact that the signal connected to the first analogue channel was at different levels at the two different TDC

pulses. The TDC pulse which occurred while the signal was above an adjustable threshold was inhibited automatically. This facility made use of the fact that most tests involve cylinder pressure measurement, thus eliminating the need for switching the flip-flop device.

The desired number of cycles which were to be averaged was entered in the setup editor and the program automatically reduced the amount if the computer had inadequate memory space. The amount of memory required to buffer the data was proportional to the product of the number of points in a window and the number of cycles to be recorded. Reducing both the width of the window and the crank angle resolution greatly increased the number of successive cycles which could be recorded.

One of the objectives of the data acquisition system was to automate the test procedure as far as possible, thus allowing the operator to concentrate on the engine and instrumentation. This was partly achieved by minimizing the keystrokes required to control the program. For this reason, when the information required for the test setup had been entered, it could be stored on magnetic disk. Normal utilization of the system did not involve entering all the information described above. The information would simply be loaded from an appropriate setup file and slightly edited to suit the needs of the test. This, and the fact that the input sockets on the cabinet were placed conveniently on the front panel, made the system highly versatile, requiring minimal time to change from one test format to the next.

The setup menu also provided an auto-calibration facility. This required the successive input of two known signals into the appropriate channel and the entry of the corresponding values in the correct units at the keyboard. The program then calculated the channel gain and offset automatically and amended the setup data

accordingly. Although this facility was best suited to calibrating the steady state channels, it was also used to determine the gain of the high speed channels. By declaring a high speed channel as a steady state channel, the gain of the channel could be determined. The calculated gain value was then transferred to the relevant high speed channel by the operator.

Due to the fact that the heat flux probe and the cylinder pressure transducer required the same housing, all tests had to be carried out in two phases. Cyclic surface temperature was recorded during the first phase and cylinder pressure, needle lift and cylinder head displacement were recorded during the second. This required duplication of certain portions of the setup data. The requirement was accommodated by the data acquisition system. Data recorded in the two phases were stored under identical file names except for a number included in the file name which represented the phase number. When the required setup had been edited and saved on disk, and all the channels had been calibrated, the setup menu was exited and the system entered the data acquisition mode.

There were three alternatives available to the operator in the data acquisition mode. Firstly, all selected channels could be monitored. Secondly, all selected channels could be recorded in the manner specified in the setup menu and finally, previously recorded data stored on disk could be loaded. If the monitoring option was selected the program entered a routine which looped until interrupted from the keyboard. All steady state channels were recorded 50 times and the averages were displayed at the top of the screen. One cycle of the high speed data were then recorded and displayed graphically on the screen. The routine was repeated with the previous values being erased as the new values were displayed. In this manner all data were continually updated at a rate determined by the number of channels being recorded. In this mode the system simulated a bank of panel meters and an

oscilloscope, thus rendering these items unnecessary.

When the engine had stabilized at the desired point the monitoring routine was interrupted and the recording routine was selected. Initially, the steady state channels were repeatedly recorded over a period of approximately five seconds. One thousand readings of each channel were averaged before the high speed data were recorded. During high speed data acquisition, the DMA controllers were used to transfer digitised data from the data acquisition board to computer memory. The data acquisition board and DMA controllers were programmed to operate in dual DMA mode. The process involved using two sixteen bit DMA channels alternately, to maintain a continuous flow of data into memory. Each channel transferred 128 kilobytes (kb) of data before issuing an interrupt.

The interrupt initiated an interrupt servicing routine automatically and prompted the other DMA channel to continue with data transfers. The interrupt servicing routine stored the central processor unit (CPU) registers on the stack, then checked to see if the data acquisition board had encountered any problems. If errors had occurred or if the required amount of data had been recorded, the routine terminated the dual DMA mode. If further data transfers were required the inactive DMA channel was reprogrammed to transfer data to an unused portion of computer memory. The CPU registers were then restored and the program waited for the subsequent interrupt. Programming the DMA controllers involved setting the amount of data to be transferred and the target address of the memory.

The data acquisition board was also programmed to operate in dual DMA mode and in the event of an error could also initiate the interrupt servicing routine by issuing an interrupt. The board recorded multiple high speed channels with the aid of what was termed the ram channel gain list. The list was set up on the

board, by the high speed data acquisition routine and included the order and voltage range of high speed channels to be recorded. With the aid of the digital I/O lines the high speed data acquisition routine commanded the digital interface to set the required window and disable the trigger pulses. These trigger pulses were re-initiated after the trigger on the data acquisition board was enabled. The digital interface ensured that the first trigger pulse received was also the first pulse of a window. In this manner it was possible to keep track of the recorded data.

On each trigger pulse all the channels in the ram channel gain list were recorded successively. The time between the recording of the successive channels was set by the on board clock to 0,667μs. The fact that these channels were not recorded simultaneously was possibly the greatest limitation of the system. The result was that the data recorded for successive channels were 0.667μs out of phase. Although this could have been overcome by a process of numerical interpolation, it was considered to be insignificant. In addition, the phase error was consistent for all the tests and would thus not affect the relative comparisons.

When the required data had been recorded or when an error had been detected, the system interrupts, which had been modified to accommodate DMA, were returned to their original state. An appropriate message was displayed on the screen and if an error had been detected, the high speed data acquisition routine was repeated unless interrupted from the keyboard. If errors had not occurred the steady state channels were recorded a second time. A second average was then determined for all the steady state channels and compared to the first average. If these values differed by a proportion greater than that specified in the setup menu then the entire recording routine was repeated, unless interrupted from the keyboard.

The DMA controllers were capable of accessing a total of sixteen megabytes (Mb) of computer memory. The first block of one Mb of memory was occupied mostly by the computer operating system and the data acquisition program. The remaining 15 Mb was available as a data buffer for high speed data acquisition. At the time of data acquisition the program which ran under the Microsoft disk operating system (DOS) was not capable of accessing more than 1 Mb of memory. The data buffers were thus limited to less than 256 kb within the first one Mb of computer memory. This resulted in the maximum number of high speed data points which could be recorded being less than 131 000. Representative averages of the signals were, however, achieved and there was thus no need for additional data points. At a later stage the information required to overcome the problem was acquired. The solution involved initiating one of the system binary input output system (BIOS) routines. The routine transferred the computer into protected mode in order to transfer blocks of data from extended memory to below the 1 Mb limit where they could be accessed by the program.

After the required high speed data had been recorded successfully the successive cycles were averaged. A facility which calculated the variance of signals was also available. The facility is useful in determining the number of successive cycles required in order to achieve a representative average. In the data acquisition menu an alternative to recording data was to load previously recorded data from disk. If this option was selected the filename extension was requested. The bulk of the file name was compiled automatically from the test heading and phase number. When data were acquired, either from disk or from the board, the data acquisition mode was terminated automatically, and the program entered the data processing mode.

The primary objective of the data processing menu was to ensure that recorded data were correct. This was done with the aid of

routines which displayed the data in graphical form. A number of important calculations were are also made. On entry into the data processing menu the options available were displayed along with the recorded steady state data. The recorded high speed data could be plotted against crankshaft angle on request. The routine assumed that needle lift was recorded on the second high speed channel. This needle lift channel was searched for the start, end and duration of injection. When injection point was located the routine searched the first high speed channel for ignition point and the ignition delay was calculated. The information was then displayed.

Cylinder pressure could be plotted against cylinder volume. The resulting curve gives some indication of the nature of the engine cycle. If the recorded window included the entire compression and expansion strokes the indicated mean effective pressure (IMEP), break mean effective pressure (BMEP) and friction mean effective pressure (FMEP) were calculated. By plotting the logarithm of pressure against the logarithm of volume it is possible to gain valuable information about the accuracy of the recorded pressure data. This facility was also included. The gradient of the curve is of particular interest because it represents the polytropic compression or expansion coefficient. The coefficient was thus calculated and plotted against crank angle for the relevant portion of the engine cycle. The coefficient equals 1,395 when adiabatic conditions prevail in the combustion chamber. The crank angle at which this occurs is of interest when heat transfer calculations are being conducted. The point was determined and the corresponding crank angle was displayed.

The final option in the data processing menu was the storage option. The option required the input of the test point number. The file name was compiled from the test heading, the test phase number and the test point number. The directory path could be

changed on request. Data describing the basic test setup were stored on the first line of the file. This included the crankshaft angle resolution, window limits and the number of steady state and high speed channels. The reason was that other programs would be able to read and interpret the recorded data. The basic setup data were followed by a blank line. The steady state data were then stored, one channel per line on the following lines. A blank line followed the last steady state channel value in order to separate it from the high speed data.

The high speed data were stored in columns. The first channel's data being stored on the extreme left, with the last channel's data being placed on the extreme right. The columns were separated by spaces. This format of storage allowed the data to be accessed with ease by other programs. Some of the programs used were based on Turbo Pascal, Professional Fortran and Lotus 123.

All the original objectives were achieved by the final data acquisition system. The system has proved to be highly versatile in application and has been used successfully by people unfamiliar with the computer languages and hardware. One of the main advantages of the system was the ease with which it could be adapted to perform functions which were not originally included. It was also clear that the system will be upgraded easily to take advantage of developments in the components which make up the system.

The system has already been upgraded from Turbo Pascal Version 3.0 to Version 4.0 during the course of the project. Data Translations recently released a new data acquisition board similar to the one used. The program was then converted to Turbo Pascal Version 5.0 and upgraded to operate on the faster data acquisition board. This gave the system the capability of digitising 250 000 readings per second at a resolution of twelve bits. The Turbo Pascal Version

5.0 compiler in conjunction with an Intel 80286 CPU running at 16 MHz and an Intel 80287 math co-processor gave the system the ability to process data at high speeds. Faster computers are also becoming available. It is thus clear that there are numerous possibilities for improving the data acquisition system.

5.5 Fuel Selection

Any research program claiming to investigate fuel quality should include the testing of a wide range of fuels representing a wide range of chemical and physical properties. The objectives of the project are, however, slightly different in that the relationship between combustion behaviour and engine stress is sought. The causes of a particular combustion behaviour are not of prime importance. A range of different types of combustion behaviour could have been achieved without changing the fuel at all. This might have been done by adjustments to the engine and fuel injection equipment.

It was, however, decided that a range of different combustion behaviours should be reached by testing a wide range of fuels and changing engine settings. This would account for the effect of fuel chemical composition on the gas temperatures in the engine. Engine manufacturers and operators appear to have some idea of expected engine life when conventional crude-oil derived diesel fuel is used. The fuel was thus considered to be the most suitable reference for relative comparisons of engine stresses and durability. The fuel refined from crude-oil at the coastal refineries, which is referred to as Coastal diesel, has been used as a reference fuel in the project. It was decided that the other commercially available fuels, namely Natref and Secunda diesel, should be tested. This was to ensure, that if differences existed, they would be detected and quantified.

Although an extensive analysis of combustion behaviour had already been conducted on a wide range of South African fuels, it was decided that this should be partly repeated (Taylor, 1987). This was because it became evident that the behaviour of the fuels in the ADE 4.236 engine deviated significantly from their behaviour in the Perkins 3.152 engine used by Taylor (1987). During the development of the heat flux probe, the confounding effects of soot were avoided by making use of a pure ethanol fuel. The fuel used for the purpose consisted of 93,5% hydrated ethanol and 6,5% of an ignition improver. The ignition improver is known as Blendol and is produced by AECI. At the time of testing there was considerable interest in the ethanol fuel as an alternative to diesel. The fact that the chemical and physical properties of the fuel are vastly different to diesel also made it highly suitable for inclusion in the tests.

Fuels and engine conditions were sought which are known to result in engine failure. From the results of Hansen et al. (1984) it is clear that the blend of 15% of ethanol and diesel exceeds the tolerance limits of some engines. This fuel and a blend of 25% ethanol and diesel was included in the tests. The latter fuel being expected to exceed the tolerance limits of most engines. Discussions with Wotherspoon (1988) revealed that if the timing on the ADE 4.236 engine was advanced by an amount which exceeded the recommended advance significantly, engine failure may occur. In order to generate unacceptable stresses in the engine a test was conducted with the timing advanced by four degrees beyond the recommended level.

A wide range of physical and chemical properties is encompassed by the fuels already described. To supplement the range a fuel was tested which consisted of 37,5% hydrotreated straight run tops (HSRT) and diesel. Blends of HSRT and diesel are of commercial interest since this would extend the available diesel resources

greatly. A summary of the fuels tested is given in table 1.

Table 1. A summary of the fuels which were tested.

Abbreviation	Test Fuel
CSTL	Coastal diesel fuel
TMNG	Coastal diesel fuel with advanced timing
SASL	Secunda diesel fuel
NAPT	37,5% HSRT and 62,5% coastal diesel fuel
15ET	15% dry ethanol and 85% coastal diesel fuel
25ET	25% dry ethanol and 75% coastal diesel fuel
ETHN	6,5% Blendol MW and 93,5% dry ethanol

5.6 Calibration and Test Procedure

In order to determine differences between fuels correctly, it is imperative that high levels of consistency be maintained during testing. A rigorous test procedure should thus be developed and followed throughout testing. Experience gained during the development of the instrumentation and data acquisition system contributed to the test procedure used.

Both the heat transfer probe and the cylinder pressure transducer were sensitive to the accumulation of soot. These devices were thus always cleaned prior to testing. The cylinder pressure transducer was soaked in carbon tetrachloride before being cleaned. The diaphragm of the device was located within a narrow slot behind the heat shield and was thus not easily cleaned. The carbon deposits were softened by the carbon tetrachloride and were removed by drawing a cotton thread through the slot. The transducer was then inspected under a microscope to ensure that no carbon remained. If carbon remained, then an ultrasonic cleaning device was used. This was, however, seldom required.

The surface thermocouple required more careful treatment to avoid damaging the gold coating. The entire cleaning process was carried out under a microscope. The soot layer was crushed by rolling a cotton thread, under tension, across the face of the probe. This was repeated until the soot had been removed. After cleaning, the gold coating was visible although slightly discoloured. The presence of soot on the surface thermocouple obviously affected the heat transfer to the probe. The amount of soot formed depended to a large extent on the nature of the fuel used in the engine.

Soot was also found on many other surfaces in the combustion chamber. Despite the fact that the measured rate of heat transfer was reduced by the presence of soot, the conclusion was reached that the occurrence represented the actual heat transfer to the components. It was thus necessary to ensure that the soot present on the probe during testing was representative of that present in the engine when running on the particular fuel. It became evident that initially soot accumulated rapidly and then appeared to reach an equilibrium thickness. The phenomenon was analysed by Hohenberg (1979) who proved that the soot layer reached an equilibrium thickness within thirty minutes after the engine was started. The effect of the soot then remained constant for the following ten hours of testing.

Testing was commenced by turning on all instruments in order to give the electronic components time to reach their normal operating temperatures. The test fuel was then prepared. Any fuels which required blending were blended immediately before testing. This was done to ensure that water contamination could not take place and that the blend was stable at the time of testing. The engine fuel system was thoroughly flushed with the test fuel before being bled. The heat flux probe was fitted to the engine and the engine was started and run at approximately 1800 r/min and 150 Nm for at least 30 minutes. This served to warm the engine and deposit an

equilibrium layer of soot on the heat flux probe.

After the warm up period all electronic components and transducers would have reached temperatures which approached normal operating temperatures. All channels were then calibrated. The data acquisition program was run. Appropriate setup data were loaded and edited to suit the requirements of the particular test. Where known conditions could not be applied to any particular channel, a constant voltage source was used to simulate transducer output. Considerable effort was made to minimize errors at all times. Any errors in the steady state data which exceeded 1% of the measurement range were considered unacceptable, while an attempt was made to achieve higher levels of consistency.

The engine speed input was calibrated by holding the speed at a known value. The auto calibration routine of the data acquisition system was used to record the channel voltage and the actual speed was entered through the keyboard. Engine speed was then changed to a second known value at the other extreme of the speed range. The channel voltage was again recorded and the actual speed was entered. Channel offset and gain were calculated and the setup data were amended automatically. The auto calibration routine then checked the two input voltages to ensure that they were adequately far apart when compared to the channel voltage range. If the difference between these voltages was too small then the calibration was rejected in order to avoid measurement errors. The fact that the speed signal was based on digital counters resulted in a relatively stable signal. The signal varied by less than 0,5% of full range throughout the project. This was confirmed by a digital pulse counter.

The torque measurement device was calibrated by applying two known torque loads. This was done with the aid of a calibrated weight hanging at the end of an arm of known length. The second point

used was zero torque load. As is the case with most balance type torque measurement devices, problems were encountered as a result of bearing friction. This resulted in hysteresis of the measured torque output. When a load was applied the output did not reach the correct value immediately. Although the correct value was rapidly approached initially, the signal then required as long as 60 seconds to reach the correct value. As a result of temperature changes during the test the zero point tended to drift slightly. Errors were, however, never allowed to exceed 1% of full range.

The fuel flow measurement device was calibrated with the aid of a mass balance. Repeated measurements of the mass of fuel contained in the measuring flask varied by less than 0,1 %. Measurements of a constant fuel flow, taken by the system, were found to vary by less than 0,2% (Taylor, 1987). The device, being based on a fixed volume, was sensitive to variations in fuel density caused by temperature changes. Fuel temperature was measured and found to vary by an insignificant amount during testing. Being a batch device, the fuel flow meter was not suited to being connected to the data acquisition system. These results were thus recorded manually.

The exhaust, water and oil channels were calibrated by alternating the input leads between two probes which were measuring different temperatures. The actual temperature values were read from the commercial panel meters which were used to process the signals. These meters were calibrated from time to time with the aid of an ice bath and boiling water. Although it is generally accepted that K type thermocouples have a maximum accuracy of 2°C, it was found that the consistency of the temperature measurements was within 1°C. When surface temperature was being recorded two of the panel meters were used to record average surface temperature and temperature within the heat flux probe.

The fact that the probe junctions were grounded resulted in interference of signals when the panel meters were connected to the data acquisition system. These two signals were thus recorded manually when surface temperature was being recorded. Fuel flow and water and oil temperature were not recorded at this stage while speed, torque and exhaust temperature were recorded by the data acquisition system.

After the steady state channels had been calibrated in preparation to measure surface temperature, the gain of the surface temperature channel was calibrated. The surface temperature channel was entered in the setup data as if it were a steady state channel. The precision voltage source was used to simulate a thermocouple signal and the auto calibration routine was used to calculate the channel gain. The differential amplifier was used to amplify the cyclic channel range to a maximum. This involved eliminating the channel offset voltage. Average surface temperature was also recorded as a steady state voltage by one of the panel meters. This information was later used to regenerate the true channel offset. The surface temperature channel was then removed from the steady state channel list and the calculated gain was entered as the high speed channel gain. Due to the fact that the surface temperature signal was not linear, the signal was recorded in μV units to allow the calculation of temperature at a later stage.

By recording surface temperature as the only high speed channel, the number of successive cycles which could be recorded and averaged was maximized. Unfortunately, in order to calculate surface heat transfer rates the entire engine cycle must be digitised. The number of engine cycles which could be averaged was thus reduced. The exact crank angle resolution required to represent transient surface temperature correctly was unknown. For this reason and in order to maintain data compatibility during data processing, the decision was made to use the same resolution as

that used to record cylinder pressure. Data were thus recorded at each ½° of engine rotation. The result was that 91 successive cycles could be recorded and averaged. This number far exceeded the number recorded by other researchers who conducted similar tests with success (Sihling and Woschni, 1977; Lawton, 1987 and Morel, Wahiduzzaman, Tree and DeWitt, 1987).

The setup data were then saved on file and the initial phase of testing was commenced. Data were recorded at a total of thirteen data points. Twelve of these data points were concentrated at two engine speeds, namely 1700 r/min and 2000 r/min. Six readings were taken at evenly distributed loads across the torque range, at each of the two speeds. The thirteenth point was recorded at zero load and 1000 r/min. The monitoring routine was used to keep track of the engine state. When the required point was reached, data were acquired by the recording routine and inspected with the aid of the data processing routines. These data were then stored on disk under a file name which was compiled from the test heading, the phase number and the number of the test point. When data had been recorded at all the required data points the engine was shut down and the heat flux probe was removed and inspected.

The pressure transducer was then fitted to the engine and the entire calibration procedure was repeated. Speed, torque, fuel flow and exhaust, water and oil temperatures were recorded during this phase of the test. Injector needle lift and cylinder head displacement were recorded along with cylinder pressure. The gain of the needle lift channel was not required since the signal was only used to determine the start and end of injection. The channel was thus never calibrated. The cylinder head displacement channel was calibrated in the same manner as the surface temperature channel. Despite the high levels of amplification, the calculated gain of both the surface temperature and cylinder head displacement channels varied by less than 0,6% throughout the project.

The engine was started and the test was repeated with data being recorded at the thirteen test points used previously. Although the engine speed could be controlled to within 1%, some difficulty was experienced with achieving exactly the same torque levels as those used to record surface temperature. It was thus decided that when comparisons were to be made between data recorded in the two phases, regressions would first be carried out on the data. The interpolation of values at any required point was thus possible. This would also be useful when comparing different fuels.

Basing comparisons on regression results had the added advantage of reducing the effects of data acquisition errors. This was because, the regression, being based on all the relevant data points, would average any extreme values. Regression values were, in effect, based on multiple observations, which are known to improve accuracy. Not recording data from the two phases at the same load did, however, present problems for some aspects of the data processing. An effort was thus made to record data at the same load points where possible. All recorded data were inspected at the end of a test to ensure that errors had not occurred. Input channels were then checked for excessive drift and electronics malfunctions. This was, however, unlikely since all channels were monitored at all times.

Accurately and consistently recorded data did not, however, guarantee accurate results. Extended data processing was required to achieve the objectives of the project. The role played by the data processing in the accuracy of the final results was possibly as great as that of the instrumentation and data acquisition. Much attention was thus given to the development of reliable and accurate computational techniques in addition to the extreme care taken in applying measurement techniques.

6. EXPERIMENTAL TECHNIQUES

Neither combustion rate nor engine stress can be determined directly from measured data. This information must be calculated with the aid of complex models of the relevant processes. For example, in order to calculate thermal stress, the temperature distribution in the component must be calculated and then used to calculate the stress distribution. Not only are these complex calculations, but the determination of the required boundary conditions is a difficult process.

Errors are easily introduced by unreliable computational models. It is thus possible that the accuracy of the final results is affected by the calculations to a greater extent than by the accuracy of the instrumentation. The experimental techniques and data processing should therefore receive as much attention as the development of the instrumentation. The differences between the commercial fuels are relatively small. If these differences are to be detected, both the instrumentation and the data processing procedure need to be extremely sensitive and consistent.

In the event of differences being detected, a conclusion must be reached as to what proportion of the difference can be attributed to measurement and calculation errors. If differences fall within the margins of accuracy of the calculations then it is difficult to reach significant conclusions. This requires a thorough statistical analysis of the results obtained from all the instruments and calculations. Confidence intervals of the accuracy and consistency of the different results should thus be established. Definite conclusions can thus be drawn on the effects of combustion on engine life.

6.1 Heat Release Analysis

In an engine there are numerous dynamic processes which occur simultaneously. It is the combined effect of these processes that determines the performance and durability of the engine. The relevant processes are as follows;

(i) air induction,
(ii) piston movement and volume change,
(iii) heat transfer,
(iv) gas leakage,
(v) change in the gas properties,
(vi) fuel injection,
(vii) combustion, and
(viii) scavenging.

The interaction of these processes determines the cylinder pressure development.

Heat release analysis normally involves the calculation of the rate of combustion by measuring pressure and calculating the contribution of the other processes. Simplified models are used to establish the contribution of the different processes. The models used differ in complexity and accuracy, with the simplest models disregarding the contribution of some processes. Combustion rate is calculated by solving thermodynamic equations which describe the interaction of the different processes in the engine.

The accuracy of the heat release analysis is determined by the accuracy of the different models and the measured pressure data. It is thus important to establish the relative importance of the different processes and model each process with appropriate care. This is usually done by comparing the amount of energy involved in each process with the fuel energy consumed by the engine. Greater accuracy is required for the calculation of processes which involve

large amounts of energy. The sensitivity of the results to errors in the different variables can be determined by introducing small changes into the inputs of the various sub-models deliberately. The resulting change in the calculated results indicates the sensitivity of the model to the variable which was changed. Processes such as gas leakage during combustion, which involve a small portion of the energy released, are often disregarded.

The heat release model used in the project was a zero-dimensional model which was originally developed at the University of Illinois, Urbana, Illinois, USA. Being zero-dimensional the model took no account of combustion chamber shape and assumed that all variables could be represented by a single value at any instant. The use of the model involved the following basic assumptions ;

(i) thermodynamic equilibrium existed in the combustion chamber at each instant,

(ii) fuel was completely converted to combustion products,

(iii) burning took place incrementaly as a homogeneous combustion, and

(iv) cylinder content was a homogeneous mixture of air and combustion products (Faletti, Sorenson and Goering, 1982).

The model was based on the first law of thermodynamics, the ideal gas laws and the equation describing piston movement (Faletti, 1981). From the first law of thermodynamics the following equation can be derived :

$$dU = \delta Q - \delta W - \Sigma h_i \cdot dm_i \qquad (1)$$

The change in internal energy of the cylinder contents is represented by dU. δQ is the heat transferred to the system and δW is the work transfer from the system. The summation term covers the energy involved in mass exchange across the system boundary. Mass exchange implies injected fuel and gas leakage. By separating

the heat transfer term, δQ, into heat released, δQ_{ch}, and heat lost to the cylinder walls, δQ_{ht}, the following equation can be obtained:

$$\delta Q_{ch} = dU_s + \delta W + \Sigma h_i \cdot dm_i + \delta Q_{ht} \qquad (2)$$

The change in sensible internal energy, dU_s, was calculated by assuming that it was a function of temperature. δW is the work done on the piston and is equal to $P \cdot dV$, where P is pressure and V is volume. δQ_{ht} is normally calculated with the aid of heat transfer theory by estimating cylinder wall temperature and transfer coefficients. Heat transfer coefficients are normally estimated by applying empirical models. One of the most popular models was developed by Woschni (1967).

Mass transfer accounts for a small proportion of the total energy involved in combustion, but its inclusion greatly complicates the analysis. Mass transfer is thus usually disregarded (Gatowski, Balles, Chun, Nelson, Ekchian, and Heywood, 1984). The result is that the rate of heat release, δQ_{ch}, is expressed in terms of variables that are either calculated or measured. Using a similar method, Krieger and Borman (1966) derived the following expression:

$$\frac{1}{M}\frac{dM}{dt} = \frac{\frac{RT}{v}\frac{dv}{dt} - \frac{\partial u}{\partial p}\frac{dp}{dt} + \frac{1}{M}\frac{dQ}{dt} - C[B]}{u - h_f + D\frac{\partial u}{\partial F} - C\left[1 + \frac{D}{R}\frac{\partial R}{\partial F}\right]} \qquad (3)$$

where

$$B = \frac{1}{p}\frac{dp}{dt} - \frac{1}{R}\frac{\partial R}{\partial p}\frac{dp}{dt} + \frac{1}{v}\frac{dv}{dt} \quad ; \quad C = T\frac{\partial u}{\partial T} \Big/ \left[1 + \frac{T}{R}\frac{\partial R}{\partial T}\right];$$

$$D = \frac{(1 + f_o)M}{f_s M_o} \quad ;$$

M = mass, kg; R = gas constant, kJ/kg.K; T = temperature, K; F = fuel air ratio; t = time, s; v = volume, m^3; u = internal energy, kJ/kg; p = pressure, kPa; dQ/dt = heat transfer, kJ/s; h_f = heat of formation of the fuel, kJ/kg; f_s = stoichiometric fuel air ratio.

This equation can be integrated numerically using an iterative process resulting in the mass rate of combustion at each crank angle (Faletti et al., 1982). The rate of energy release is equal to the product of the mass rate of combustion and the calorific value of the fuel.

It is well known that simplified models of processes are responsible for the introduction of most errors in heat release analysis. In order to minimize the need for modelling, as many of the relevant variables as possible were recorded. Few models are capable of accounting for the effect of chemical and physical differences between fuels. Thus the effect of these differences would be reflected best by recorded data. The following variables were recorded for use in the calculation of heat release rate ;

(i) cylinder pressure,
(ii) combustion chamber wall temperature for the calculation of heat transfer rate,
(iii) intake air temperature,
(iv) gas leakage past the piston rings and valves,
(v) fuel consumption rate, and
(vi) air flow rate through the engine.

Cylinder pressure is the most important input into the heat release model. The accuracy of the pressure data is largely dependent on knowledge of the signal range and offset. Signal range can be determined by calibrating the pressure transducer with the aid of a dead weight tester. A calibration showed that the transducer gain deviated from the value specified by the manufacturer by less

than 0,8%. The gain specified by the manufacturer is the same for all the Kistler 6121 pressure transducers. This implied that the specified value was not actually measured for the particular transducer used. The transducer had thus not deteriorated significantly from manufacture. The transducer had been used for an extended period of time before the testing for the project commenced. The period over which testing took place was relatively short when compared to the total number of hours that the transducer had worked. The measured gain was thus used in the calculation of pressure instead of the value specified by the manufacturer.

Piezo-electric pressure transducers do not have a stable offset and thus cannot provide absolute pressure values. The researcher is forced to shift the pressure curve to a point which is considered to represent the actual absolute pressure. The method most commonly used by researchers to set the pressure offset is to equate the cylinder pressure during the valve overlap with some value related to atmospheric pressure. A unique method based on measured data was developed during the project.

The mass of air in the combustion chamber per stroke was calculated from the measured air flow rate. Intake air temperature measured at the inlet valve was used as an estimate of air temperature in the combustion chamber at the end of the intake stroke. This value was known to underestimate the actual value, but the magnitude of the error was relatively small. Regardless of the magnitude of the error, it would be consistent for all the fuels tested and would thus have no detrimental effect on the relative comparisons. The temperature T, mass M and volume V of the air in the cylinder, could thus be estimated at the moment when the inlet valve closed. By assuming that during the intake stroke, air obeyed the ideal gas laws, the following equation was derived:

$$P = \frac{M \cdot R \cdot T}{V} \qquad (4)$$

By assuming a value for the gas constant R, and taking a few simple measurements, it was thus possible to calculate the pressure P at the beginning of the compression stroke. This was a significant improvement on other methods which rely on assumptions.

The signals from piezo-electric pressure transducers can be affected by the thermal shock which occurs during combustion (Kach and Adamczyk, 1985 and Taylor, 1987). The Kistler 6121 pressure transducer used in the project was fitted with a heat shield which was designed to eliminate the problem. The pressure transducer was also sensitive to build-up of carbon on the diaphragm and required careful cleaning. It was thus necessary to check all pressure data for measurement errors.

A number of methods for checking the pressure data were used. By integrating pressure with volume, the work involved in the compression and expansion strokes can be calculated. The difference between the work of compression and the work of expansion can be used to calculate the indicated mean effective pressure. The difference between this value and the break mean effective pressure is an indication of engine friction and is referred to as friction mean effective pressure. Engine friction is the result of the combined effect of the following factors ;

(i) friction of bearings and pistons,
(ii) the work of pumping air through the engine,
(iii) the work of pumping lubricating oil,
(iv) the work involved in fuel injection,
(v) cooling fan and water pump load, and
(vi) alternator load.

Due to the fact that all these losses escalate with increasing speed, engine friction tends to rise significantly with speed. If the speed is held constant and the load is varied, some of the factors contributing to friction will increase while others

decrease. Increased load leads to higher temperatures. Increased oil temperature could reduce bearing friction and the work of pumping oil. The pistons reach optimum shape at higher loads which could reduce piston friction. Air flow through the engine decreases with load, thus reducing the pumping work while the work involved in fuel injection increases. Whether the total engine friction increases or decreases with increasing load is uncertain. The total engine friction would, however, vary by a relatively small amount at constant engine speed.

By analysing the FMEP calculated from cylinder pressure recorded at varying load and constant speed, it is possible to get an indication of the accuracy of the pressure data. Calculated FMEP should not change significantly with load at constant speed (Hardenberg, 1986 and Taylor, 1987). A second method of investigating the accuracy of the pressure data is by plotting the logarithm of pressure versus the logarithm of volume. The relationship between pressure P and volume V at any instant in the combustion chamber during compression and expansion is described by the following expression:

$$P \cdot V^{\alpha} = \text{constant} \qquad (5)$$

By taking the logarithm of this function, the following equation can be derived:

$$\log(P) = - \alpha \cdot \log(V) + \text{constant} \qquad (6)$$

It is thus evident that the gradient of the plot of the logarithms of pressure and volume represent the polytropic constant α at that instant. The polytropic constant for adiabatic compression is equal to 1,395. If the gas is being heated then the coefficient exceeds the value of 1,395 and vice versa. It is known that in an engine, during initial compression, the gas is heated by the cylinder walls while late in compression the walls are heated by the gas. At some point during the compression stroke adiabatic

conditions will exist. The value of the polytropic constant should thus be greater than 1,395 early in the compression stroke and less than 1,395 towards the end of the compression stroke. This implies that the compression curve should form a concave line on the logarithmic plot. By calculating the polytropic constant from measured data and plotting it against crank angle, the accuracy of the recorded data can be investigated further. Of particular interest is the crank angle at which adiabatic compression occurs.

Possibly the second most important aspect to consider for heat release analysis is the phasing of cylinder volume with recorded pressure data. This is determined by the accuracy of calibration of the crankshaft encoder. Any error in the phasing between measured pressure and calculated volume results in significant errors in calculated heat release, FMEP and polytropic constant. Reliable techniques for calibrating the shaft encoder are thus necessary.

Although both the calculation of heat release and FMEP are sensitive to the phasing of pressure data with crank angle, they are not easily used for calibration as it is difficult to establish the correct value for these variables. By assuming that adiabatic compression occurs at a particular crank angle, it is possible to vary the phasing of data until the calculated polytropic constant equals 1,395 at the required point. The actual point at which adiabatic compression occurs cannot be defined conclusively.

Increased compression ratio results in an increase in the rate at which air temperature rises during the compression stroke. If cylinder wall temperature does not change significantly then increased compression ratio will lead to adiabatic compression earlier in the compression stroke. Any changes in cylinder materials or cooling lead to changes in the cylinder wall temperature. Increased wall temperature results in the point of

adiabatic compression being retarded. It is thus unlikely that the exact point at which adiabatic compression occurs can be calculated accurately. This point is not a constant, but is in fact dependent on factors such as engine design and running conditions.

The most practical method of calibrating the crankshaft encoder is to analyze the logarithmic plot of motoring pressure versus volume. This is illustrated in figure 10. The compression curve should yield a slightly concave line and the expansion line should return initially along the identical path. The relative position of the compression and expansion lines near peak pressure reflects on the change in the internal energy of the air in the combustion chamber. If the two lines form a loop, it implies that the work done on the piston is positive for that portion of the cycle which is incorrect.

In the region of TDC the internal energy of the air in the combustion chamber decreases at a rate equal to the rate of heat transfer to the cylinder walls. This is because the rate of change of volume approaches zero at this stage. The decrease in internal energy immediately before peak pressure can be expected to be similar to the decrease during the equivalent instant immediately after peak pressure. The polytropic constant, which is related to the change in internal energy, is thus unlikely to differ significantly for these two instants. The gradient of the compression and expansion lines in the logarithm plot should thus be identical before and after peak pressure. If these lines form an acute angle it implies that there has been an inflection in the rate of heat transfer which is incorrect.

By ensuring that the compression and expansion lines had the same gradient at the point of peak pressure, it was possible to calibrate the phasing of cylinder pressure data to an accuracy well

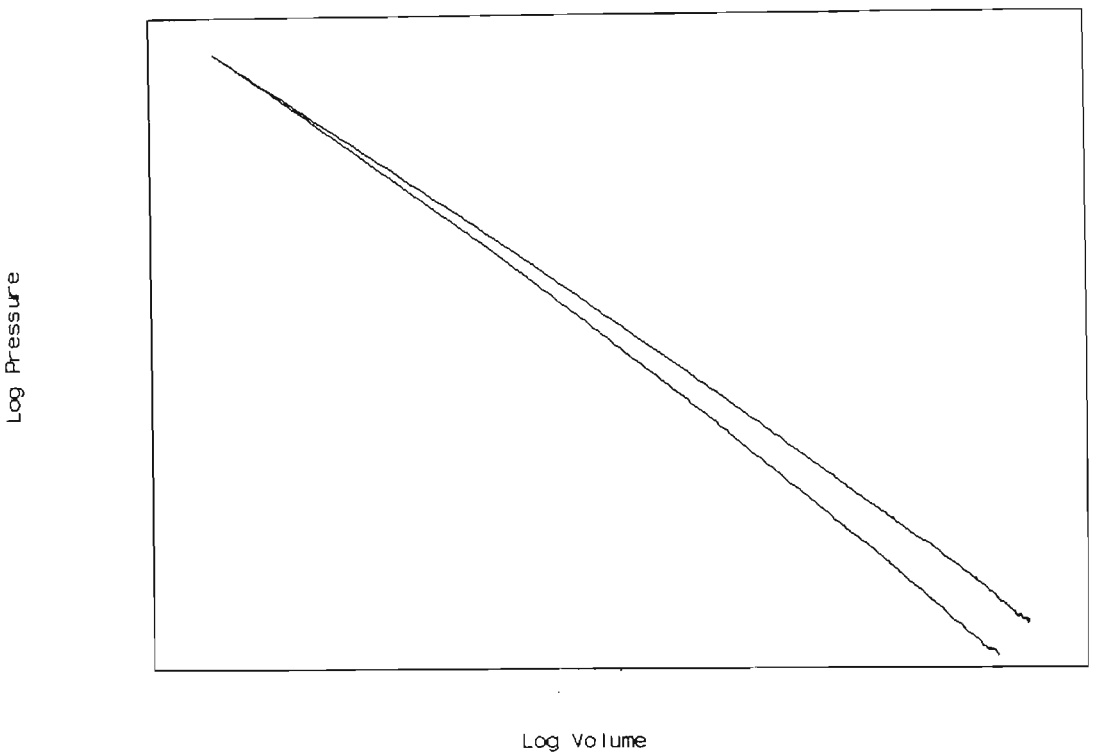

Figure 10. Logarithm of motoring pressure versus the logarithm of volume.

within the resolution of measurement. Callahan, Yost and Ryan (1985) stated that the line for expansion should initially return along the same path as that of the compression line in the logarithm plot of motoring pressure versus volume. This implies that there is negligible heat transfer in the region of TDC. The rate of heat transfer is in fact at a maximum in the region of TDC. The compression and expansion lines should thus be slightly separated in the region of TDC and diverge gradually with increasing volume.

The point at which peak motoring pressure occurs normally precedes TDC by between 0,8 and 1,0°C.A. (Amann, 1985). This is as a result

of heat transfer from the air to the combustion chamber walls. This information is, however, difficult to use for purposes of determining the true phasing between pressure and volume.

The rapid pressure rise associated with ignition is responsible for creating resonance in the combustion chamber (Timoney, 1987a). High rates of pressure rise also lead to increased gas velocities past the heat shield of the pressure transducer which could cause pressure fluctuations. The result is, that shortly after ignition high frequency pressure fluctuations are often superimposed on the pressure signal. By studying equation 3 it can be seen that the rate of heat release is highly dependent on the rate of pressure rise. Hence, any fluctuations in measured pressure are magnified in the calculated heat release rate.

The problem can be overcome by data smoothing. Smoothing, however, has the effect of reducing inflections in the data. This has a significant effect on the calculated rate of heat release during premixed combustion. In order to smooth the data and avoid distorting the results adversely, a system was used where smoothing was only commenced from a point 2°C.A. after the peak rate of pressure rise. A weighted five point moving average method was used. Due to the fact that these fluctuation were the result of high rates of pressure rise, smoothing was not required before the peak rate of pressure rise had been reached. The method was found to reduce fluctuations in the calculated heat release rate adequately without distorting the results significantly (Taylor, 1987).

It can be seen in equation 3 that volume and the rate of change of volume play a large role in the calculation of the rate of heat release. A high level of accuracy was therefore required for the calculation of cylinder volume. Volume was calculated from data which described the engine geometry. For the calculation the

following information was used;

(i) compression ratio,

(ii) cylinder bore,

(iii) piston stroke, and

(iv) connecting rod length.

All the information except compression ratio was described with adequate accuracy by the engine manufacturer specifications.

Compression ratio should be calculated with extreme care. To calculate compression ratio it is necessary to measure the clearance volume of the cylinder used for testing. The clearance volume of the ADE 4.236 engine comprises the piston bowl, the valve recesses, the space between the piston and the cylinder head and the annular gap between the piston and the cylinder liner above the piston rings. The volumes of the piston bowl and valve recesses were measured by covering them with a perspex sheet and filling the cavity which was formed with liquid. A thin film of grease was used as seal between the perspex and the metal. The liquid was poured in through a small hole in the perspex sheet. The effect of the perspex was to reduce the role played by the liquid meniscus. The volume between the piston and the liner was determined by measuring the difference between the diameter of the piston and the cylinder liner.

The size of the gap between the piston and the cylinder head was initially thought to be equal to the thickness of a used gasket. When a number of used gaskets were measured, it was found that their thickness was 1,58 mm. This figure yielded a compression ratio of 15,23:1. Inaccurate results which appeared to originate from this value and the fact that the manufacturer specifies a value of 16:1, indicated that the calculated ratio was incorrect. An attempt was thus made to measure the actual gap between the piston and the cylinder head. This was achieved by placing a length of 1,5 mm soldering wire between the piston and cylinder

head. The wire was inserted through the injector hole. The engine was then rotated over TDC so that the wire was squashed between the piston and the cylinder head. The soldering wire being inelastic maintained its distorted form. The thickness of the flattened section of the wire was then measured. This process indicated that the gap between the piston and cylinder head is 0,97 mm when the engine is cold.

With the aid of finite element analysis it is possible to calculate the thermal distortion of the piston. The average distortion of the piston crown relative to the gudgeon pin was calculated to be 0,17 mm. By assuming that the expansion of the engine block is similar to that of the crankshaft and connecting rod, it was concluded that the average gap between the piston and cylinder head is 0,8 mm. The compression ratio calculation was repeated and yielded a value of 16,41:1.

Heat transfer between the cylinder walls and the gases in the combustion chamber was calculated from measured surface temperature. The time history of surface temperature at the pressure transducer location was used to calculate the heat transfer rate at the point. In order to carry out a reliable finite element analysis, the spatial distribution of surface temperature was determined. The spatial distribution which was used in the finite element analysis was also used to calculate the net rate of heat transfer out of the combustion chamber.

There are a number of advantages in using measured heat transfer data. Firstly, the surface heat flux probe is capable of detecting differences in heat transfer resulting from different fuel properties. This cannot be expected from the commonly used heat transfer models such as the one developed by Woschni (1967), which rely mainly on pressure data. Secondly, regardless of the fuel used, all the heat transfer models have shortcomings. The results

of Taylor (1987) and Timoney (1987a) proved that most of the error in the heat release calculations results from the inability of the Woschni (1967) equation to calculate the contribution of radiative heat transfer.

An additional advantage of using the measured data to calculate heat transfer rate was that the heat release results provided feedback on the accuracy of the measured heat transfer data. Heat transfer normally involves less than 20% of the energy released during combustion. It is thus evident that any error in the calculated heat transfer rate is reduced to one fifth in the heat release results. Thorough investigations into the consistency of heat transfer rate calculated from measured data showed that a high level of repeatability was achieved.

The mass of the gasses in the combustion chamber appears repeatedly in equation 3. It is thus clear that the accuracy of the heat release analysis is highly dependent on the accuracy with which the mass is calculated. The mass of air in the combustion chamber at the beginning of the compression stroke is determined by the induction processes. Pressure losses in the air intake system and heating result in the density of the induced air being lower than that of the ambient air.

By measuring the airflow through the engine and assuming that it was evenly distributed between the cylinders, it was possible to calculate the mass of air in the combustion chamber. The accuracy of the calculated mass is equivalent to the accuracy with which the airflow can be measured. Although extreme care was taken to ensure that the airflow was measured accurately, any errors would be the same for all the fuels tested. The relative comparisons would thus not have been affected by any errors in the calculated air mass.

The validity of the assumption that gas leakage plays an insignificant role during combustion was tested by measuring the total gas leakage past the piston rings. Measurements indicated that the maximum gas leakage at any load was 1200 liters per hour. This represented less than 2% of air induced into the engine. A small proportion of the measured leakage actually occurs during combustion since combustion occupies less than one tenth of the working cycle. The assumption that gas leakage is negligible, is therefore correct.

In an effort to take the role of injected fuel into account, the combustion chamber mass contents were continually updated. Instead of increasing the mass at a rate equal to injection rate it was increased at a rate equal to combustion rate. In this manner the only fuel in the combustion chamber that was not accounted for was the injected fuel that was undergoing preparation. The injection duration is normally more than four times the ignition delay. The fuel unaccounted for at any instant, would thus not exceed one quarter of the total fuel charge.

To calculate the thermodynamic properties of the entire combustion chamber, it is necessary to know the amounts and properties of the different gasses present. During the compression stroke the combustion chamber contains air and residual gasses from the previous stroke. The amount of residual gas in the chamber is not easily measured and thus needs to be estimated. The clearance volume represents 6,1% of the maximum cylinder volume. If the assumption is made that the scavenging process during valve overlap succeeds in displacing approximately 18% of the burnt gasses in the clearance volume, then it can be deduced that the residual gas fraction is 5%. Taylor (1987) used a value of 3,5%. The reason for the lower value is that the compression ratio of the engine used was higher and the clearance volume thus represented a smaller fraction of maximum cylinder volume.

The equilibrium composition of the combustion chamber contents is calculated using a procedure developed by Strehlow (1982). The procedure uses the Weinberg technique and allows dissociation of the combustion products to be accounted for. A procedure developed by Savage (1982) then uses the equilibrium composition, pressure and temperature to calculate the thermodynamic properties of the mixture (Faletti et al., 1982). The Krieger-Borman equation requires the input of the energy of formation of the fuel. The energy of formation of the fuel and some of the thermodynamic properties were calculated on the basis of the carbon-hydrogen-oxygen ratio of the fuel.

The determination of the ratio required chemical analysis of the fuel. The results were, however, relatively insensitive to large errors in the carbon-hydrogen-oxygen ratio. Increasing the hydrogen proportion by 22% had no effect on calculated peak rate of heat release. The calculated cumulative heat release increased by 1,3%. Increasing the oxygen proportion from zero, to two sixteenths of the carbon proportion, reduced the calculated peak rate by 0,82%. The calculated cumulative heat release decreased by 1,5%. Chemical analyses of most of the fuels tested had been carried out by Taylor (1987). The ratios of blends not analysed were calculated from the proportions and from the chemical formulae of the fuels used in the blending process.

Knowledge of the sensitivity of the heat release results to errors in the various inputs is useful in the determination of the confidence interval of the final results. A thorough investigation into the sensitivity of the heat release model to input errors was carried out by Taylor (1987). The fact that heat release analysis relies on numerous assumptions, models and measurements, can result in the accumulation of large errors. It is thus important to have methods by means of which the accuracy of the final results can be

monitored on a continual basis.

Calculated heat release rate before and after combustion should be zero. This can be used to get an idea of the accuracy of the entire calculation. If the rate of heat release is calculated from motoring pressure data, some idea of the accuracy of the model can be gained. Any deviation from zero is incorrect and the magnitude of the deviation is an indication of the calculation error. The deviation from zero of calculated rate of heat release for motoring conditions, as a percentage of full scale is shown in figure 11. It can be seen that the maximum deviation from zero was less than 1% of the normal full scale value. This is, however, not fully representative of the actual running conditions.

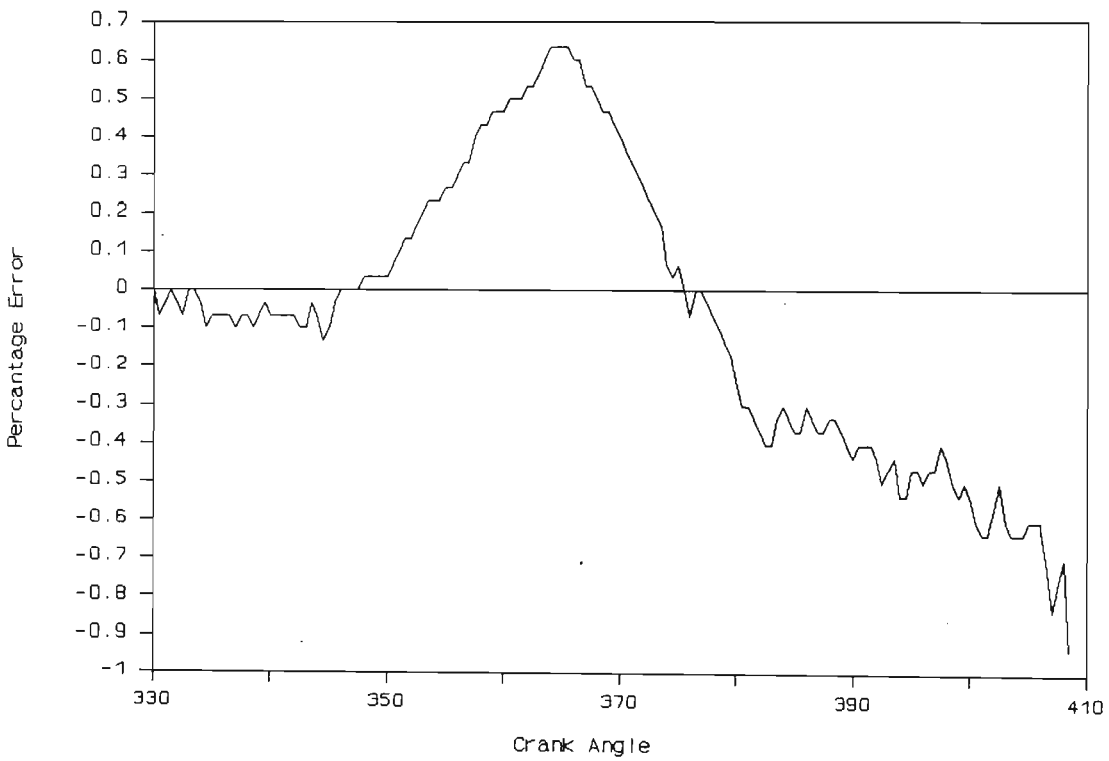

Figure 11. Deviation of heat release rate from zero as a function of crank angle, calculated from motoring pressure data.

By integrating heat release rate over the full duration of combustion, it is possible to calculate the net energy released. By comparing this amount with the energy injected in the form of fuel an energy balance can be conducted. Most of the injected fuel energy should be accounted for by the heat release model. Energy involved in incomplete combustion of the fuel would, however, be undetected by the model. The latent heat of evaporation of water in the combustion products would also be undetected by the model. The reason for this is that this energy is never released as sensible heat and does not contribute to pressure development. The lower calorific value of the fuel should thus be used for the comparison.

At high equivalence ratios where smoke formation and incomplete combustion can occur, it is reasonable to expect the model to underestimate the fuel consumption. The ratio of calculated to measured fuel consumption is best expressed on a percentage basis. The ratio is of particular interest because it indicates the cumulative error of the entire heat release analysis. Timoney (1987a) referred to the ratio as the implied combustion efficiency.

The heat release model which was finally used achieved an extremely high level of accuracy when compared to the results of Taylor (1987) and Timoney (1987a). For all data except those recorded at zero load and maximum fueling, the model accounted for between 90 and 105% of the fuel consumed. The vast majority of these results lay between 95 and 100%. This was despite the fact that the emphasis was placed on achieving high consistency for the purpose of relative comparisons. This was the result of the attention which was focused on improvements in the measurement and calculation of the information used in the analysis. Possibly the most important improvement was the use of heat transfer data which

were based on measured information. These data accounted for both convective and radiative heat transfer adequately. A typical heat release curve is illustrated in figure 12. It is interesting to note that the latent heat of evaporation of the fuel prior to ignition, was detected. The calculated combustion rate before and after combustion also tended to approach zero.

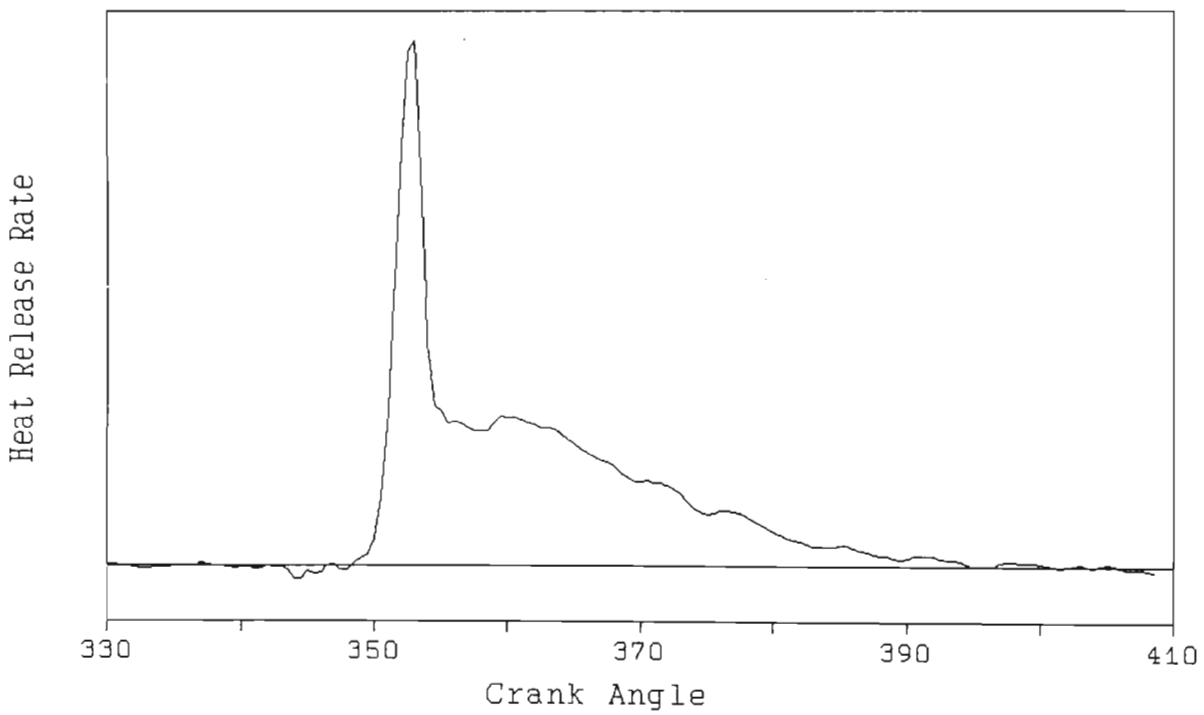

Figure 12. An example of a typical heat release curve.

6.2 Heat Transfer

Both the calculation of combustion rate and engine stress required reliable information describing the rate of heat transfer in the combustion chamber. For heat release analysis the net rate of heat transfer out of the combustion chamber as a function of time, was required. Stresses in the engine were calculated with the aid of finite element analysis. In order to perform finite element

analysis, heat transfer coefficients were required as a function of time and location. The analysis also required the knowledge of gas temperatures. In addition to instantaneous heat transfer coefficient and gas temperature, the average heat transfer coefficient and gas temperature were also required.

Gas temperatures and heat transfer rates and coefficients were calculated from a number of different measurements. Transient surface temperature recorded by the surface thermocouple was used to calculate transient surface heat transfer rate at the probe. Average heat transfer rate was indicated by the difference between the temperatures of the two junctions in the heat flux probe. The integral of the transient heat transfer rate was also used to determine average rate of heat transfer. Cylinder pressure in conjunction with recorded inlet and exhaust temperature were used to calculate transient and average gas temperature.

If the assumption is made that the heat transfer in the combustion chamber wall is single dimensional then the relationship between temperature T, time t and distance from the surface x, is described by the Fourier equation:

$$\frac{\delta T}{\delta t} = \alpha \cdot \frac{\delta^2 T}{\delta x^2} \qquad (7)$$

The constant α represents the thermal diffusivity of the wall material. By solving the equation it is possible to derive an expression describing temperature as a function of time and distance from the wall.

Measured combustion chamber wall temperature was represented by values recorded at discrete time intervals. Information in this form is not easily applied in mathematical equations. A means of expressing these recorded data as a function of time was required. This was achieved by performing a Fourier analysis on the recorded

surface temperature data. Surface temperature was then expressed as a Fourier sine expansion of the form :

$$T_{w(x=0)} = T_{wm} + \sum_{i=1}^{\infty} [\, A_i.\cos(i\phi t) + B_i.\sin(i\phi t)\,] \qquad (8)$$

Where $T_{w(x=0)}$ is the transient wall temperature at the surface,
T_{wm} is the average surface temperature,
ϕ is the angular frequency of the engine cycle and
A and B are the Fourier coefficients.

By solving the Fourier equation and expressing the result in the form of a Fourier sine expansion, it is possible to derive an equation for temperature as a function of time, location and the Fourier coefficients. This equation can then be differentiated with respect to x for the conditions at the surface to yield an equation for temperature gradient at the material surface (Sihling and Woschni, 1977). The rate of heat transfer across the material surface is equal to the product of the temperature gradient and the thermal conductivity of the material. The following equation for the rate of heat transfer at the surface can then be derived:

$$\dot{q}_{(x=o)} = - \dot{q}_m - K_w \cdot \sum_{i=1}^{\infty} \left[\frac{i\phi}{2\alpha}\right]^{\frac{1}{2}} . [(B_i - A_i)\sin(i\phi t) + (B_i + A_i)\cos(i\phi t)] \qquad (9)$$

where $\dot{q}_m$ is the average rate of heat transfer and K_w is the thermal conductivity of the cylinder wall material.

By substituting the Fourier coefficients, determined from the Fourier analysis of each set of recorded data, into this equation, it was possible to calculate the transient surface heat transfer rate. When performing the Fourier analysis of recorded data a number of alternatives arose. Firstly, the time required to perform the analysis was highly dependent on the order of the analysis selected. While increasing the order tended to improve

the accuracy, it also took longer to reach completion. Secondly, higher resolution of the recorded data was also responsible for extending the time taken to complete the analysis. It was thus necessary to determine what resolution and order were required to achieve an expression which represented the recorded data adequately.

Due to the fact that the rate of heat transfer is highly dependent on the rate of temperature change, any noise in recorded surface temperature was magnified in the calculated heat transfer rate. The fact that surface temperature was recorded at high gain and that the conductors were unscreened over a considerable length, resulted in high frequency noise in the recorded signals. Despite the fact that much of the noise was eliminated by the averaging process, it became clear that data smoothing was required. A study was carried out into the simultaneous effects of smoothing, changing the data resolution and changing the order of the Fourier analysis.

An attempt was made to reach a situation where smooth results could be achieved rapidly without compromising accuracy. It was found that by reducing the resolution to two crank-shaft degrees, the time required to conduct the analysis was greatly reduced. In order to avoid discarding valuable recorded data and to achieve smoothing, a method was required which would take all data into account. This was achieved by performing a weighted five point moving average on the half degree data at each two degree interval. A Fourier analysis was then conducted on the smoothed two degree data. This resulted in a situation where the speed of analysis was greatly increased, where data were smoothed and where all recorded data had contributed to the data which were analysed.

A 200th order Fourier analysis was conducted with unsmoothed data at half degree resolution and then repeated with an order of 100

on the smoothed two degree data. It was found that the peak rates of heat transfer differed by 0,4% while the integral of the heat transfer curves differed by 0,7%. The smoothed data yielded a far smoother curve while the analysis was eight times as fast. It was concluded that the impact of the smoothing and reduction of resolution on the calculated rate of heat transfer was negligible. It was also found that increasing the order of the analysis beyond 120 made no significant improvement to the results.

It is evident from equation 9 that the temperature distribution in the combustion chamber wall is determined to a large extent by the material properties. Morel, Keribar and Blumberg (1988) indicated that given a particular rate of heat transfer, the magnitude of the temperature swing during the engine cycle depended on material properties. Increased heat capacity and thermal conductivity both reduced the temperature swing of the combustion chamber surface. The heat flux probes which were used for the project were made up of seven different materials, namely;

(i) chromel,
(ii) alumel,
(iii) gold,
(iv) cast iron,
(v) stainless steel,
(vi) ceramic cement, and
(vii) magnesium oxide.

All these materials played a role in the nature of the heat transfer through the probe. The role played by the different materials was thus investigated in order to gain an understanding of what was actually being recorded. The cast iron, stainless steel, ceramic cement and magnesium oxide were not considered to have had a significant effect on the probe output. The relative locations of these materials was thought to encourage single dimensional heat flux in the probe. The mass of gold present in

the probe was such that it would not have made a significant contribution. The important materials in the probe were chromel and alumel. The heat capacity of any particular alloy type tends to vary by a small amount with changing alloy proportion. Thermal conductivity on the other hand varies considerably with alloy proportion.

Chromel and alumel, both being nickel based alloys can be expected to have similar heat capacities. This cannot, however, be said for their thermal conductivities. The temperature swing of the chromel and alumel surfaces could thus differ. It was also clear that the temperatures of the chromel and alumel surfaces would not necessarily be the same at any point in the engine cycle. The output voltage of the probe is the sum of the voltages of the two junctions, namely the chromel-gold junction and the gold-alumel junction. The fact that the temperatures of the two junctions could differ, implied that the surface thermocouple would no longer behave as a K type thermocouple. The output voltage of the probe would thus represent an average of the temperatures at the two junctions.

The temperature to voltage gain of the two junctions would determine the weighting of the two junction temperatures in the resulting average. These junction gains can be assumed to be linear over the relatively small range of temperature swing. The result is that the rate of heat transfer calculated from the average temperature is a weighted average of the heat transfer actually occurring in the two materials. In the application of equation 9 for the calculation of surface heat transfer it was difficult to determine what value to use for thermal conductivity. It was understood that the correct value would be a weighted average of the conductivities of the two materials. The correct weighting would be some function of the two junction gains.

It was concluded that, although the recorded voltage did not represent an actual temperature exactly, it did represent an average of the surface temperatures. The assumption was made that the average temperature to voltage gain did not differ significantly from that of a K type thermocouple because junction gains are almost linear over a small range. There was also no doubt that increases in temperatures would yield increases of the same order in the output voltage. The shape of the surface temperature curve is, however, of greatest importance in the calculation of heat transfer and was correctly represented by the recorded data. The form of the calculated rate of heat transfer would thus represent the actual situation although the range would not necessarily be correct.

The results of Taylor (1987) and Timoney (1987a) indicated that if the rate of heat transfer was correctly calculated then all the injected fuel would be accounted for by heat release analysis. It was thus decided that this fact should be used to determine the unknown average thermal conductivity. The range of the calculated heat transfer curve was scaled in such a manner that the calculated fuel consumption equalled the measured fuel consumption. Calculated rate of heat transfer was scaled by entering a hypothetical material conductivity. This was done for two different fuel tests at all engine conditions, except maximum fueling and zero load. An average value was then calculated. The average value represented the average thermal conductivity of the relevant probe materials. The value was found to be within 7% of 61 W/m.K on a 95% level of confidence. This value was then used consistently throughout the project. Error in the value subsequently had no effect on the relative comparisons of fuels.

In the application of equation 9, knowledge of the average rate of heat transfer is required. The rate of heat transfer is equal to the product of temperature gradient and thermal conductivity. The

average temperature gradient was initially calculated from the temperatures recorded by the two thermocouples in the probe. Temperature gradient was assumed to be equal to the difference between these two values divided by the distance between the second probe and the surface. As was the case for the surface thermocouple, the correct thermal conductivity was unknown. This was because there were two materials of unknown thickness as well as contact resistances between the surface and the second thermocouple.

An additional limitation was that the resolution of the measurement of temperature difference was only 2°C. This resulted from the fact that average surface temperature and the temperature at the second thermocouple were recorded with a resolution of 1°C. This and the small range of the temperature difference of less than 70°C could lead to errors of more than 2,9% of full range in calculated heat transfer rate.

A better method for the calculation of the average rate of heat transfer was thus required. By calculating the polytropic constant from pressure data throughout the compression curve, it is possible to determine where in the cycle adiabatic compression occurs. Adiabatic compression implies that there is zero heat transfer to the air in the combustion chamber. Initially it was assumed that the surface heat transfer curve should be zero at the point where adiabatic compression occurred. This allowed the surface heat transfer curve to be offset by the correct amount and obviated the need to determine the average heat transfer rate prior to calculation. An example of the calculated rate of heat transfer over an entire engine cycle is illustrated in figure 13. The average rate of heat transfer could then be calculated by integrating the surface heat transfer rate throughout a cycle.

It was thus possible to compare the temperature difference between the surface and the second thermocouple with the calculated average heat transfer rate. The average heat transfer rate was known to be directly proportional to the temperature gradient. The average heat transfer rate was thus plotted against measured temperature difference for a large number of load conditions taken from different tests. This showed that at a particular speed the relationship between the two variables was linear but the regression lines did not pass through zero. Readings taken at two different speeds formed separate lines with different offsets. The conclusion was drawn that the criteria used to determine the offset of the heat transfer curve was slightly incorrect. This implied that zero heat transfer at the surface does not correspond with the point of adiabatic compression of the bulk gas in the engine.

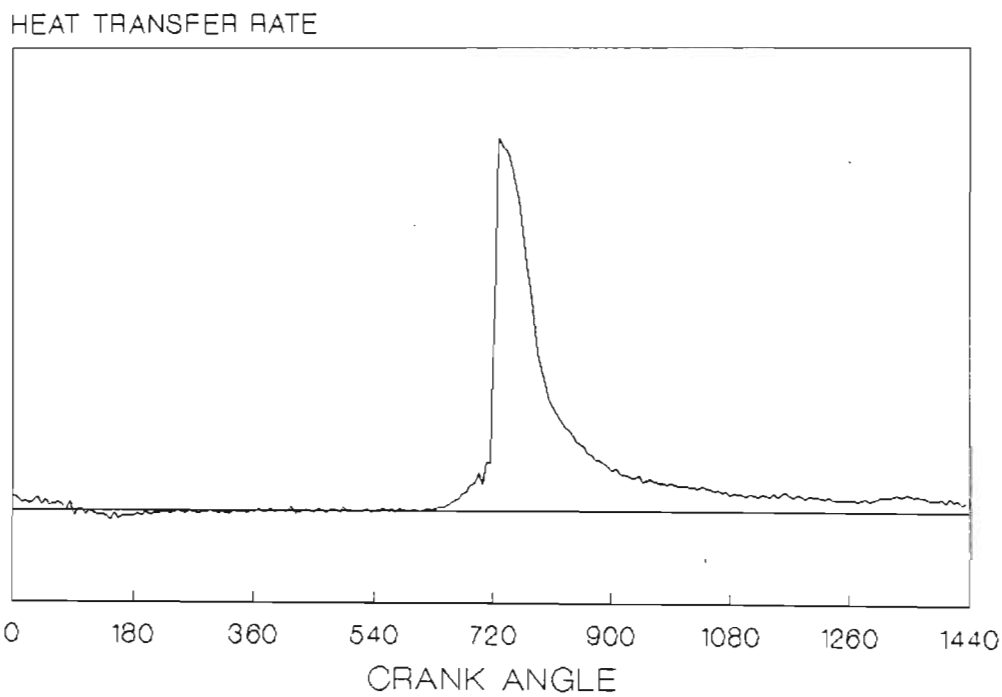

Figure 13. An example of the rate of heat transfer calculated from measured surface temperature.

This observation was supported by the findings of Lawton (1987) who indicated that zero heat transfer rate occurred far earlier in the cycle than the point of adiabatic compression. The explanation for this is that during the intake and early compression stroke, the boundary layer is heated by the combustion chamber walls. The temperature of the boundary layer is thus considerably higher than the bulk gas temperature. Compression results in an increase in air temperature at a rate determined by the gas laws. The temperature of the boundary layer which is higher at the outset remains higher than the increasing bulk gas temperature. The heat transfer at the combustion chamber surface is determined by the temperature difference between the wall and the boundary layer.

The boundary layer will equal wall temperature earlier in the cycle than the bulk gas. At the point where boundary layer temperature equals wall temperature, there can be no heat transfer between the wall and boundary layer. At this point the boundary layer is hotter than the bulk gas and thus heats the gas in the combustion chamber. Heat would thus be removed from the boundary layer rapidly, retarding it's temperature increase due to compression. Beyond this stage the boundary layer also loses heat to the combustion chamber walls. The bulk gas temperature continues to increase at a rate slightly higher than that due to compression. Bulk gas temperature will thus soon equal that of the boundary layer which results in adiabatic compression. The bulk gas will consequently experience adiabatic compression slightly later in the cycle than the point where zero surface heat transfer occurs.

Lawton (1987) did not, however, have any means to determine where in the cycle zero heat transfer occurred. The results of Lawton (1987) indicate that this occurred at bottom dead centre which is not credible because compression has not yet commenced at this point. Rao and Bardon (1985) stated that due to high turbulence

in the engine, the boundary layer is very thin and would have negligible thermal capacitance. This statement contradicts the observations of Lawton (1987). It was concluded that although the phenomenon described by Lawton (1987) did in fact take place, the effects were possibly not as significant as he had made them out to be.

In an attempt to determine the true zero point, the heat transfer calculation was repeated for numerous sets of independent data while the assumed zero point was varied. Linear regressions of average heat transfer rate on temperature difference were conducted for each assumed zero point. Changing the zero point resulted in the regression lines being shifted vertically. By a process of interpolation and iteration three different zero points were achieved for the three different speeds used for testing. These zero points resulted in all the calculated rates of heat transfer falling on the same line. An indication of the consistency with which heat transfer was determined is shown in figure 14.

A linear regression showed that 99,1% of the variation in the calculated average rate of heat transfer was accounted for by the measured temperature difference. The offset from zero of the regression line was found to be 0,22% of full scale which was proved to be insignificant. Error in the determination of temperature difference made a greater contribution to variation in the regression than errors in the calculated average rate of heat transfer. There was, however, no means by which the actual confidence interval of the heat transfer measurement and calculation could be determined.

A statistical analysis of the data displayed in figure 14 was conducted and showed that all recorded data fell within the 90% confidence interval for predictions of the regression. The confidence interval was equivalent to less than 8% of full range.

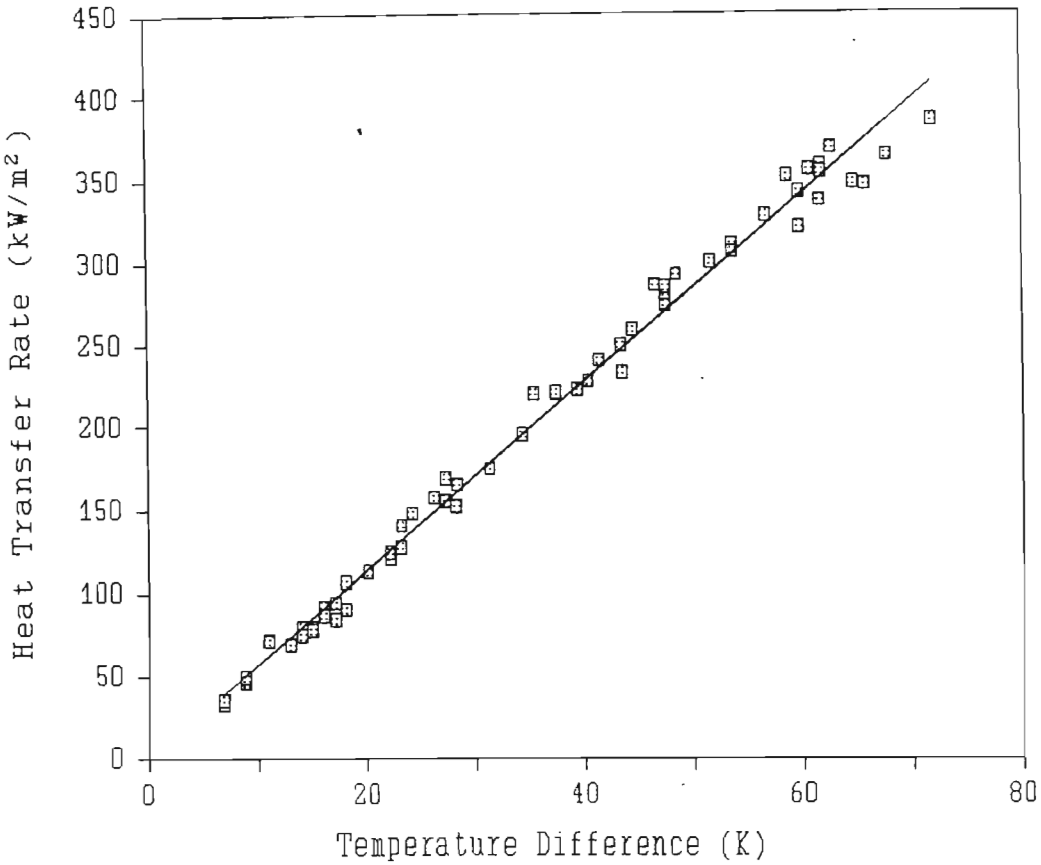

Figure 14. Calculated Average rate of heat transfer plotted against measured temperature gradient.

The confidence interval of the measured temperature difference was at least 6%, due to poor resolution and measurement error. This indicated that the confidence interval of calculated rate of heat transfer was within 2% of full range. Differences in the average rate of heat transfer were measured with different fuels at the same engine condition. These differences amounted to as much as 10% of full scale. On the basis of the deduced confidence interval there can be no doubt that the differences measured between fuels were significant.

The calculated zero heat transfer points were as follows:

1000 r/min = 113,0°C.A. before TDC
1700 r/min = 103,0°C.A. before TDC
2000 r/min = 91,5°C.A. before TDC

The fact that the point advanced with decreasing speed was highly credible. Heat transfer, which was the cause of the effect, is highly dependent on time. Reduced time due to increased speed should thus reduce the role played by the effect and cause the zero point to approach the point of adiabatic compression. The point of adiabatic compression was found to be in the region of 55°C.A. before TDC. The analysis illustrated the sensitivity with which the instantaneous heat transfer rate was calculated. The good correlation between calculated heat transfer rate and measured temperature difference illustrated the consistency with which the heat transfer rate was calculated. The high linear correlation coefficient proved that the assumptions made in the calculation of heat transfer rate had been valid.

The gradient of the regression line correlating average heat transfer rate with temperature gradient was an indication of the thermal conductivity of the materials in the probe. The gradient was directly proportional to the value calculated for the average thermal conductivity of the materials in the surface thermocouple. The method of calculation of the average thermal conductivity could thus be verified by investigating the gradient of the regression line. The thermal resistance per unit area of the materials between the surface and the second thermocouple could be calculated from the gradient.

The thermal resistance was calculated by multiplying the distance between the surface and the second thermocouple with the inverse of the gradient of the regression line. The thermal resistance was the result of the contribution of the following separate resistances;

(i) the resistance of the cast iron probe material,
(ii) the contact resistance between the cast iron and the ceramic cement,
(iii) the thermal resistance of the ceramic cement, and

(iv) the contact resistance between the ceramic cement and the second thermocouple.

The distance between the second thermocouple and the surface was 2,3 mm. It was assumed that this was made up by 0,3 mm of ceramic cement and 2 mm of cast iron. The thermal conductivities of the ceramic cement and the cast iron were 2,3 W/m.K and 58 W/m.K respectively. From this information it was possible to calculate the contact resistances between the cement and the metals. The fact that the ceramic cement was bonded to both the cast iron and the thermocouple would result in low contact resistances. The calculated contact resistance of 6,7E-06 m^2.K/W confirmed this observation. A second approach was to assume that the contact resistance was negligible and then calculate the thicknesses of the cast iron and ceramic cement. The calculation indicated that the thicknesses of the cast iron and ceramic cement were 1,968 mm and 0,332 mm respectively. The fact that both these calculations yielded credible results indicated that the use of the energy balance to determine the surface thermocouple properties was valid.

Transient heat transfer coefficient was calculated by dividing the transient heat transfer rate by the momentary difference between surface temperature and gas temperature. Gas temperature was calculated from measured cylinder pressure, exhaust temperature and inlet temperature. During the intake stroke it was assumed that air temperature in the combustion chamber was equal to the temperature of the air in the inlet manifold. This was known to underestimate the actual air temperature because the air is heated by the inlet valve and the combustion chamber walls during the intake stroke. The error was, however, both relatively small and consistent and would thus not affect the relative comparisons.

During the compression and expansion stroke the gas temperature was calculated from measured pressure with the aid of the ideal gas

laws. The mass of the air in the combustion chamber was calculated from the volumetric efficiency. In order to account for the mass of the injected fuel, the air mass was increased by the mass of the injected fuel, at a point 20°CA after TDC. Gas temperature during the exhaust stroke was assumed to be equal to exhaust temperature. This value was known to underestimate the actual temperature but the error was consistent. Efforts to reduce errors in the calculation of gas temperature, such as by estimating heat transfer to the valves, were considered to be unnecessary. This could introduce additional errors and detract from the relative comparisons.

Surface heat transfer coefficients and gas temperatures were required as inputs to the finite element analysis, for the calculation of heat transfer rates and material temperatures. In addition to transient values of heat transfer coefficient and gas temperature, average values were required to perform the finite element analyses. Average gas temperature was calculated by averaging the gas temperature through the entire engine cycle. It was, however, discovered that the average heat transfer coefficient should not be calculated in the same manner.

The equation for the rate of heat transfer to the combustion chamber wall is as follows:

$$q(t) = h(t) \cdot (T_{gas}(t) - T_{wall}(t)) \qquad (10)$$

Where h is the heat transfer coefficient, t is time and T_{wall} and T_{gas} are the wall and gas temperatures respectively. The equation for the average rate of heat transfer is thus:

$$q_{ave} = \frac{1}{2\pi} \int_0^{2\pi} h(t).(T_{gas}(t) - T_{wall}(t))dt \qquad (11)$$

Seale and Taylor (1971), Woschni (1979) and Woschni and Fieger (1979) stated that a representative value for the average heat transfer coefficient can be calculated by simply integrating the heat transfer coefficient over an entire cycle. This implies that:

$$\int a.b \; dt = \int a \; dt . \int b \; dt, \quad \text{where a and b are functions of time.}$$

This relationship is mathematically incorrect. In actual fact the correct average heat transfer coefficient cannot be calculated from the transient heat transfer coefficient alone. If a correct average heat transfer coefficient exists at all, the calculation of the average would require the inclusion of transient temperature difference as well as heat transfer coefficient.

The surface temperatures which were to be calculated by the finite element analysis would be of a similar order as those measured by the probe. It was assumed that it was acceptable to calculate both average gas temperature and average heat transfer rate by integrating these variables over one cycle. The average rate of heat transfer should be equal to the product of the average heat transfer coefficient and the difference between the average wall and gas temperatures. The average heat transfer coefficient was thus calculated on this basis by using the following equation:

$$h_{ave} = q_{ave} \; / \; (Tg_{ave} - Tw_{ave}) \qquad (12)$$

Where h_{ave} is the average heat transfer coefficient, q_{ave} is the average heat transfer rate, Tw_{ave} is the average wall temperature and Tg_{ave} is the average gas temperature. The finite element analysis calculated heat transfer rates and surface temperatures on a basis similar to that of equation 12. Average heat transfer coefficients calculated on this basis were thus considered to be most representative for application in the finite element analyses.

Both the measurement and calculation of heat transfer in the engine was a complex process. It was therefore necessary to validate all the data recorded by the heat flux probe and verify the associated experimental techniques. This was done by plotting the calculated average rate of heat transfer against the measured temperature difference in the probe for every reading used. This is displayed in figure 14. The regression of heat transfer rate on temperature difference yielded a R^2 value of 99,1%. This indicated that 99,1% of the variation in calculated heat transfer rate was explained by the measured temperature difference. A study of the residuals of the regression showed that the maximum residual was 5% of full scale. The average residual was found to be less than 2% of full scale. It was concluded that the entire measurement and calculation procedure for the determination of heat transfer at the probe was consistent to within 2%.

The rate of heat transfer at any instant is highly dependent on the location in the combustion chamber (Seale and Taylor, 1971; Woschni and Fieger, 1979; Morel, Wahiduzzaman, Tree and DeWitt, 1987 and Morel, Keribar and Blumberg, 1988). The rates of heat transfer measured at the probe were thus not representative of what was happening at other locations in the combustion chamber. In order to conduct representative finite element and heat release analyses, it was necessary that the spatial distribution of heat transfer in the combustion chamber be taken into account. Since the spatial distribution was not measured, it was necessary to develop a model based on published data which would represent the spatial distribution. In the development of a representative finite element model for the engine piston an extensive study was conducted into the spatial distribution of heat transfer. The spatial ditribution is discussed in the same section as the finite element analysis.

The results of Woschni and Fieger (1979) were considered to be the most easily applied. These results also included the spatial distribution of heat transfer in a combustion chamber which was similar in shape to that of the test engine. The application of these published data, however, required that a number of assumptions be made. Given a particular spatial distribution in the combustion chamber, the following assumptions were made;

(i) the rate of heat transfer at any point on the piston crown, outside the combustion bowl, was identical to the rate at the point on the cylinder head directly above it,

(ii) an increase in the rate of heat transfer at the probe would accompany proportional increases at all other locations in the combustion chamber,

(iii) the shape of the rate of heat transfer curve was the same at all locations,

(iv) all locations experienced zero heat transfer rate at the same instant, and

(v) there was no variation in the rate of heat transfer in a circumferential direction.

The net rate of heat transfer to the combustion chamber wall was calculated by integrating the product of area and the rate of heat transfer over the entire combustion chamber surface. The rate was then used in heat release analysis. The spatial distribution which was used in the finite element analysis was also used to calculate the net rate of heat transfer for heat release analysis. Due to the nature of finite element analysis a continuous distribution was not used. The spatial distribution was represented by discrete values at each surface element of the finite element model instead.

The fact that calculated rates of heat transfer yielded accurate heat release results indicated that the assumed spatial distribution was valid. On the whole the good correlation between the different calculations and known facts indicated that the

entire technique used to determine heat transfer rates was valid.

6.3 Dynamic Mechanical Stress

In order to investigate the effect of high rates of pressure rise on engine stresses, the displacement of the cylinder head was measured. This was done by recording the voltage output from the strain gauges of the instrumented cylinder head bolt, as a high speed channel. It was evident that cylinder head displacement was predominantly a function of cylinder pressure. However, it was noticed that the shapes of the pressure and cylinder head displacement signals differed in the period following ignition. Cylinder head displacement tended to lag behind pressure immediately after ignition. It then rose rapidly to a peak value before oscillating about a value which tended to follow the pressure decrease during the expansion stroke. The oscillations decayed before the end of the expansion stroke. An example of a pair of displacement and pressure signals is illustrated in figure 15.

The behaviour of the cylinder head relative to the engine block can be described by a mass-spring-damper model (Miyamoto et al., 1980). To investigate the relationship between cylinder pressure development and the resulting cylinder head strain, a model was developed which described the behaviour of the cylinder head. The cylinder head was modelled as a single mass attached to the engine block by two springs and a viscous damper. The springs represented the stiffness of the gasket and the cylinder head bolts. Movement of the mass spring damper system was initiated by the force of gas pressure acting on the area above the piston. The engine block, although far heavier than the cylinder head, also moved to a certain extent. It was thus modelled as a separate mass attached to the ground by a spring and a viscous damper. The complete model is illustrated in figure 16.

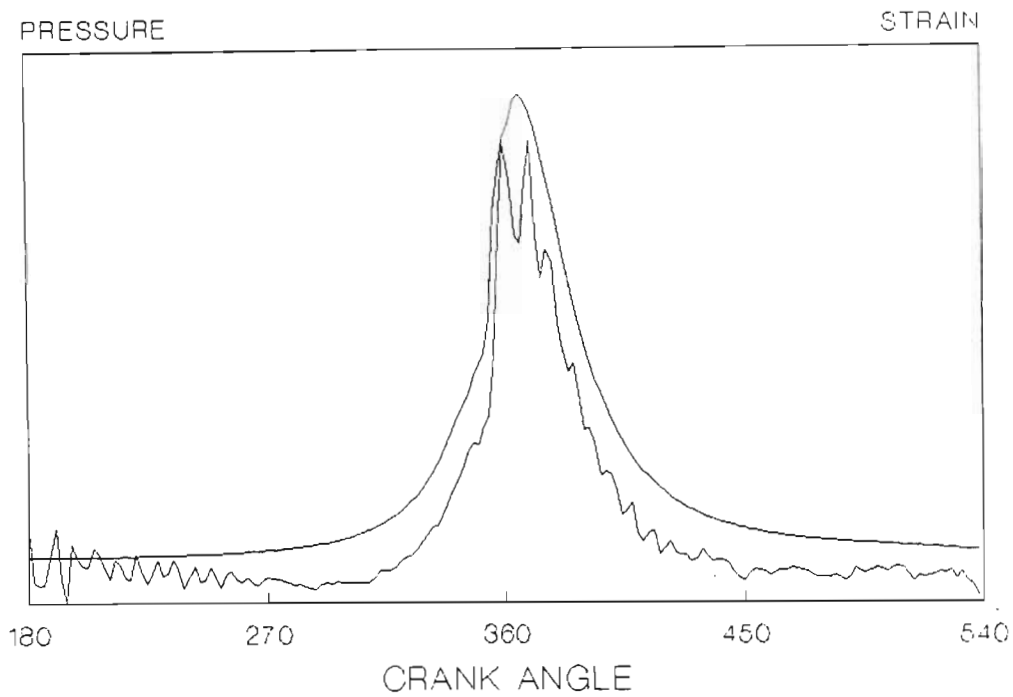

Figure 15. Cylinder pressure and cylinder head displacement measured simultaneously.

The equation describing the movement of the cylinder head is as follows:

$$P(t).A = m_h.\ddot{x}_h + C.(\dot{x}_h-\dot{x}_b) + (K_1+K_2).(x_h-x_b) \quad (13)$$

where P(t) is pressure as a function of time,

A is the area of cross-section of the piston,

m_h is the mass of the cylinder head,

x_h and x_b are the displacement of the cylinder head and engine block as functions of time respectively,

C is the viscous damping coefficient,

and K_1 and K_2 are the gasket and cylinder head bolt stiffnesses respectively.

The output from the instrumented cylinder head bolt was in fact equivalent to $x_h - x_b$. The assumption was made that the

acceleration of the engine block was negligibly small when compared to that of the cylinder head. This assumption is justified by the fact that there is a large difference between the mass of cylinder head and the mass of the engine block. Cylinder head acceleration was thus assumed to be equal to the second differential of the signal from the cylinder head displacement transducer.

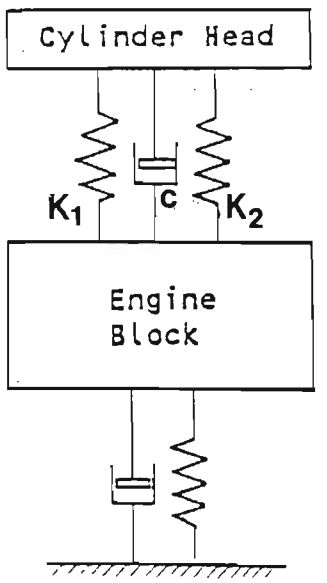

Figure 16. The mass-spring-damper model which was used to predict the movement of the cylinder head.

In order to calculate cylinder pressure from measured cylinder head displacement the following equation was derived:

$$P(t) = (m_h.\ddot{x}_r + C.\dot{x}_r + K.x_r)/A \qquad (14)$$

where x_r was equal to $x_h - x_b$ which was measured by the transducer and K was equal to $K_1 + K_2$. $\ddot{x}_r$ and $\dot{x}_r$ were calculated by numerical differentiation of the transducer signal. The mass, stiffness and damping factors were determined by an iterative process. The method was capable of calculating cylinder pressure to within 4% of full range. The inclusion of measured cylinder head acceleration would have increased the accuracy of the calculation if greater accuracy were required (Miyamoto et al., 1980).

For the purposes of the project it was, however, of greater importance to calculate component stresses from cylinder pressure. The calculation of strain from pressure proved to be more complex than the calculation of pressure from strain. Strain could not be calculated directly from cylinder pressure. A predictor corrector method was required. The method required a number of initial assumptions to be made. It was assumed that at the end of the intake stroke, the position, velocity and acceleration of the cylinder head were equal to zero. The assumption was made on the grounds of the fact that cylinder pressure deviated from atmospheric pressure by a small amount during the entire exhaust and intake strokes. The cylinder head was assumed to have come to rest during this period. Acceleration measurements made by Taylor (1984) on a single cylinder research engine showed that the acceleration of the cylinder head did approach zero during this stage of the cycle.

Strain was calculated progressively at each half degree interval from the beginning of the compression stroke to the end of the expansion stroke. At each instant i, an initial estimate of position x and velocity $\dot{x}$ was made on the basis of the position, velocity and acceleration of the preceding two time intervals. The equations used for these two calculations were as follows:

$$x(i) = x(i-2) + 2 \cdot dt \cdot \dot{x}(i-1) \qquad (15)$$

$$\dot{x}(i) = \dot{x}(i-2) + 2 \cdot dt \cdot \ddot{x}(i-1) \qquad (16)$$

Acceleration was then calculated on the basis of these estimates and equation 14 by using the following expression:

$$\ddot{x}(i) = (P(i) \cdot A - C \cdot \dot{x}(i) - K \cdot x(i))/m_h \qquad (17)$$

Velocity and position were then re-calculated from the estimated acceleration and their values at the preceding point. This was done on the basis of the following equations:

$$\dot{x}(i) = \dot{x}(i-1) + dt \cdot (\ddot{x}(i) + \ddot{x}(i-1))/2 \qquad (18)$$

$$x(i) = x(i-1) + dt\cdot(\dot{x}(i) + \dot{x}(i-1))/2 \qquad (19)$$

Equations 17, 18 and 19 were repeated until the calculated values of position, velocity and acceleration converged. It was found that at most points a third calculation of position, velocity and acceleration was unnecessary. In other words the second estimate of position and velocity did not differ significantly from the original estimate. This was because of the small time intervals used and the efficient estimates made by equations 15 and 16.

For purposes of statistical analysis and comparison with other engine variables it was necessary to quantify the measured cylinder head strain. The variable most relevant in the determination of component life is the strain amplitude. It was for this reason that the strain amplitude of the cylinder head bolt was used to represent measured cylinder head displacement. Strain amplitude was calculated by subtracting the minimum strain from the maximum strain during the cycle. This value was then recorded along with speed, torque, heat release parameters and heat transfer parameters at each engine condition for each fuel. A statistical analysis of all these data was then conducted.

6.4 Finite Element Analysis

The objective of conducting finite element analyses was to evaluate the relative effects of measured differences in loading on engine life. The literature is not conclusive on the relative roles played by the different forms of engine loading. Finite element analysis was thus used to determine the significance of the different engine loadings.

The most simple analysis was the calculation of the stresses which were caused by static pressure and steady heat transfer. By calculating the transient stresses which resulted from dynamic

pressure, transient gas temperature and varying heat transfer coefficient, the significance of the high cycle loadings was determined. The relevance of the low cycle loading was determined by calculating the transient stresses which resulted from step changes in engine load. The relative significance of the different types of component loading then formed the basis of an analysis into the effect of fuel combustion on engine life.

The engine piston is certainly the component which is most often analysed with the aid of finite element analysis. There are a number of possible reasons for this fact. Firstly, the piston appears to be the most vulnerable component in the immediate vicinity of the combustion chamber. It is the piston which places the greatest constraints on the application of poorer fuels, the use of higher power ratings and the achievements of lower emissions and fuel consumption (Sander and Schoeckle, 1979; Buchta, 1981; Wacker and Sander, 1982 and Reipert, Moebus and Schellmann, 1983). Secondly, the piston is to a large extent physically independent of other engine components. The piston can thus be modeled with relatively high accuracy without modelling other engine components. It is fortunate that the component in the engine which is most vulnerable, is also the most easily modelled with the aid of finite element analysis.

In order to portray the relative effects of the different types of loading and different fuels adequately, it was necessary to develop a representative model of the piston. In an attempt to identify the important aspects of modelling a piston, an analysis of published results was conducted. Most finite element analyses of engine pistons had been conducted by piston manufacturers. It was apparent that the requirements of accurate piston design far exceeded the requirements of the project. The NISA II finite element analysis package developed by the Engineering Mechanics Research Corporation was used in the project. The program is

capable of running on an IBM compatible personal computer. In order to reduce costs the demonstration version of NISA II was purchased which is limited to 50 elements and 200 nodes. This did, however, place some constraints on the analysis, in that a well optimized model had to be developed.

Most pistons have at least one plane of symmetry. The result is that the geometry can be fully represented by half of the piston. Some pistons which have two planes of symmetry can be represented by one quarter of the piston. The crown and skirt of the ADE 4.236 piston were to a large degree axi-symmetric. The piston could thus be relatively well represented by a rotationally symmetric finite element network (Reipert et al., 1983). It was the objective of the project to investigate stresses in the region of the piston crown. Fuel related failures had occurred in this region. Representing the piston as an axi-symmetric solid involved modelling the geometry in two dimensions as a function of radius and distance from the base.

Schockle (1981) stated that axi-symmetric piston models have been used with success for many years although they were of limited value in the calculation of gudgeon pin stresses. Saugerud and Sandsmark (1979) and Reipert, Moebus and Schellmann (1983) stated that, if correctly applied, axi-symmetric models yielded accurate results. Assanis and Badillo (1988) used a highly simplified two dimensional model to obtain successful results. Reipert et al. (1983) proved that an axi-symmetric model calculated the temperature distribution in a piston accurately. The results of Reipert and Buchta (1981) showed that the thermal distortion of the piston is relatively axi-symmetric particularly in the region of the crown. Radial distortion of the skirt in the gudgeon pin plane and perpendicular to this plane was found to differ by less than 5%. The results of Buchta (1981) showed that piston crown stresses were relatively independent of their location relative to the

gudgeon pin plane. It was concluded that although small variations existed in the stresses around the piston crown in the circumferential direction, these variations would be independent of differences between fuels.

The alternative to performing an axi-symmetrical piston analysis is to perform a full three-dimensional analysis. Not only does the preparation time of a three dimensional analysis exceed that of the axi-symmetric model, but the processing time is considerably longer. It is for these reasons that an axi-symmetric finite element model was used. Possibly the greatest limitation of the model was the fact that the piston bowl was not centrally located in the piston crown. This resulted in a slightly different radial thickness of the piston crown in different planes relative to the gudgeon pin plane. Sander and Schoeckle (1979) stated that increased radial thickness of the crown resulted in higher stresses. This was confirmed by the fact that the damaged pistons which were studied, had all failed at the point where the radial thickness of the crown was the greatest. Munro et al. (1986) showed that in the case of a piston with an offset bowl, the stress at the point of maximum radial thickness was often less than that at other locations. The stress at this point did, however, become tensile which would explain observed cracking.

The accuracy of the axi-symmetric model was largely dependent on the radial thickness chosen to represent the piston geometry at each height from the base. If the larger radial thickness of the piston crown was used, the model would overestimate thermal stresses. This would also result in an overestimation of the piston stiffness and thermal capacity. For these reasons the radial thickness of the model at each height from the base was made equal to the average piston thickness at that height. The average piston thickness was determined by sectioning a piston at various heights from the base. The surface area of each section was then

measured. The wall thickness of the model was selected by ensuring that the surface area of a section of the model at any height, was identical to that of the actual piston. The result was that the axi-symmetric model would contain the same amount of material as the actual piston. The model would thus have the same thermal capacity and mass as the actual piston. The vertical distribution of the material in the model would also be identical to that of the piston.

After choosing a representative piston geometry it was necessary to reduce the geometry into finite elements. The accuracy of any finite element analysis is largely dependent on the manner in which the geometry is broken down into a finite element mesh. Theoretically, increasing the number of elements and nodes increases the accuracy of the analysis. Wu and Chiu (1986) compared two axi-symmetric finite element models, one comprising 119 nodes and the other comprising 172 nodes. The difference between the results of the two models was found to be insignificant. This indicated that extending the resolution beyond a certain point was unnecessary. Munro (1979) stated that the advanced element libraries which have evolved, permit accurate calculations without a need for large element numbers. The element library of the NISA II package was known to contain the most current technology. It can be seen in the results of Buchta (1981) that even a coarse finite element model is capable of representing the relative stress distribution in a piston accurately.

The simplified axi-symmetric piston geometry was divided into 50 axi-symmetric elements. These elements included 181 nodes. The ADE 4.236 piston which is manufactured by Karl Schmidt, Johannesburg, South Africa, is a composite piston. A steel expansion control band and a cast iron piston ring carrier are cast into the aluminium piston. The large differences between the thermal properties and expansion rates of these three materials

made it necessary for them to be taken into account. The finite element mesh which was used for the analysis is illustrated in figure 17. This figure also illustrates the stress distribution and distortion which was calculated by the model for a typical cylinder pressure loading. The inclusion of the expansion control band and piston ring carrier resulted in a small amount of compromise in the shape of some of the elements. It can, however, be seen in figure 17 that all the elements in the region of the piston crown approach optimum shape. A study of the element distortion indices confirmed this observation. The finite element mesh used in the project was relatively fine when compared with those referred to in the literature as being coarse.

The accurate representation of the piston geometry is possibly the most simple aspect of the analysis of an engine piston. It is the representation of boundary conditions and constraints that pose the greatest challenge in piston analysis. It was for this reason that the determination of representative boundary conditions and constraints received considerable attention.

The piston is constrained in the vertical direction by the gudgeon pin which opposes gas pressure forces. The gudgeon pin exerts a force on the piston at the upper surface of contact between it and the piston. This force is only applied to two locations on either side of the piston. The use of an axi-symmetric model required the assumption that the constraints were also axi-symmetric. This would certainly result in the misrepresentation of pressure induced stresses in the piston skirt and gudgeon pin boss. This, however, did not apply to stresses in the piston crown. Vertical constraints were applied to all the nodes which were the same distance from the base, as the upper edge of the gudgeon pin. This constrained the piston model successfully. The assumption of axial symmetry obviated the need for additional external constraints. The nodes which lay on the central axis of the model did, however,

require to be constrained. The assumption of axial symmetry implied that these nodes could neither move horizontally nor rotate. They were, thus constrained in rotation and in the horizontal direction.

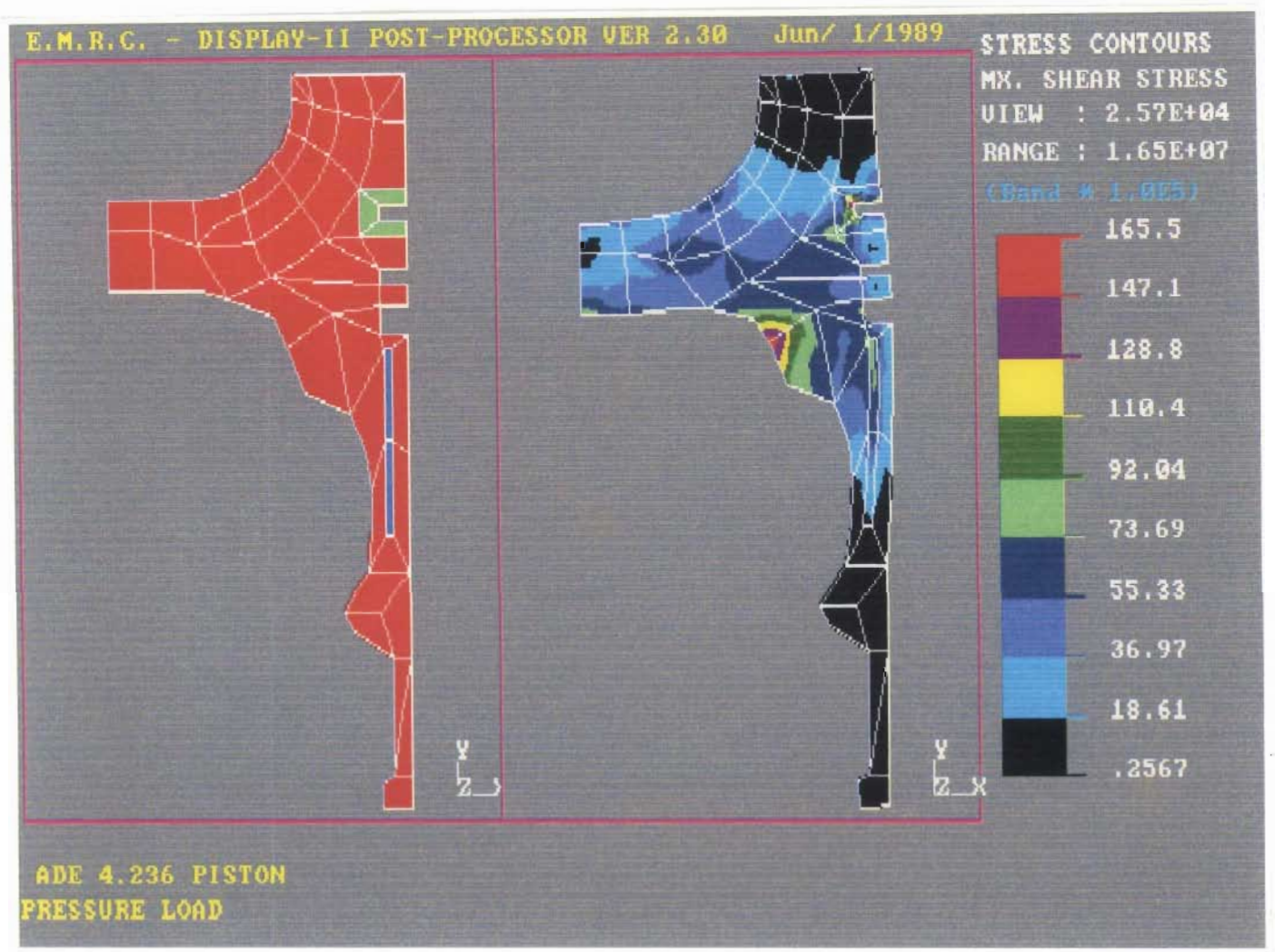

Figure 17. The finite element mesh, showing the expansion control ring and the piston ring carrier. A stress distribution calculated for a typical pressure loading is also illustrated along with the exaggerated distortion.

The piston is subjected to a number of forces other than cylinder pressure and the resulting gudgeon pin force. The reciprocating nature of the engine results in acceleration forces and side thrust on the piston skirt. From the results of Reipert and Buchta (1981) it can be seen that the effect of side pressure on the piston skirt has an insignificant effect on the piston crown. Acceleration forces were not only totally independent of the fuel used, but they were also considered to play a negligible role in stresses at the crown. Side thrust on the piston skirt and acceleration were thus not included in the analysis.

Cylinder pressure forces were accounted for by applying an evenly distributed pressure over the entire piston crown. Pressure was also applied to the region between the upper piston ring and the piston crown. Pressure was assumed to be uniform throughout the cylinder. The pressure values used were thus equal to recorded cylinder pressure. The representation of thermal boundary conditions required information describing both the ambient gas temperature and the heat transfer coefficient. It was assumed at the outset that by affecting cylinder pressure, gas temperature and heat transfer coefficient, the nature of the fuel affected piston stresses. In order to determine the effects of the fuel on piston stresses, it was necessary to apply the measured boundary conditions in the finite element model correctly.

The heat transfer coefficient between the cylinder gasses and the piston crown varies considerably between different locations in the combustion chamber (Seale and Taylor, 1971; Woschni, 1979; Woschni and Fieger, 1979; Morel, Wahiduzzaman, Tree and DeWitt, 1987 and Morel, Wahiduzzaman and Fort, 1988). It was thus desirable to account for the spatial distribution in the finite element model. A study of the various spatial distributions reported in the literature was conducted. Circumferential variation in heat transfer was unquestionably small and could be neglected (Seale

and Taylor, 1971 and Sarsten, 1979). This was further justification for the use of an axi-symmetric model. It was also evident that the spatial distribution was highly dependent on the combustion chamber size and shape (Seale and Taylor, 1971). Many of the reported distributions were thus irrelevant in the development of the model. Numerous researchers were able to show relative values at a few discrete points, but were unable to display a full distribution (Roehrle, 1978; Morel, Wahiduzzaman, Tree and DeWitt, 1987 and Morel, Wahiduzzaman and Fort, 1988).

Woschni and Fieger (1979) provided the most applicable results in that they displayed a continuous distribution of heat transfer coefficient across the piston crown. Not only was their method of calculating the distribution accurate, but the shape of the piston used was similar to the one used in the project. The heat transfer coefficient at each element on the piston crown was calculated by integrating the distribution reported by Woschni and Fieger (1979) over that element. The coefficient was then expressed as a fraction of the coefficient at the piston bowl lip. The actual coefficient at each element was calculated by multiplying the value determined at the probe with the fraction for that element. This method involved the assumption that the relative distribution of heat transfer coefficient was independent of all factors other than piston shape.

The relative distribution of heat transfer coefficient which was derived from the results of Woschni and Fieger (1979) is displayed in figure 18. The distribution was also used for the calculation of the net rate of heat transfer out of the combustion chamber. This allowed the heat flux probe to be calibrated by performing an energy balance. Seale and Taylor (1971) indicated that the heat transfer coefficient at any point in the combustion chamber was largely a function of the distance from the centre line of the cylinder. It was thus possible to derive the relative distribution

of heat transfer coefficient at the cylinder head. The derivation also assumed that the coefficient at any point on the cylinder head would be similar to that at the corresponding point on the piston. The heat transfer coefficient at the cylinder liner was deduced from the results of Roehrle (1978).

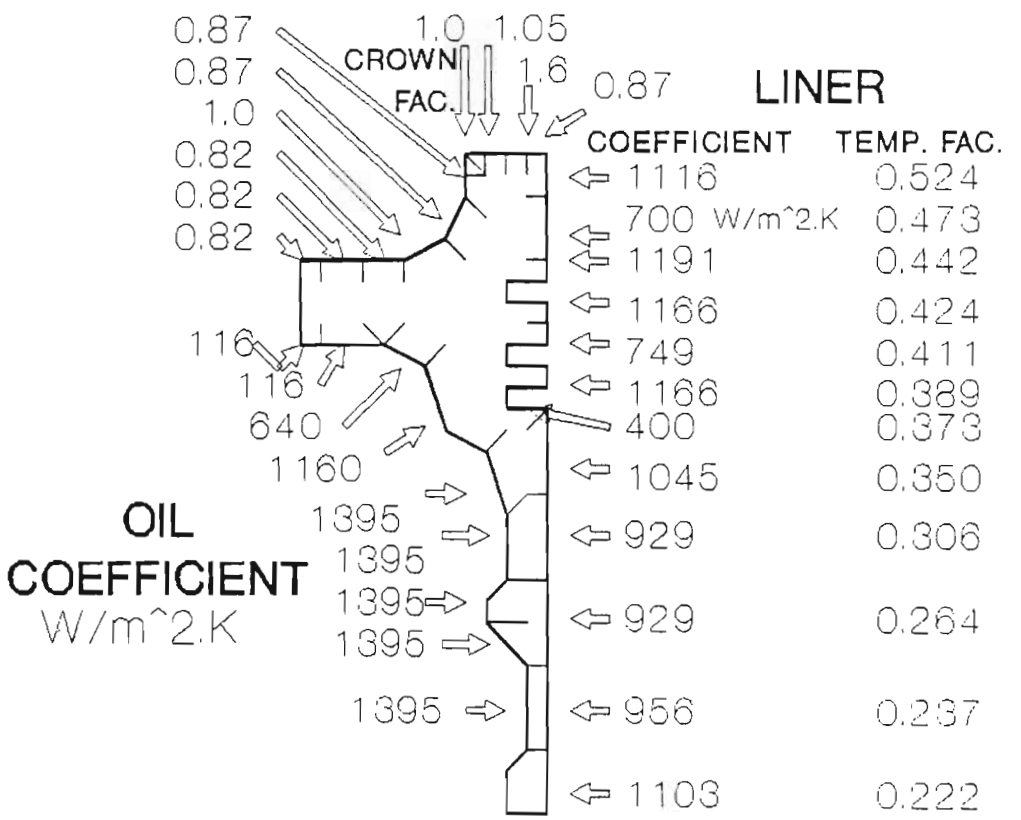

Figure 18. Boundary conditions for the piston model. Actual coefficients for the sides of the piston are displayed. Multiplication factors are displayed for the crown coefficients and apparent liner temperature.

The location of the maximum value of heat transfer coefficient, outside the piston bowl, corresponded with an observation reported by Hardenberg (1986). Hardenberg (1986) stated that turbulence in the squish zone, caused by gas rushing out of the combustion

chamber after ignition, resulted in high coefficients. The turbulence which started at the piston bowl lip affected the area outside the piston bowl, resulting in maximum heat transfer coefficients at this point.

The assumption was made that the gas temperature in the combustion chamber was uniform at all times. It was understood that limitations of both this assumption and the assumed constant relative distribution could introduce errors. Woschni (1979), however, stated that owing to the high thermal conductivity of aluminium, the effect of the spatial distributions on the piston temperature distribution was small. Any errors in the spatial distributions would thus have an insignificant effect on the calculated temperature distribution. The assumed uniform gas temperature and spatial distribution of heat transfer coefficient would thus be adequate for the calculation of relative stresses.

The heat which is transferred to the piston from the combustion gasses, is dissipated through heat transfer to the cylinder liner and engine oil. The temperature distribution in the piston is determined by the combined effects of heating of the piston crown and cooling of the lower regions of the piston. Accurate representations of the boundary conditions which result in this heat dissipation are thus as important as the representation of the combustion chamber boundary conditions.

The sliding contact between the piston and the cylinder liner is responsible for conducting much of the heat away from the piston. Heat transfer across this interface is determined by the temperature gradient and the heat transfer coefficient. Not only does the cylinder liner temperature decrease from the cylinder head downwards, but the piston reciprocates over a region of the liner. The temperature adjacent to any point of the piston side wall at any instant is thus dependent on the position of the piston. The

temperature is not easily determined. A study of reported cylinder liner distributions was conducted. Haddad and Watson (1984) and Munro et al. (1986) displayed typical cylinder liner distributions. These distributions showed that the liner temperature decreased exponentially from the cylinder head downwards.

It was decided that the distributions provided by Haddad and Watson (1984) and Munro et al. (1986) could be used in conjunction with heat transfer theory to develop a model which would predict liner temperatures. A simple model was required which would be consistent and representative, while being able to portray the effects of the measured differences in heat transfer rate. It was concluded that the variables which should be included in such a model are as follows;

(i) average cylinder gas temperature,
(ii) average heat transfer coefficient between the combustion chamber gasses and the walls,
(iii) cooling water temperature,
(iv) the thickness of the press fitted cylinder liner and the surrounding engine block,
(v) heat transfer coefficient between the engine block outside the cylinder and the cooling water,
(vi) the contact resistance between the cylinder liner and the engine block, and
(vii) the distance from the cylinder head.

Unlike most of the cylinder liner, the point on the liner immediately below the cylinder head experiences gas temperature and gas heat transfer coefficients for the entire cycle. Single dimensional heat flux between the combustion gasses and the cooling water was assumed to take place at this point. By calculating the combined thermal resistance of the heat transfer coefficients, contact resistance and material conductivities, it was possible to calculate the heat transfer rate through the cylinder wall. The

product of the heat transfer rate and the thermal resistance of the gas to wall heat transfer coefficient was equal to the temperature difference between the gas and the wall. It was thus possible to calculate the surface temperature of the cylinder liner at the top of the combustion chamber. The assumption was made that neither liner temperature nor coefficient varied circumferentialy.

The decrease in liner temperature away from the cylinder head was then addressed. Liner temperature tended to approach the coolant temperature in an exponential manner towards the bottom of the cylinder. It was thus decided that the significant variables in the distribution of liner temperature were distance from the cylinder head and temperature difference between the liner and the coolant. At each point of the distributions reported by Haddad and Watson (1984) and Munro et al. (1986) the difference between liner temperature and coolant temperature was calculated as a function of relative distance from the cylinder head. The difference at each point was then compared to liner temperature nearest the cylinder head. Both these distributions showed similar trends. By performing a polynomial regression on these distributions an equation for the relative temperature gradient between the liner and coolant was derived. With the equation it was possible to calculate the surface temperature at any point on the liner from the temperature calculated for the liner adjacent to the cylinder head. The cylinder liner temperature distribution could thus be determined from measured temperatures and heat transfer coefficients with the aid of the model.

The fluctuating liner temperature adjacent to each element on the piston was represented by an apparent average temperature. The average liner temperature apparent to any point on the piston is equal to the time average of the temperature of the surface which it covers. The nonlinear temperature distribution of the liner and

the changing velocity of the piston make it impossible to calculate the apparent temperature by simple averaging. The apparent liner temperature at each element on the piston was thus calculated by integrating the liner temperature numerically at each point that the element passed over during a cycle. An expression was thus derived for the apparent liner temperature at each element as a function of measured temperatures and heat transfer coefficients.

The equation which was used for the calculation of the liner temperature apparent to each element of the piston was as follows:

$$T_{apparent} = T_{water} + T_{factor} \cdot (T_{liner} - T_{water}) \qquad (20)$$

where $T_{apparent}$ was the apparent surface temperature at the face of each element. This temperature was used for the calculation of heat transfer at the surface. T_{water} was measured water temperature and T_{liner} was the temperature of the liner at the cylinder head, calculated from measured gas temperature, heat transfer rate and water temperature. The multiplication factor T_{factor} was calculated by numerical integration, over one cycle, of the relative temperature difference between liner temperature and water temperature, as a function of distance from the cylinder head. The multiplication factors calculated for each of the elements which came into contact with the liner are illustrated in figure 18.

Due to variations in contact pressure, clearance and lubricant thickness, the heat transfer coefficient between the piston and liner varies from one location to the next. Haddad and Watson (1984) gave typical values of heat transfer coefficient at different locations on the piston wall. They also gave examples of the heat transfer coefficients between the piston rings and the piston and liner. The distribution reported by Woschni and Fieger (1979) was, however, again considered to be the most applicable in the project. The heat transfer coefficient at each element was thus derived. The coefficients which were used are illustrated in figure 18.

The piston rings are responsible for carrying a large amount of heat from the piston to the liner. They were, however, not included in the finite element analysis. The cooling capabilities of the piston wall would thus be misrepresented. In order to avoid this limitation the heat transfer coefficients of the elements on either side of the piston rings were adjusted to compensate for the absence of the piston rings. This was done by ensuring that the thermal resistance at the surface of these elements was equal to their actual thermal resistance in parallel with the thermal resistance of half of the piston ring. The calculated heat transfer coefficients at the surface of these elements were thus higher than their actual value. Although the heat flux would be misrepresented slightly at the piston ring grooves, the heat flux on the whole was better represented.

The distribution of heat transfer coefficient between the bottom of the piston and the lubricating oil is well documented by Woschni and Fieger (1979). The nature of the oil cooling system played a significant role in these coefficients. One of the systems reported on by Woschni and Fieger (1979) was similar to that used in the ADE 4.236 engine. The heat transfer coefficients at the elements which came into contact with the oil were thus determined from this information and are also illustrated in figure 18. The ambient temperature was assumed to be equal to measured oil temperature.

In addition to the geometry and the boundary conditions, knowledge of the material properties was required. This included both mechanical and thermal properties. In the event of stresses exceeding the elastic range of the material, the inclusion of the elasto-plastic properties in the model is sometimes considered necessary (Saugerud, 1981 and Dowling, 1982). Buchta (1981), however, stated that as long as the region undergoing plastic

deformation was small, elastic material properties provided accurate results. Buchta (1981) showed that the regions predicted to experience plastic deformation were similar for both the elastic and elasto-plastic analyses of an aluminium piston.

The version of the NISA II package that was used for the work did not have the capability of incorporating elasto-plastic properties into the model. Initially it was assumed that if the piston of the ADE 4.236 engine experienced any plastic deformation, the deformation would be limited to a small portion of the entire piston. The assumption was thus made that the use of elastic material properties was acceptable. The pistons of the ADE 4.236 engine are made of Karl Schmidt KS 1275 aluminium alloy. All the relevant properties of the alloy, including the non-linear temperature dependent properties, were provided by Buchta (1989).

It was found that the use of a temperature dependent, linear material model resulted in a gross overestimation of stresses in the piston crown. The stresses in a large proportion of the piston crown exceeded the yield point of the alloy by a considerable margin. This indicated that the piston crown did in fact experience plastic deformation. The NISA II program was unfortunately not capable of accounting for non-linear material response.

In order to account for plastic deformation the temperature dependent non-linear stress strain curves were divided into 21 subdivisions on the basis of plastic strain. These curves were then digitised and regressions as a function of temperature were conducted. The result was that the actual material properties were represented by 21 hypothetical temperature dependent linear materials. Each of the hypothetical materials could be used at individual elements to represent a small range of the nonlinear material response. This method is illustrated in figure 19. This

overcame the limitations of the NISA II program and allowed the actual stiffness of the material to be approximated with acceptable accuracy.

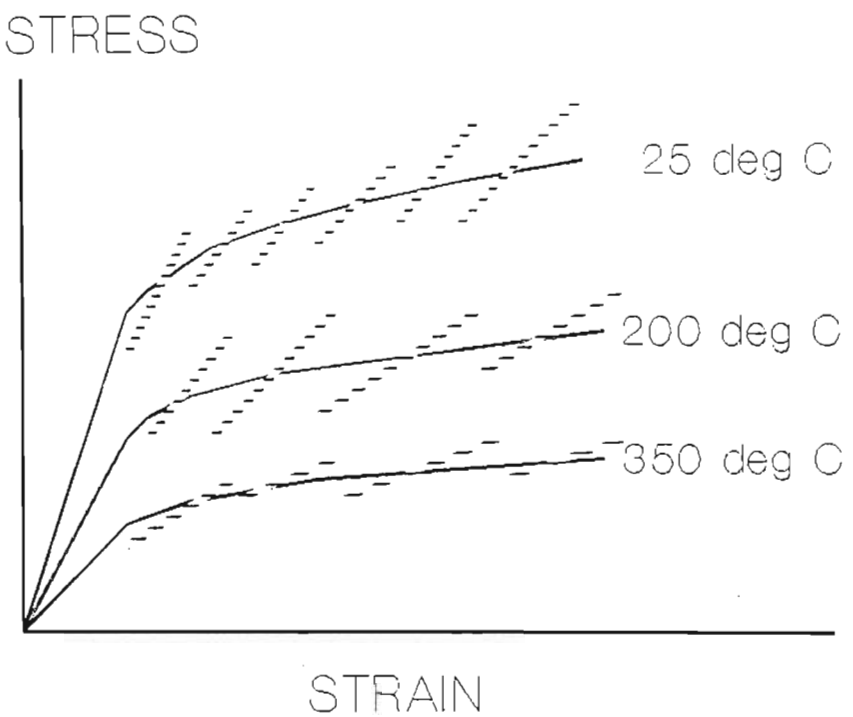

Figure 19. An illustration of the method used to approximate non-linear material response. Each of the hypothetical linear materials, represented by the dotted lines, could be used to approximate the true material over a small strain range.

A process of manual iteration was then used to determine which of the hypothetical materials was required at each element. The process was extremely time consuming. The inclusion of nonlinear material response relieved stresses in the region of the piston crown greatly. The result was that the stress in many of the elements which appeared to yield initially, dropped to below yield point. For each analysis a situation was reached where the material used at each element approximated the conditions which

would actually apply when plastic deformation took place.

A complete finite element model of the ADE 4.236 engine was thus derived. The model represented the geometry, materials, constraints and boundary conditions of the piston in an axi-symmetric form. The accuracy with which the results of a model represent the actual conditions is limited by the accuracy with which the boundary conditions are known. A simplified model is thus unlikely to represent all aspects of a piston correctly. It was, however, believed that the model which was used, yielded reliable and consistent results, particularly in the region of the piston crown.

The objective of the research was to determine the relative effect of the nature of combustion on engine life. Finite element analysis was used to calculate component stresses and temperatures from measured engine variables. The results of the finite element analysis were then used to calculate the expected component life. The life of a component is affected by numerous factors. In order to calculate the expected life of any component, it is necessary to identify the factors which contribute to the failure of the component. These factors should then be included in the analysis. The factors which could play a role in the failure of diesel pistons are as follows:

(i) material properties,
(ii) temperature,
(iii) environmental affects,
(iv) creep,
(v) high cycle pressure loading,
(vi) high cycle thermal loading,
(vii) low cycle loading, and
(viii) transient load variations.

Both Saugerud (1981) and Dowling (1982) stated that the present fatigue theory does not account adequately for all the factors which have an effect on component life. Despite this fact it was necessary to establish a procedure which could be used to calculate the relative component life under different conditions. It was for this reason that the different factors affecting piston life were investigated.

The fatigue strength of aluminium is relatively poor, particularly at high temperatures. The fatigue strength of aluminium at room temperature is approximately 40% of that of cast iron. At temperatures commonly found in the region of the piston crown the strength of aluminium is reduced to less than 25% of that of cast iron (Wacker and Sander, 1982). Increased thermal loading has the combined effect of increasing stresses and weakening the material. The effect of temperature on fatigue strength was thus accounted for by applying temperature dependent material properties in all calculations. The information provided by Buchta (1989) describing the properties of the piston alloy, included the necessary information. Material temperatures were determined from the results of the finite element analysis.

The environment in the combustion chamber is extremely hostile. Piston life is certainly affected by the chemical attack from the fuel and combustion deposits. This is aggravated by the combined effects of high temperatures and fuel impingement. The existing technology is not capable of accounting for most of the environmental factors which affect component life (Dowling, 1982). Quantification of fuel spray impingement was not carried out in the project although it was known to contribute to failure. It was assumed that the variation in the effects of fuel spray impingement with different fuels was insignificant when compared to the variation in other factors which contribute to failure. It was for these reasons that the chemical, mechanical and thermal

effects of the injected fuel on the piston were not taken into account.

Saugerud and Sandsmark (1979) and Saugerud (1981) indicated that creep plays a significant role in piston failure. Munro (1979), Sander and Schoeckle (1979) and Buchta (1981) indicated that cyclic fatigue plays a predominant role in piston failure. This discrepancy appears to be related to both the size and the application of the piston. The former application being marine where high loads are maintained for extremely long periods of time in large engines. The latter application appears to be general purpose automotive type applications where loads tend to fluctuate more rapidly and more often.

The relevant application in the project is automotive and agricultural, where the role of creep is expected to be far less than that of cyclic fatigue. The calculation of the extent of creep is a complex process which is highly dependent on empirical data which are not yet documented adequately (Saugerud, 1981). It is for these reasons that the effects of creep were not directly calculated. Creep is dependent on material temperature and stress which were used to calculate the cyclic fatigue life of the piston. By accounting for the relative effects of fuels on cyclic fatigue, the relative effects of creep were also accounted for to a certain extent.

On the basis of the fact that failures of actual pistons were known to occur at the piston bowl lip, it was decided that all component life calculations should be carried out at this point. The fact that the finite element piston model was designed to be most accurate in the region of the piston crown, also contributed to the decision. Although the piston skirt and the expansion control ring constrained the upper portions of the piston correctly, it was felt that fatigue life calculation in these components would not

be representative. It was thus assumed that the temperatures and thermal and pressure induced stresses calculated at the piston bowl lip could be used to calculate representative engine life. The calculation of correct component life from this information was, however, a difficult task.

In order to establish a representative method of calculating component durability from finite element results, a study of methods recommended by other researchers was conducted (Sander and Schoeckle, 1979; Buchta, 1981; Saugerud, 1981; Schockle, 1981 and Dowling, 1982). It was concluded that the method most relevant and applicable to diesel engine pistons was that used by Sander and Schoeckle (1979), Buchta (1981) and Schockle (1981). The method involved calculating representative thermal and pressure induced stresses at the critical points.

Representative stresses were calculated from the finite element results with the aid of Tresca's criterion which is a maximum shear stress theory. For both the high cycle pressure stresses and the low cycle thermal stresses, the cyclic stress amplitude was then calculated. The high cycle stress amplitudes for both the engine idle condition and the high load condition were assumed to be equal to the maximum pressure induced stress. The difference between the thermal stress levels at idle and high load was used as the low cycle stress amplitude.

The resulting strain amplitude was determined from the stress-strain curves at the appropriate temperature. The strain amplitude was then used in conjunction with the Woehler (life-strain) curves of the material to determine the fatigue life. The Palmgren-Miner method was used to calculate the partial damage resulting from each of the three cyclic loads. The three loads being;

(i) high cycle pressure load at high power,

(ii) high cycle pressure load at idle conditions, and

(iii) low cycle thermal load.

The method relied on tensile stress-strain curves to determine strain for both tension and compression from calculated stress. This implied that the assumption had been made that the stress-strain curves for compression were the mirror image of those for tension. Neither Sander and Schoeckle (1979), Buchta (1981) nor Schockle (1981) made any mention of the assumption. Results of a strain cycle test of the alloy used in the ADE 4.236 piston, displayed by Buchta (1981), illustrate that the stress-strain relationship in compression does approach being a mirror image of the tensile curve. This is particularly true for lower values of stress.

In order to calculate cyclic strain amplitudes from the different finite element analyses it was necessary to assume a model which described the material behaviour throughout the life of the piston. The fact that part of the piston crown experienced plastic deformation complicated the analysis greatly. Plastic deformation would only take place during the first few engine cycles and not throughout the piston life. The finite element analyses conducted were in fact only representative of the first cycle experienced by the piston. After the first few cycles the piston would experience residual tension in part of the piston crown and compression in the surrounding material, on cooling. The analysis of such a piston was, however, not possible. The conventional model could, however, yield the correct strain amplitudes if correctly applied.

The material behaviour model which was used to describe the processes experienced by the material at the piston bowl lip had the following stages, as illustrated by figure 20:

(i) The bowl lip alloy was originally stress free.

(ii) With the application of engine load the piston warms and experiences linear thermal stress.

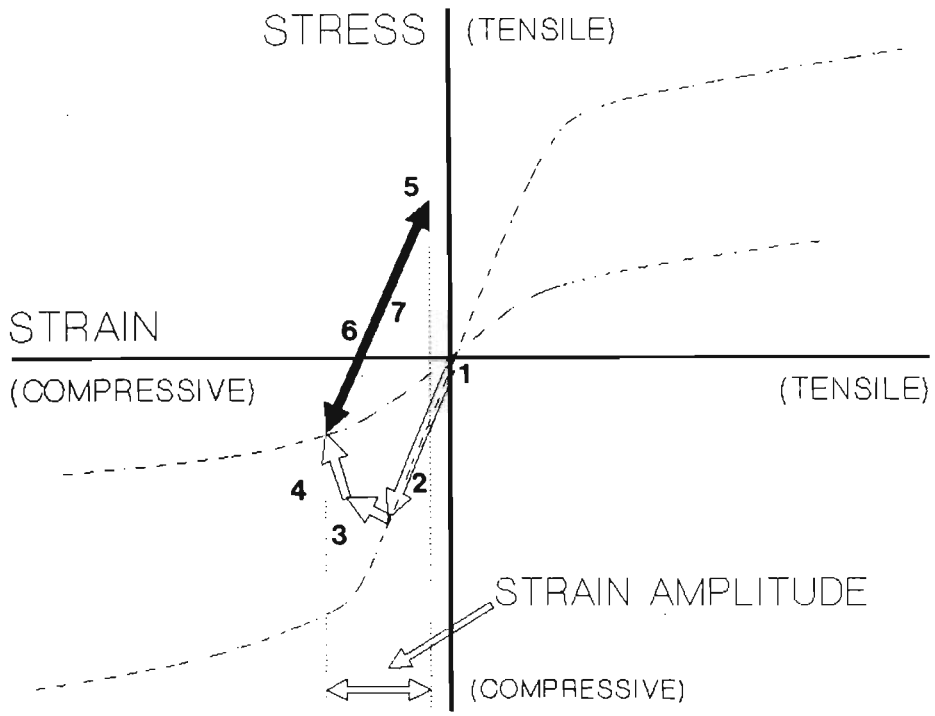

Figure 20. The stress-strain cycle which was used to determine strain amplitudes for the calculation of piston life.

(iii) The piston temperature continues to rise, resulting in stress increase and weakening of the alloy.

(iv) When the yield point is reached plastic deformation occurs. It was assumed that all plastic deformation took place in the first cycle.

(v) When the engine is stopped the piston cools and the material which did not undergo plastic deformation attempts to return to it s original form. It is, however, resisted by the deformed alloy in the piston crown. The assumption was made that the amount of deformed alloy was such that it would not distort the rest of the piston by a significant amount. The deformed alloy would thus be forced

back to its original form leaving it in tension.

(vi) A repeat of the original load would result in the material experiencing elastic deformation back to the same point last achieved under load. Any loading which did not exceed the original loading would thus result in elastic deformation.

(vii) If the engine were to cycle between two different loads the piston material would experience linear deformation and the strain amplitude would be determined in the manner illustrated in figure 20.

With these assumptions it was possible to calculate cyclic strain amplitudes for various piston loadings.

The role played by the rate of pressure rise on component stresses is not clearly defined. The results of Miyamoto et al. (1980) proved that high rates of pressure rise can result in peak stresses which exceed what would be expected from the prevailing pressure values. This phenomenon was investigated by measuring strain with the cylinder head displacement transducer. These measurements would, however, have little bearing on the piston. The role of the rate of pressure development on piston stresses was thus investigated with the aid of the finite element model. This was done by first performing an eigenvalue analysis in order to determine the natural frequencies of the piston. This information was then used to calculate the dynamic response of the piston while being subjected to an extreme dynamic pressure cycle. The resulting strains gave an indication of the role played by the rate of pressure development. This analysis proved that high cycle pressure loading on the piston can be represented by the peak pressure value alone. High cycle pressure loading was thus accounted for by calculating the static stresses which resulted from peak pressure.

High cycle thermal loading of the piston was investigated by performing a transient heat transfer analysis of the piston. An extreme engine condition was selected and the instantaneous gas temperature and heat transfer coefficients were calculated. These transient thermal boundary conditions were then applied to the piston model. The transient temperatures at selected points on the piston were thus calculated throughout the cycle. Stresses were also calculated at various points in the cycle. The range of variation in the calculated stresses gave an indication of the significance of the high cycle thermal load. It was found that piston stresses varied by an insignificant amount as a result of high cycle thermal loading.

The calculation of transient thermal load and fatigue life requires the assumption of a representative load cycle. There is, however, no single representative load cycle (Saugerud, 1981). The assumption was made that for purposes of relative comparison it would be applicable to alternate engine load between no load and a load which approached maximum power. The load cycle used for the calculation of piston life included the following stages;

(i) zero load at a speed of 1000 r/min for 2 minutes,
(ii) increase to a BMEP of 700 kPa at a speed of 2000 r/min over 2 seconds,
(iii) maintain a BMEP of 700 kPa at 2000 r/min for 2 minutes, and
(iv) return to zero load at 1000 r/min over two seconds.

The load cycle is similar to those applied by Munro (1979), Sander and Schoeckle (1979), Buchta (1981) and Francis (1986). The load cycle which changed frequently from idle to more than 80% of rated engine power, was considered to be more severe than most applications of the engine. Although maximum loads are achieved in automotive applications, the load seldom fluctuates as frequently as in the above load cycle. In agricultural

applications it is possible for the load to fluctuate in a manner similar to that described in the above load cycle. This would occur in heavy draft operations where the machine is frequently forced to stop and turn. It was concluded that the use of the above load cycle to calculate component life would result in relevant comparisons of the effect of each fuel on durability.

The stresses resulting from transient load variations were investigated by varying the thermal boundary conditions in a manner which corresponded with the above cycle. The temperature distribution in the piston was recorded at successive intervals. The recorded transient temperature distributions were then used to calculate transient thermal stresses. It was found that unlike the results of Munro (1979) and Francis (1986), the transient thermal stress gradually increased to the equilibrium value. At no stage did the transient thermal stress exceed the equilibrium value significantly.

This implied that maximum thermal stress could be represented by the equilibrium value resulting from maximum engine load. Low cycle thermal loading was thus accounted for by calculating the thermal stresses at maximum load and at engine idle conditions. Engine life could thus be calculated by considering the range of high cycle pressure stress at a frequency of 1000 cycles per minute and low cycle thermal stress at a frequency of 15 cycles per hour. The material temperatures relevant to the calculations were obtained from the results of the finite element analysis.

In order to calculate the average temperature distribution at each engine condition a static heat transfer analysis was carried out. This was done by applying average thermal boundary conditions to the piston. Measured oil and cooling water temperatures were used while the calculated average gas temperature and average heat transfer coefficient were applied at the piston crown. The static

finite element analysis then calculated the temperature of each node of the piston model. This temperature distribution was then used with peak cylinder pressure in a static stress analysis. The static stress analysis not only calculated both thermal and pressure induced stresses, but also calculated the combined stress distribution.

For each fuel maximum strain was determined using the plastic material model. The strain amplitude between the cold piston condition and idling was then calculated using the elastic model. When cycling, the strain varied between maximum strain and the strain at the idle condition as indicated by the solid arrow in figure 20. The cyclic strain amplitude was thus calculated by subtracting the strain amplitude between the cold and idle conditions from the maximum strain. Temperature dependent strain-life curves were then used to determine the expected component life from the calculated strain amplitude. A regression was conducted on the strain-life curves so that life could be calculated from material temperature and strain amplitude. The fact that material temperature varied by a large amount during the cycle complicated the calculation. An average of maximum temperature and the temperature at idle was finally used. The expected engine life was thus calculated for each fuel. Calculated life, temperature and stress were then compared with measured and calculated combustion and heat transfer parameters. This was done with the aid of statistical analyses.

6.5 Statistical Analysis

The different measurements and analyses conducted in the project generated vast quantities of data and numerous different variables. It was thus impractical to attempt to determine trends and relationships between variables without the aid of statistical methods. Even the graphical methods which are most commonly used were not adequate. In order to perform a statistical analysis of the results it was necessary to quantify the results of the different analyses for each of the tests. This was done by defining simple variables which could represent the results of each

analysis adequately.

The results of heat release analyses were well quantified by Hansen et al. (1987) and Taylor (1987). Taylor (1987) found that a large number of the variables commonly used to quantify heat release rate were inter-dependent. It was thus evident that there would be no advantage in the determination of some of the variables which have been used previously. In this manner the tedious determination of some of the variables such as the duration of premixed combustion was avoided. The variables which were determined from the heat release results are listed in table 2 along with their units and definitions.

Table 2. List of variables with units and definitions.

Variable	Units	Definition
Speed	r/min	*Engine speed at which data were recorded
Torq	Nm	Load at which data were recorded
MEP	kPa	*Brake mean effective pressure
Fuel	kg/h	Fuel consumption rate
Power	kW	Engine power
IMEP	kPa	Indicated mean effective pressure
SFC	kg/kW.h	Specific fuel consumption
Therm		*Thermal efficiency
Volef		Volumetric efficiency
Air	kg/h	Air consumption
Equiv		Equivalence ratio
%Bnt		Implied combustive efficiency
Pmax	kPa	*Maximum cylinder pressure
TGmax	K	*Maximum gas temperature
dPdt	MPa/s	*Maximum rate of pressure rise
dEdt	MW/kg	*Maximum apparent rate of heat release
dEpt	°CA	*Crank angle at which maximum apparent rate of heat release occurred
Ignit	°CA	Ignition point
End	°CA	End of combustion
Txst	°C	*Exhaust temperature
TWater	°C	Water temperature
Toil	°C	Oil temperature
TGave	°C	*Average gas temperature
Injec	°CA	Injection point
InDur	°CA	*Injection duration
Delay	°CA	*Ignition delay
CmDur	°CA	*Combustion duration
Smoke	Bosch	*Exhaust smoke level

* represents the variables which were included in the statistical analysis.
°CA denotes crank angle.

The results of the heat transfer analysis were also reduced by extracting average and peak values. In order to investigate the timing of heat transfer rate with respect to the timing of combustion, the point at which peak heat transfer rate occurred was recorded. The variables used to quantify the calculated rate of heat transfer are listed in table 3 along with their units and definitions.

Table 3. List of variables related to heat transfer with units and definitions.

Variable	Units	Definition
Speed	r/min	*Engine speed at which data were recorded
Torq	Nm	Load at which data were recorded
BMEP	kPa	*Brake mean effective pressure
TWmax	°C	Maximum wall temperature
TWmin	°C	Minimum wall temperature
TWave	°C	*Average wall temperature
TWtwo	°C	Temperature at the second thermocouple
MxCoef	$kW/m^2.°C$	*Maximum transient heat transfer coefficient
PtCoef	°CA	Point of maximum heat transfer coefficient
TrnsMx	kW/m^2	*Maximum transient heat transfer rate
TrnsPt	°CA	*Point of maximum heat transfer rate
TrnsAve	kW/m^2	*Average rate of heat transfer
TransNett	kJ	Net heat transfer during combustion
CoefAve	$kW/m^2.°C$	Average heat transfer coefficient

* represents the variables which were included in the statistical analysis.

The study of damaged pistons showed that the most common failure location was the piston bowl lip. The values of temperature, stress and life at this region were thus used to quantify the results of the finite element analysis. Measured cylinder head strain was simply quantified by extracting the amplitude of the strain signal. The variables used to quantify both the finite element analysis and cylinder head displacement are listed in table 4.

Table 4. List of variables from finite element and cylinder head displacement analyses.

PstTmp	°C	*Piston bowl lip temperature.
StrAmp		Piston bowl lip strain amplitude.
Life	h	*Piston life.
Strain	μV	*Cylinder head bolt strain amplitude.

* represents the variables which were included in the statistical analysis.

Two separate statistical analyses were then conducted. The first analysis involved consolidating all the variables from each test. Data recorded at engine idle conditions were not included in the analysis. Each variable was represented by twelve observations for each of seven tests, thus resulting in a sample size of more than 80 observations of each variable. The advantage of such a large sample was that any correlations observed would be conclusive. The large sample size would also contribute to narrow confidence intervals of regressions. The main objective of the analysis was to reach definite conclusions on the relationships between heat release variables and heat transfer rates.

Multiple observations of the finite element results were, however, not available for the statistical analysis. This was because the finite element analysis was used to determine engine life under cycling conditions for each test. This implied that only one observation of each variable for each test was available. The finite element results were thus not included in the analysis. All the inputs into the finite element analysis such as gas temperatures and heat transfer

coefficients were, however, included in the analysis. Exhaust smoke was only recorded at a single load point for each of the tests. Unlike the finite element results it was considered to contribute to the variations in both the heat release and heat transfer variables. Exhaust smoke was thus included in the analysis as a dummy variable.

A second analysis was then conducted to investigate the variation in the results of the finite element analysis. In this analysis the sample size was reduced to a single observation of each variable per test. Each variable was thus represented by seven observations. The value of each of the variables at a speed of 2000 r/min and a load of 700 kPa was used in the analysis. These values were determined by first conducting a third order polynomial regression of each variable as a function of load using all the data recorded at 2000 r/min. These regressions were then used to determine the value of the variable at 2000 r/min and 700 kPa. This process not only made it possible to interpolate between measured points, but also had the effect of averaging data. The points that were thus determined were relatively insensitive to outliers and were representative of most of the recorded data. The objective of the analysis was to investigate the effect of the different fuels and engine timing on the life of the engine, given the same speed and load conditions. The analysis was also conducted at a speed of 1700 r/min and load of 700 kPa. Finite element results were, however, not calculated at this engine speed condition.

Both these analyses were conducted with the aid of STSC Statgraphics. The extent of the correlation between variables was of greater interest than the actual relationships between these variables. This was investigated by recording the R^2 value which is the square of the correlation coefficient. The

R^2 value represents the proportion of the variation in the dependent variable that can be accounted for by the regression. The stepwise variable selection capability of Statgraphics was used to determine the significant independent variables. Independent variables were selected successively in order of decreasing significance, while the R^2 value was recorded at each stage. The sign of the coefficients were also recorded in order to show the effect of the independent variables on the dependent variable. By studying the effect of each variable on the R^2 value, it was possible to determine the relative role played by the independent variables on the dependent variables. The relationships between the different variables were thus identified.

7. DISCUSSION OF RESULTS

Six different fuels were tested and an additional test was conducted on coastal diesel with the injection timing advanced. The data recorded from these seven tests were then processed. Processing included the calculation of heat transfer rate, heat release rate, piston temperature, piston stresses and piston life. Values representing all relevant variables were then stored and used in a statistical comparison of the fuels. The relationships between different variables were then investigated. A summary of all the results is provided in the document while all the project data and results have been lodged at the Department of Agricultural Engineering, University of Natal, Pietermaritzburg, RSA.

7.1 Heat Release Analysis

The accuracy achieved in the analysis of all the data was indicated by the implied combustive efficiency. The average implied combustive efficiency of the 80 heat release analyses conducted was 95,5%. By excluding the analyses on data recorded at zero load and maximum fueling, the average increased to 97,4%. The 95% confidence interval of the average which was ± 1,1%, indicated that the heat release analysis achieved high levels of accuracy on a consistent basis. This is particularly evident when it is considered that the variation in implied combustive efficiency is the result of errors in fuel flow measurement and calorific value as well as error in the analysis. The fact that the average was slightly lower than 100% was satisfactory since it is unlikely that all the fuel will burn under ideal conditions in the engine.

The sensitivity studies proved that cumulative heat release which was the basis of implied combustive efficiency was far more

sensitive to errors in the analysis than peak rate of heat release. It was thus deduced that the accuracy of calculated peak rate of heat release was higher than that of the implied combustive efficiency. The confidence interval of calculated peak rate of heat release was also considerably smaller than that of implied combustive efficiency. A summary of the heat release results of all the tests is listed in table 5. This table includes all the significant variables for each fuel at a particular load and two different speeds.

Table 5. A summary of the heat release results and smoke measurements for all the tests.

Speed = 2000 r/min					BMEP = 700 kPa		
	CSTL	TMNG	SASL	NAPT	15ET	25ET	ETHN
Smoke	4.69	3.83	4.25	4.04	3.69	3.3	0.21
Delay	7.5	8.8333	7.3333	7.3333	8.25	9	10.166
Pmax	8298.5	9172.4	8217.3	8278.4	8363.4	8827.3	9294.2
TGmax	2231.3	2375.4	2320.7	2278.7	2196.6	2387.4	2331.1
dPdt	13953.	16858.	12484.	14337.	16957.	23817.	10655.
dEdt	2326.5	2916.2	2102.4	2394.5	2763.7	4117.3	2190.4
dEpt	357.45	353.54	356.46	357.55	358.33	358.42	359.24
Txst	607.03	632.41	619.51	613.76	592.24	640.11	547.61
Therm	0.3184	0.3095	0.3214	0.3137	0.3267	0.3248	0.3173
InDur	20.197	19.907	19.620	20.571	20.417	21.487	25.127
CmDur	45.017	38.767	43.663	45.354	44.661	40.220	37.797
TGave	530.51	558.35	559.13	542.97	520.66	566.99	515.50
Speed = 1700 r/min					BMEP = 700 kPa		
	CSTL	TMNG	SASL	NAPT	15ET	25ET	ETHN
Delay	7.1666	7.8333	6.6666	7.3333	8	8.5	9.6666
Pmax	8245.9	9464.4	8367.2	8319.8	8733.9	8789.7	9563.0
TGmax	2081.7	2288.0	2209.4	2148.7	2156.8	2221.6	2248.9
dPdt	10911.	13244.	10989.	11946.	16957.	16742.	10470.
dEdt	1710.4	2253.6	1746.6	1900.5	2544.2	2963.2	2009.9
dEpt	355.76	352.12	355.39	356.24	356.19	357.26	357.00
Txst	539.81	606.20	553.03	550.13	525.51	575.84	515.60
Therm	0.3252	0.3048	0.3246	0.3243	0.3267	0.3242	0.3110
InDur	17.372	18.468	17.810	17.850	17.550	18.946	22.970
CmDur	48.938	47.042	46.919	47.840	43.818	44.176	36.261
TGave	480.02	529.72	512.53	497.28	486.14	515.96	487.78

In order to investigate the range of variation and to determine which fuels lay at the extremes the maximum and minimum values were extracted from table 5. This information is displayed in table 6.

Table 6. Extreme values of the heat release variables and smoke density.

	Speed = 2000 r/min BMEP = 700 kPa		Speed = 1700 r/min BMEP = 700 kPa	
	Maximum	Minimum	Maximum	Minimum
Smoke	4.69 CSTL	0.21 ETHN		
Delay	10.166 ETHN	7.3333 SASL	9.6666 ETHN	6.6666 SASL
Pmax	9294.2 ETHN	8217.3 SASL	9563.0 ETHN	8245.9 CSTL
TGmax	2387.4 25ET	2196.6 15ET	2288.0 TMNG	2081.7 CSTL
dPdt	23817. 25ET	10655. ETHN	16957. 15ET	10470. ETHN
dEdt	4117.3 25ET	2102.4 SASL	2963.2 25ET	1710.4 CSTL
dEpt	359.24 ETHN	353.54 TMNG	357.26 25ET	352.12 TMNG
Txst	640.11 25ET	547.61 ETHN	606.20 TMNG	515.60 ETHN
Therm	0.3267 15ET	0.3095 TMNG	0.3267 15ET	0.3048 TMNG
InDur	25.127 ETHN	19.620 SASL	22.970 ETHN	17.372 CSTL
CmDur	45.354 NAPT	37.797 ETHN	48.938 CSTL	36.261 ETHN
TGave	566.99 25ET	515.50 ETHN	529.72 TMNG	480.02 CSTL

It is interesting to note that while the rates of combustion and pressure rise varied by as much as 94% of the reference value, peak pressure varied by less than 16%. Calculated peak rates of heat release for all the tests are plotted as a function of load in figure 21. Variation in peak pressure is illustrated in a similar manner in figure 22. There can be no doubt that the heat release results are significant since the variation in calculated rate of heat release is many orders of magnitude greater than the confidence interval of the analysis. The same applies to recorded pressure, where measured variations far exceed expected measurement errors.

The broad range of combustion rate and peak pressure illustrated in figures 21 and 22 indicated that the fuels selected for testing

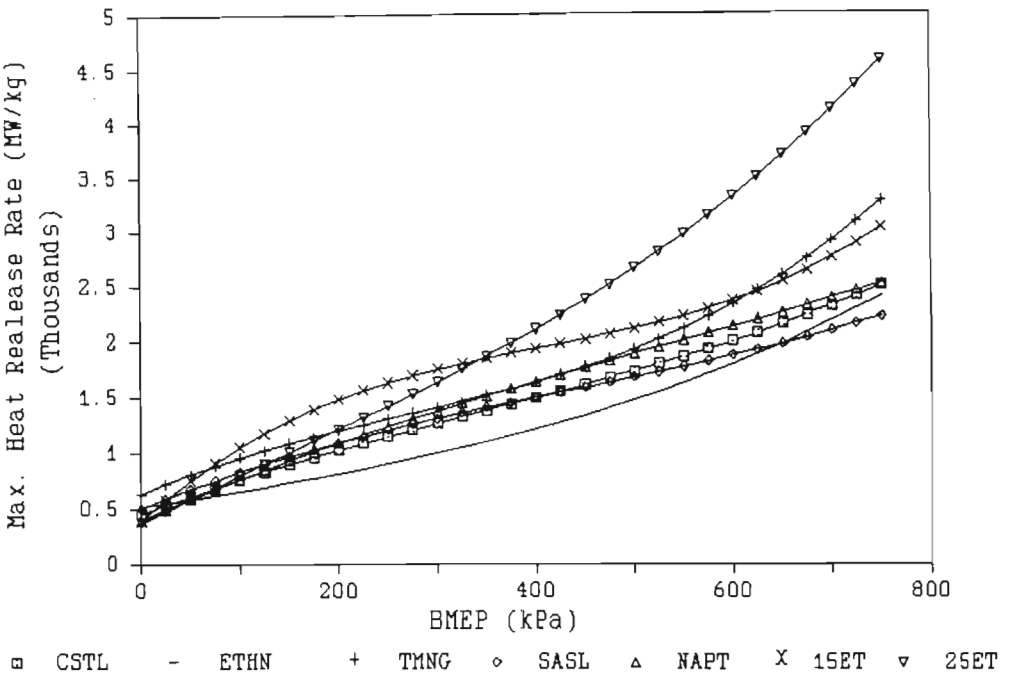

Figure 21. Peak rate of heat release for the different tests as a function of load.

were a representative sample. Not only did the peak combustion rate vary, but factors such as the relative rates and durations of premixed and diffusion combustion varied. This is illustrated in

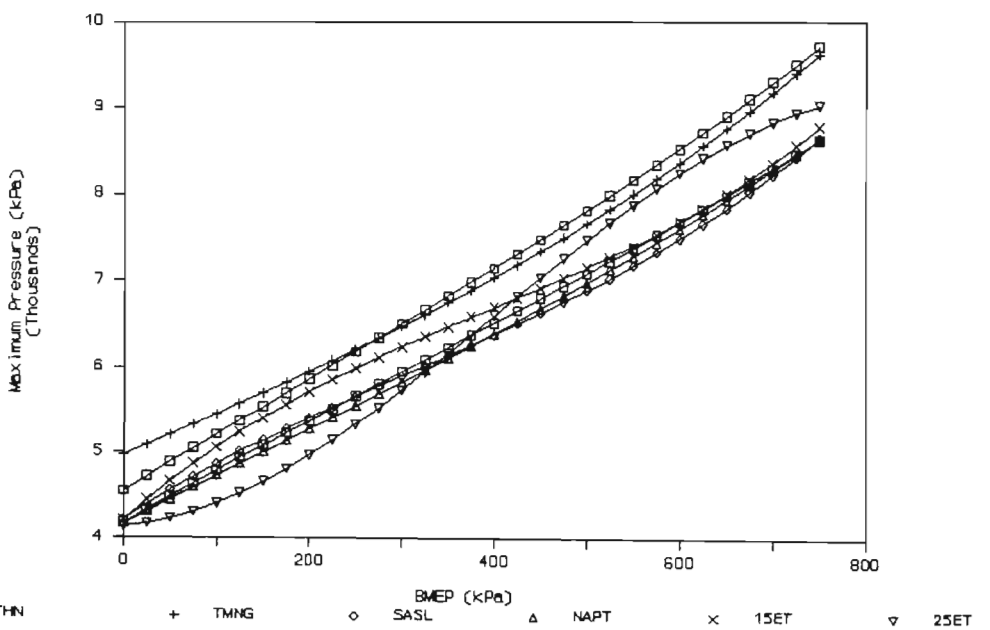

Figure 22. Peak pressure for all the tests as a function of load.

figure 23 where the calculated rate of heat release at a particular engine condition is plotted for coastal diesel, the 25% ethanol blend and ethanol.

The ethanol fuel resulted in the highest peak pressure while it had the lowest rate of pressure rise. The reasons for the low maximum rate of pressure rise are the moderate peak rate and retarded timing of the peak rate of combustion. This fuel exhibited a particularly gradual rate of increase of combustion rate after ignition. The unusually compact distribution of combustion rate, short combustion duration and relatively advanced injection timing are the cause of the high peak pressure.

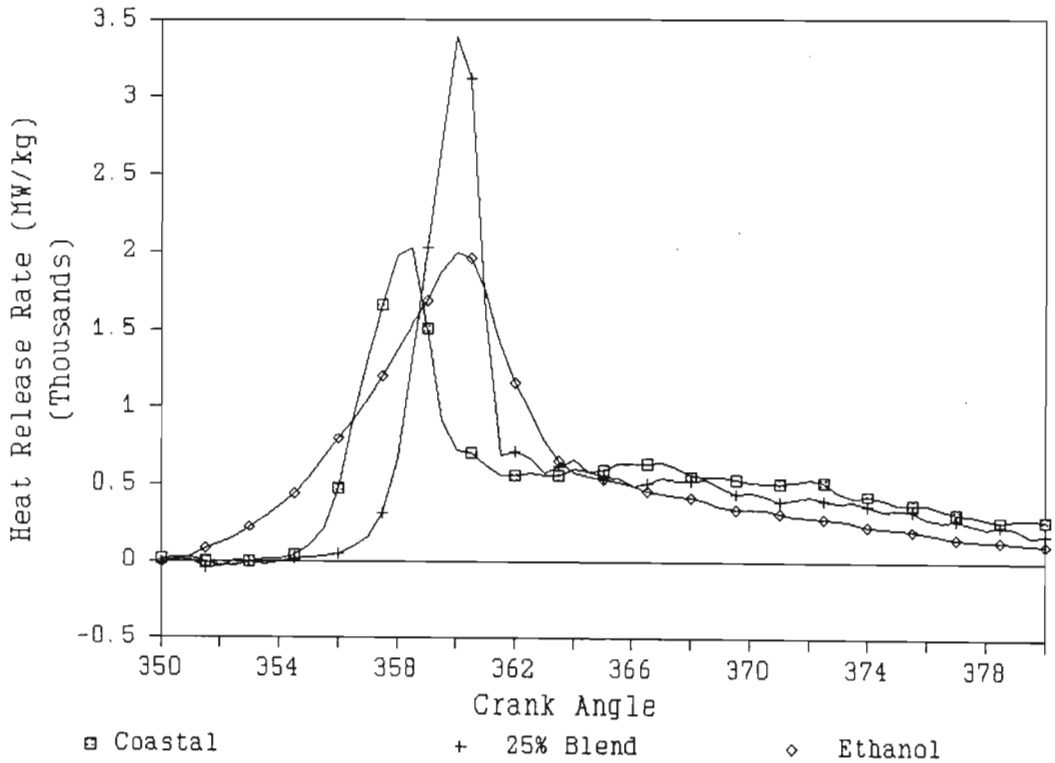

Figure 23. Heat release curves for coastal diesel, the 25% ethanol blend and ethanol at 2000 r/min and 200 Nm.

The addition of ethanol to coastal diesel tended to reduce the smoke emission while the ignition delay increased. The increased ignition delay resulted in higher rates of energy release and pressure rise. This led to increased peak pressures. The extended

ignition delay tended to minimize the increase in peak pressure by retarding combustion. Peak gas temperature is normally expected to increase with peak pressure. The addition of ethanol, however, increases the heat capacity of combustion products. This compensated for the increased peak pressure, to some extent, by limiting the increase in gas temperature. The addition of ethanol also tended to reduce exhaust temperature to a point. The reduced calorific value due to the addition of ethanol increased the duration of injection. The duration of combustion was reduced by the increased addition of ethanol. These observations correspond with the results of Taylor (1987).

Differences between the combustion of coastal diesel and Secunda diesel were found to be small. Secunda diesel displayed slightly superior behaviour at 2000 r/min while coastal performed slightly better at 1700 r/min. The differences were on the whole relatively insignificant. The addition of 37,5% hydrotreated straight run tops to coastal diesel had a surprisingly small effect on the nature of the combustion. Rate of pressure rise was increased by less than 10% while peak pressure was lower at 2000 r/min and higher at 1700 r/min.

Advancing injection timing by four degrees had a significant effect on the nature of combustion and the pressure development. Although the ignition delay was slightly increased the ignition point was advanced significantly. The advance, along with increased combustion rate, resulted in significant increases in both rate of pressure rise and peak pressure. Exhaust temperature was also increased. The increased exhaust temperature was one of the reasons for the reduction in thermal efficiency which amounted to as much as 6,3%. Further investigation of the results required a statistical analysis. This also allowed the heat release results to be compared with the results of the heat transfer and finite element analyses.

7.2 Heat Transfer

The success of the entire project depended on the sensitivity and repeatability with which heat transfer rate was measured. It was necessary to ensure that factors such as varying ambient conditions and non-representative soot layer on the probe had not played a significant role in the measured variations in heat transfer. This was done by repeating the heat transfer measurements for all the tests at the end of the project. Readings were taken at a single load point and then compared to the data recorded previously. It was found that the original data correlated well with the data recorded at the end of the project. Differences in the measured rate of heat transfer were thus proved to be representative of the actual conditions in the engine during the various tests.

The role played by soot was also investigated. A test was run at constant load starting with a clean probe. Readings were taken at frequent intervals for forty five minutes. The variation with time, in the measured rate of heat transfer was then investigated. Coastal diesel was used since it produced the highest smoke levels. The investigation proved that the 30 minute period allowed for the probe to become fouled, was adequate. The rate of heat transfer reached an equilibrium state within minutes of the engine being started.

The measured rate of heat transfer did, however, fluctuate in a cyclic manner. These fluctuation could not be attributed to variation in speed or load. Similar variations were observed by Hohenberg (1979) and Saugerud (1981) but neither of these researchers could offer any explanation. It is thought that these fluctuation were the result of instability of the cooling system or ambient air temperature. The magnitude of the fluctuations were, however, small when compared to the measured differences between fuels. Measured heat transfer rates were thus

representative although the fluctuations were expected to have a detrimental effect on correlations to a limited extent.

The investigation and the good correlation between calculated average rate of heat transfer and measured temperature difference proved that the measured differences between the different tests were significant. The linear correlation between average rate of heat transfer and the measured temperature gradient proved that the assumptions made in the calculation of heat transfer rate were valid. The measured heat transfer data were thus proved to be valid. A summary of the heat transfer results at two particular load conditions are displayed in table 7.

Table 7. A summary of the heat transfer results at two speed settings.

Speed = 2000 r/min				BMEP = 700 kPa			
	CSTL	TMNG	SASL	NAPT	15ET	25ET	ETHN
TWave	298.31	328.79	294.35	298.96	305.88	325.62	348.55
MxCoef	3.0084	2.8579	3.2374	3.3811	3.3340	2.7506	3.7392
TrnsMx	4550.9	4609.3	4741.3	5013.2	4796.9	4727.8	6198.8
TrnsPt	364.04	360.12	362.62	362.90	363.45	364.50	361.85
TrnsAve	337.06	357.17	333.39	337.50	331.99	349.48	342.64

Speed = 1700 r/min				BMEP = 700 kPa			
	CSTL	TMNG	SASL	NAPT	15ET	25ET	ETHN
TWave	282.43	304.61	272.69	275.49	284.84	303.45	328.22
MxCoef	3.4417	2.8321	3.1205	3.5105	3.1692	3.0278	4.3342
TrnsMx	4569.0	4282.6	4535.5	4800.0	4704.6	4777.6	5707.6
TrnsPt	365.54	358.87	362.75	362.38	362.20	362.66	359.10
TrnsAve	314.62	338.55	309.22	309.94	311.14	336.51	331.05

In order to get an idea of the range of variation in the different variables the maximum and minimum values of each variable were extracted. This information is displayed in table 8 along with the name of the fuel corresponding with the maximum and minimum

values.

Table 8. Extreme values of the heat transfer variables at two speed settings.

	Speed = 2000 r/min BMEP = 700 kPa				Speed = 1700 r/min BMEP = 700 kPa			
	Maximum		Minimum		Maximum		Minimum	
TWave	348.55	ETHN	294.35	SASL	328.22	ETHN	272.69	SASL
TrnsMx	6198.8	ETHN	4550.9	CSTL	5707.6	ETHN	4282.6	TMNG
TrnsPt	364.50	25ET	360.12	TMNG	365.54	CSTL	358.87	TMNG
TrnsAve	357.17	TMNG	331.99	15ET	338.55	TMNG	309.22	SASL

The range of variation in surface temperature was found to exceed 50°C for the different tests. Although variations in ambient conditions contributed to this variation, there was no doubt that the fuel used was responsible for most of the measured variation. The maximum rate of heat transfer was found to vary by a greater extent than average rate of heat transfer. Maximum and average rates of heat transfer are shown as a function of load, respectively in figures 24 and 25.

It can be seen in figure 26 that the shape of the calculated rate of heat transfer was highly dependent on the engine timing and the fuel used. An indication of the repeatability of the heat transfer measurement and calculation can be derived by comparing the rates of heat transfer calculated during the compression stroke. Variation in wall temperature, inlet temperature, soot layer and injection were expected to result in some variation in heat transfer during compression. It can, however, be seen in figure 26 that, despite these factors, calculated heat transfer rate during compression correlated well for the different tests. Variations in combustion behaviour were thus clearly the most significant cause of the measured variations in heat transfer rate. Recorded heat transfer data were found to be significant in that

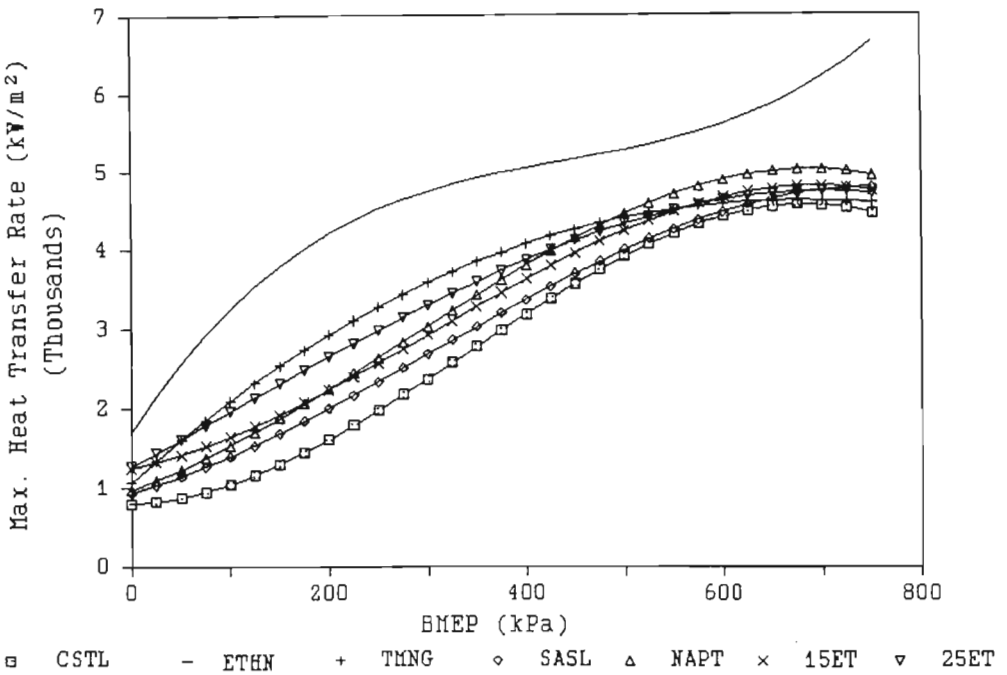

Figure 24. Maximum rate of heat transfer at 2000 r/min.

the measured variations far exceeded measurement errors. The experimental procedures and calculation techniques, including all assumptions, were thus proved to be correct.

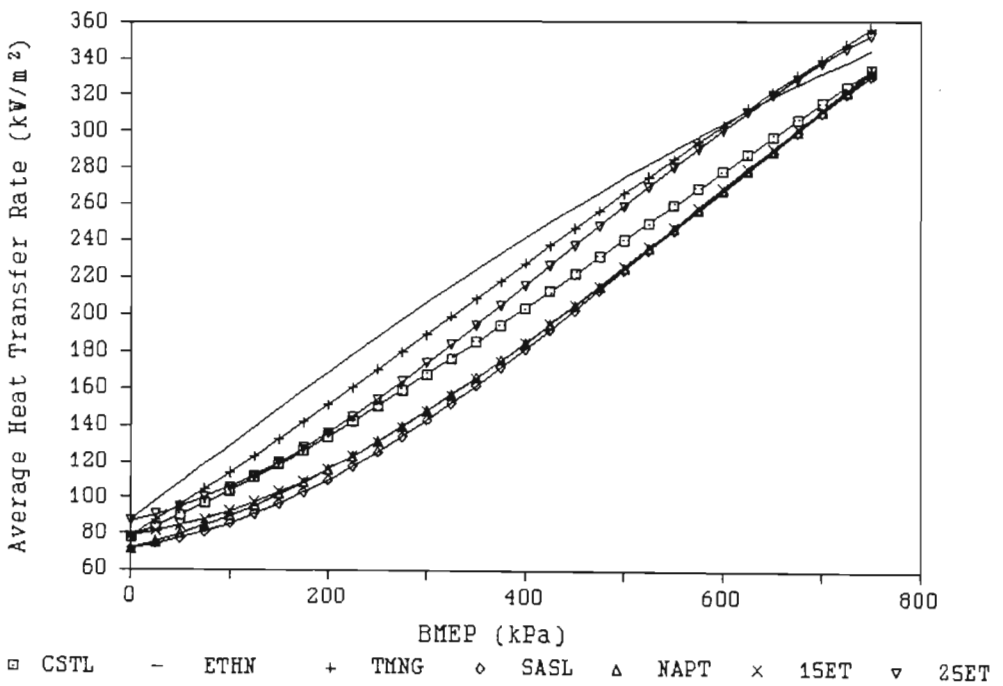

Figure 25. Variation of average rate of heat transfer with load at 2000 r/min.

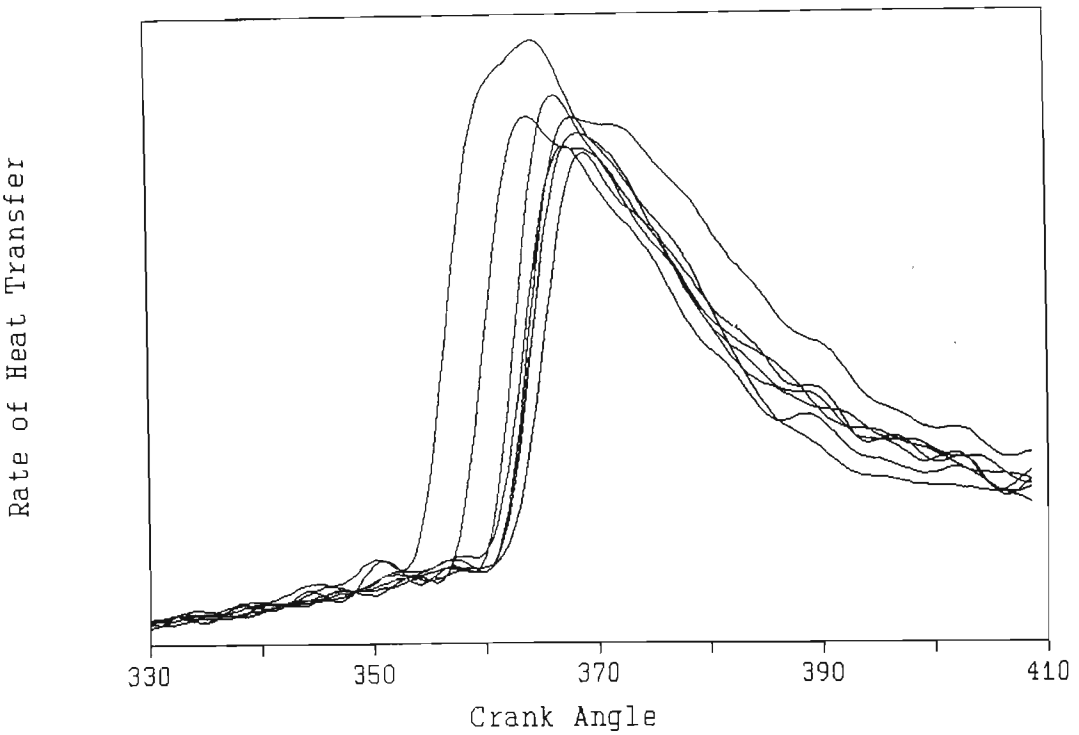

Figure 26. Rate of heat transfer calculated from measured surface temperature for all the tests at 2000 r/min and 150 Nm.

7.3 Finite Element Analysis

The results of the finite element analysis were found to correspond well with published results, particularly the calculated temperature distributions (Sander and Schoeckle, 1979; Buchta, 1981; Wacker and Sander, 1982 and Reipert et al., 1983). Piston temperatures were found to be slightly higher than those reported by other researchers. This was, however, to be expected since the pistons of the ADE 4.236 engine were known to be more susceptible to piston erosion and to cracking than those of other engines. In addition to this fact, many of the fuels tested were of far lower quality than the conventional diesel fuels.

The presence of the cast iron piston ring carrier and steel expansion control ring did not have a significant effect on the temperature distribution in the piston, but played a significant role in thermal stresses. Due to the large differences between the thermal expansion coefficients of the different metals in the piston high stresses resulted even at engine idle conditions. Both the piston ring carrier and expansion control ring tended to constrain the expansion of the aluminium alloy placing it in compression. Life predictions were only conducted at the piston bowl lip because the finite element model was designed to be most accurate at this location and because failures were known to occur at this location in practice.

The rate at which a load is applied to a structure can play a role in the magnitude of the resulting stresses in that structure. As the time of application approaches zero, so the transient peak stress approaches a value equal to double the static stress. Whether or not this effect plays a significant role in the stresses in engine components, depends on the ratio of stiffness and inertia of the component and the rate at which the load is applied. The rate of load application in the engine was proved to be highly dependent on the fuel used. This was indicated by the fact that the peak rate of pressure rise varied by more than 120% of the lowest value, as a result of fuel properties. The nature of combustion would thus affect the stresses in any components which are sensitive to the rate of pressure rise.

It was thus necessary to ascertain whether or not the stiffness-inertia ratio of the piston was such that it was affected by the rates of pressure rise occurring in the engine. This was done by performing a transient dynamic finite element analysis on the piston. It was found that dynamic stresses in the piston were directly proportional to cylinder pressure to within 0,2%. An analysis of the discrepancy between cylinder pressure and stresses

showed that the discrepancy was due to piston inertia. During rapid pressure rise the piston stresses lagged behind pressure and when the pressure dropped the stress overshot.

Peak dynamic strain was 1,8% lower than the strain calculated by a static analysis where a steady pressure equal to peak cylinder pressure was applied. This difference was attributed to the fact that the two calculation methods involved large and different calculation procedures. Round-off errors and acceptable calculation errors could be responsible for a discrepancy of as much as 1,8%.

These analyses proved that the rate of pressure application did not have a significant effect on the levels of mechanical stress in the piston. The peak pressure was thus all that was required for the calculation of mechanical stresses in the piston. Static analyses were subsequently used to determine the pressure induced strain amplitude for the purpose of life prediction.

Thermal stresses were then investigated. The transient analysis of piston temperature during one engine cycle showed that only the material at the surface was affected by high cycle thermal loading. The range of measured cyclic temperature variation was 28,4°C at the probe, while the range of calculated temperature variation at the bowl lip was only 14,7°C. Calculated temperature variation in the material on the crown outside the piston bowl was only 9,4°C. Calculated transient surface temperature variations at different locations in the piston are illustrated in figure 27. The reason for the lower range of surface temperature variation at the piston was that the thermal heat capacity and thermal conductivity of the aluminium alloy was far greater than that of the probe. The shape of the calculated surface temperature curves were, however, similar to that of the measured curve.

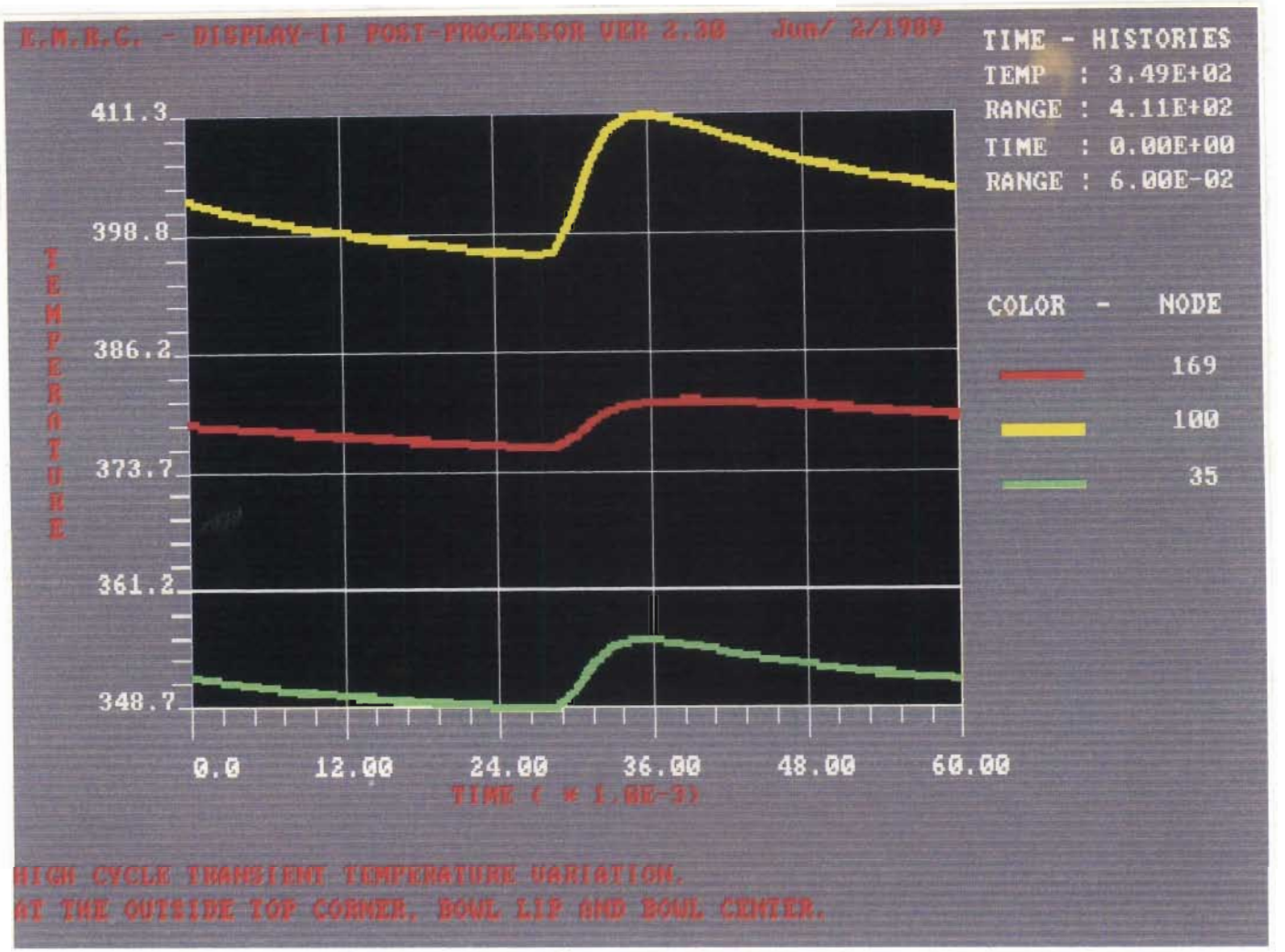

Figure 27. Calculated transient temperature at three locations in the piston over one engine cycle. The piston bowl lip temperature is represented by node 100, the outside corner of the piston crown by node 169, and the centre of the combustion bowl by node 35 in the finite element model.

The strain amplitude which would result from high cycle thermal loading was then determined. Both plastic and elastic analyses were conducted. The results of both these analyses showed that the strain amplitude resulting from high cycle thermal loading was not large enough to play a significant role in fatigue failure of the piston. The strain amplitude calculated using the elastic analysis

was considered to be more representative for purposes of life prediction. The analysis indicated that high cycle thermal loading played no role at all in piston failure.

The effect of a step change in engine load was then investigated. A transient heat transfer analysis showed that the piston took at least 100 seconds to approach an equilibrium temperature distribution after a large load step. This can be seen in figure 28. Temperature gradient across the piston, however, reached a maximum within 20 seconds of the change in load. Temperature gradient then decreased slightly as the temperatures approached equilibrium. At the time when the temperature gradient was greatest, the actual piston temperatures were well below the equilibrium temperatures.

A non-linear thermal stress analysis on this temperature data predicted extremely high transient stresses shortly after the load step. This was because the material in the region of the piston bowl lip was placed under compression at a time when it was at a relatively low temperature. The result was that the material, being cool, could resist the compressive strain by experiencing high stress levels. As the material approached equilibrium temperature it's stiffness and yield point decreased. The bowl lip would then yield and thus relieve stresses in the piston considerably. A non-linear analysis was thus found to yield a transient stress peak shortly after a step change in engine load. This corresponded with the results of Munro (1979) and Francis (1986). This, however, only applies to an unused piston which is rapidly loaded for the first time and should thus not be used to predict the life of the piston.

A piston which undergoes plastic deformation as a result of thermal stresses becomes pre-stressed after the first few cycles whereafter it experiences elastic deformation. Linear thermal stress analyses

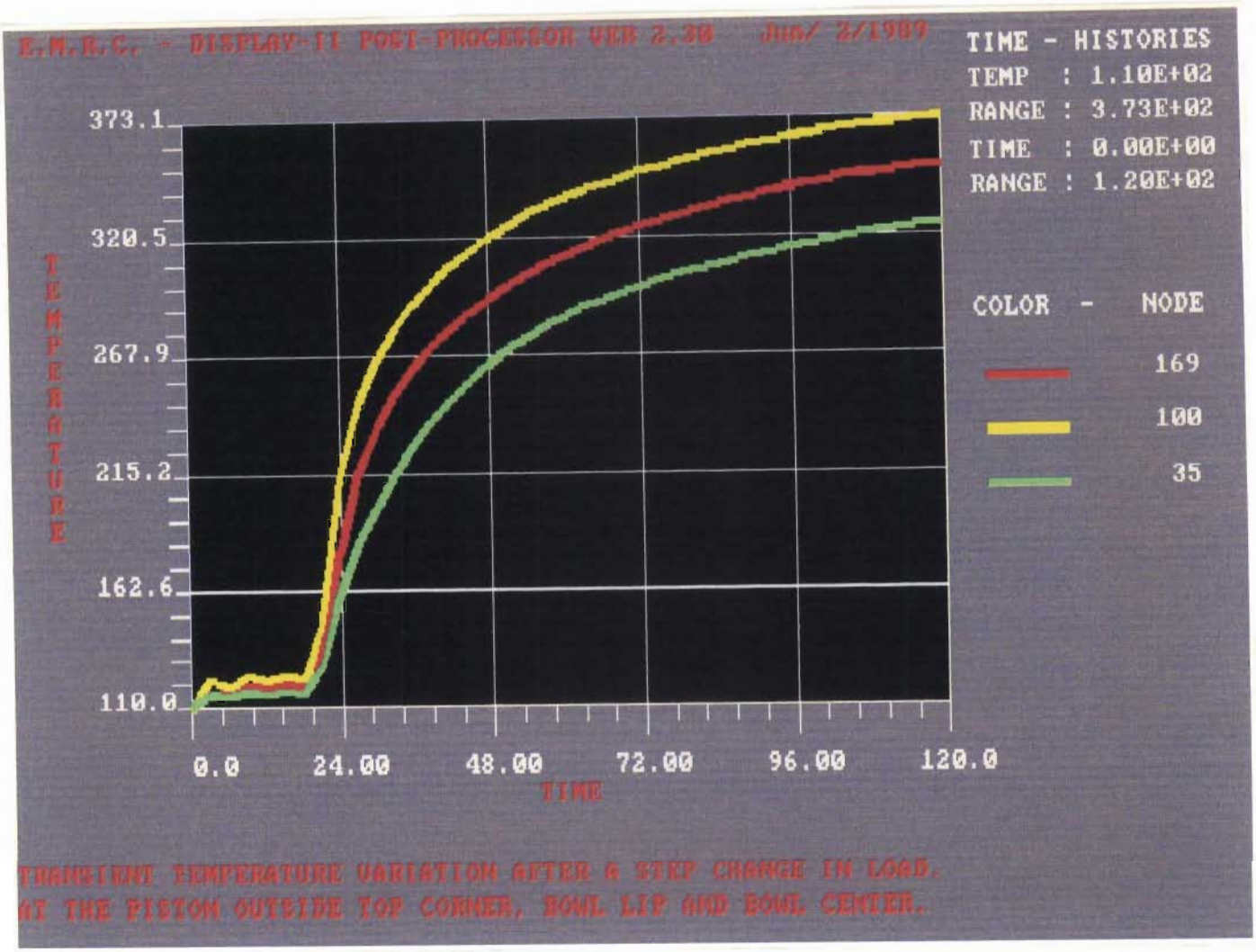

Figure 28. Transient piston temperature resulting from a step change in engine load. The piston bowl lip temperature is represented by node 100, the outside corner of the piston crown by node 169, and the centre of the combustion bowl by node 35 in the finite element model.

were then conducted and indicated that thermal stresses after a load step never exceeded the equilibrium value. It was thus not necessary to conduct transient temperature and stress analyses to determine the actual strain amplitude. Low cycle thermal strain amplitudes were thus determined by first conducting a steady state heat transfer analysis and then conducting a non-linear static

Figure 29. Temperature distributions for coastal diesel with standard and advanced timing and for the ethanol fuel.

dimensional finite element model represented the actual conditions in the engine adequately. The inclusion of the expansion control ring and the piston ring carrier in the model was important. These two elements play a significant role in the thermal deformation of the piston. This observation is supported by the fact that the clearance required between this piston and the liner is half of that required for solid aluminium pistons. This is because thermal deformation is not controlled in the solid aluminium piston. It

is interesting to note that the range of variation in predicted piston life far exceeded the variation in any of the variables which were used in the calculation. It is thus evident that piston life is highly sensitive to variation in thermal loading.

Table 9. A summary of the finite element results for all the tests.

	CSTL	TMNG	SASL	NAPT	15ET	25ET	ETHN
PstTmp	351.3	377.5	351.6	353.3	353.4	373.3	381.8
StrAmp	1.6554	1.8993	1.6578	1.6731	1.6726	1.8609	1.9360
Life	8012.7	3721.2	7944.3	7535.5	7542.4	4159.0	3352.3

7.4 Dynamic Mechanical Stress

Dynamic mechanical stresses were investigated in two ways. Firstly, by investigating measured cylinder head displacement and secondly, by calculating dynamic mechanical strain in the piston. The finite element analysis proved that rates of pressure rise, even with the worst fuel, were not fast enough to affect the piston stresses. The stiffness to mass ratio of the piston was too high for dynamic effects to play a role. Rates of pressure rise did, however, affect the cylinder head displacement.

Measured cylinder head displacement was not directly proportional to cylinder pressure. Displacement tended to lag behind peak pressure and then overshoot when the pressure dropped. The cylinder head then oscillated. Theoretical cylinder head displacement was calculated from measured cylinder pressure with the aid of the mass-spring-damper model that was developed. An example of measured and calculated cylinder head displacement is illustrated in figure 30. In a similar manner cylinder pressure was calculated from measured cylinder head displacement. An

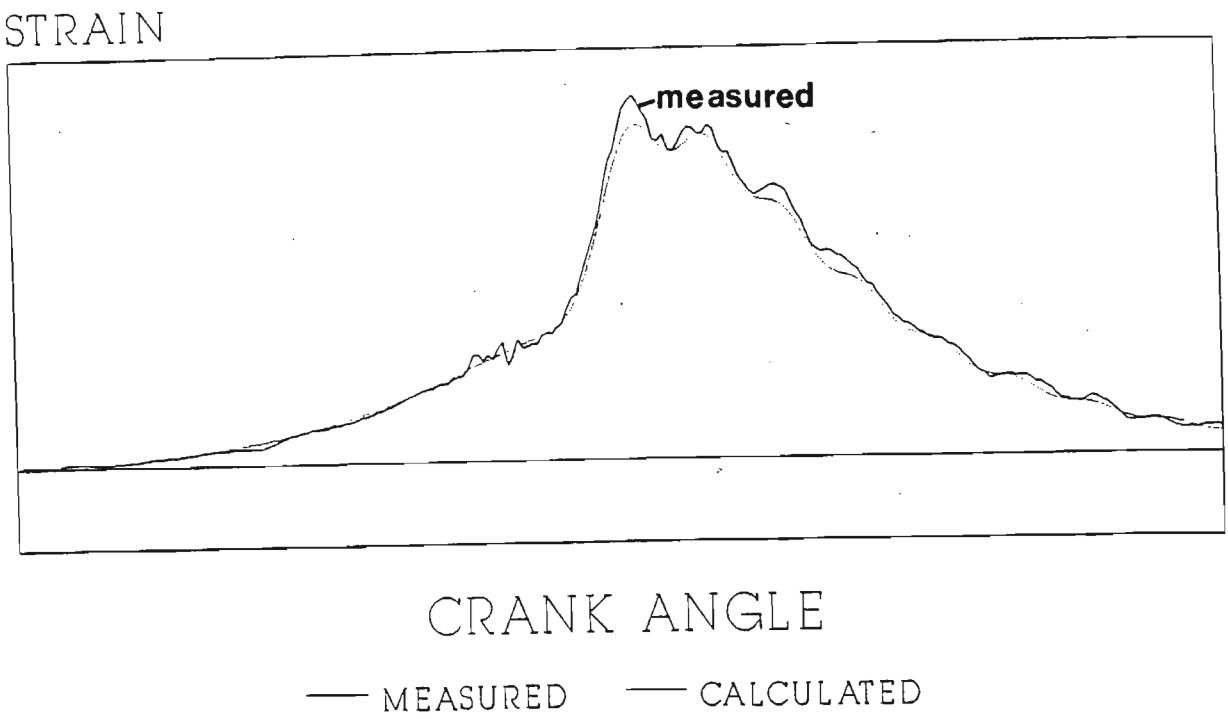

Figure 30. Measured and calculated cylinder head displacement at 1700 r/min and 191 Nm.

example of measured and calculated cylinder pressure is illustrated in figure 31.

It was found that calculated pressures and displacements correlated well with measured data. These results proved that the relationship between dynamic stress and pressure development was determined by the stiffness, mass and damping of the system.

The relative roles of peak pressure and peak rate of pressure rise in measured strain were then investigated. This was done by performing a statistical analysis on all the measured data. It was found that 99,90% of the variation in measured cylinder head displacement amplitude was accounted for by the variation in peak pressure and peak rate of pressure rise. This was achieved by conducting a linear regression of strain on peak pressure and peak

rate of pressure rise with a constant of zero. There should in fact be no constant in the regression, since a pressure and rate of pressure rise of zero would yield zero strain.

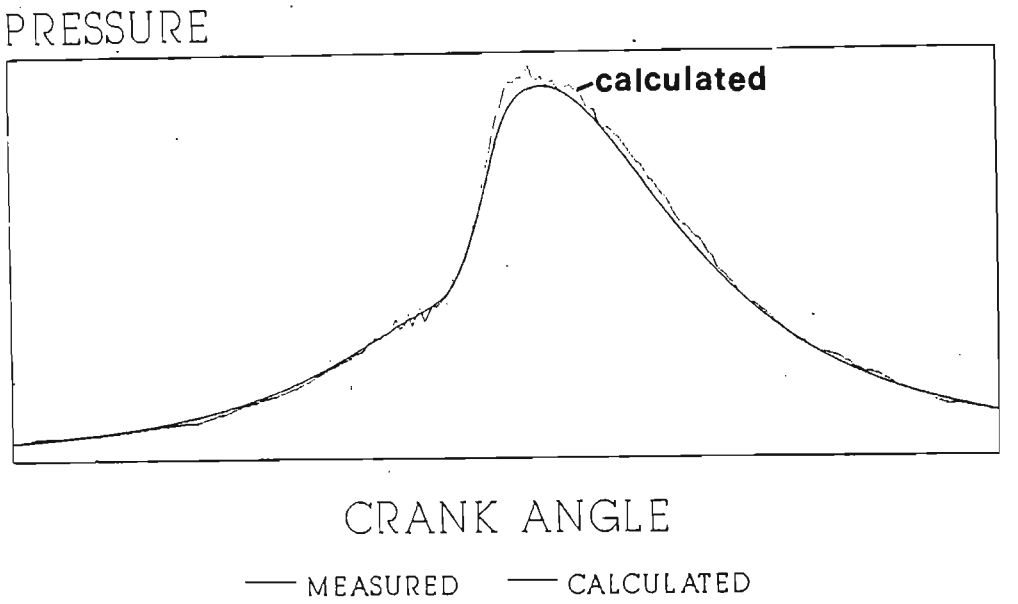

Figure 31. Measured and calculated cylinder pressure at 1677 r/min and 191 Nm.

The strong correlation between cylinder pressure and strain proved that a high standard of accuracy had been maintained throughout the measurement of strain. This was despite the fact that the strain signal was extremely small. The measurement and calibration techniques used for the project were clearly accurate and consistent at all times. It is important to note that identical calibration procedures were used for the calibration of the surface temperature measurement.

The relationship between strain amplitude and peak pressure and maximum rate of pressure rise is as follows:

$$\text{Strain Amp.} = 0{,}024208 \cdot P_{max} + 0{,}004101 \cdot dP/dt \qquad (21)$$

The significance of the contributions to cylinder head displacement, of pressure and rate of pressure rise can be determined by considering the results for coastal diesel. At 2000 r/min and 700 kPa, peak pressure was 8298,5 kPa and the maximum rate of pressure rise was 13953 MPa/s. If the rate of pressure rise were to increase by 20,8% to that measured when the timing was advanced, without a change in peak pressure, then equation 21 would predict a 4,6% rise in strain. If the rate of pressure rise increased by 70,7% to that measured for the 25% ethanol blend, without a change in pressure, then strain would increase by 15,7%. Cylinder head bolt strain is thus affected significantly by extreme variations in rate of pressure rise as would be the case with other engine components which have low stiffness to mass ratios. The piston, cylinder liner and cylinder head flame plate would, however, be affected to a smaller extent. This is confirmed by the results of the transient dynamic finite element analysis.

Possibly the only component which could suffer detrimental effects as a result of high rate of pressure rise, is the crankshaft. Not only does it have a low stiffness to mass ratio (Miyamoto, 1980), but it is also known to fail from time to time. The crankshaft usually fails at the main bearing journals and not at the big end bearing journals. This implies that failure is the result of reversed torsion and not reversed bending. Since high rates of pressure rise occur in the region of top dead centre, they would only affect the bending stresses in the crankshaft and not the torsional stresses. It is thus unlikely that the rate of pressure application has a significant effect on the mechanical loading of those components in the diesel engine which are prone to failure. Rates of pressure rise should thus only be controlled in order to achieve noise reduction (Hardenberg, 1986), reduced vibration and smooth engine operation.

The information required was in fact the relative role played by the independent variables on the dependent variable. This was best illustrated by the square of the correlation coefficient or the R^2 value. The R^2 value represents the proportion of the variation in the dependent variable which can be explained by the regression. The statistical analyses were normally limited to multiple linear regressions. Since the objective of the analyses was to determine the relative role of different variables, non-linear regressions were seldom applied. Care was taken to keep the ratio of the number of regression coefficients to the number of observations at realistic levels.

The results of the complete statistical analysis are illustrated in table 10. In this table the maximum and minimum values of each variable are displayed along with the range of variation expressed as percentages of the reference and maximum values. The data for coastal diesel were used as reference values. The independent variables are then displayed in order of decreasing significance along with the sign of the regression coefficient. Variables not illustrated did not play a significant role in the variation in the dependent variable. Variables which were clearly the effect of the dependent variable and not the cause, were excluded from the regression. Independent variables were added to the regression one at a time and the R^2 value at each stage was recorded. The R^2 values are listed below each variable in table 10.

It can be seen in table 10 that most of the variation in recorded variables could be attributed to the variation in other variables. Almost all the variation in peak pressure, gas temperature, rate of pressure rise, cylinder wall temperature and heat transfer rate could be attributed to variations in measured or calculated variables. This served to indicate that these variables were in fact determined precisely. It was, however, evident that the variation in some of the primary variables such as peak rate of

heat release, combustion duration, ignition delay and exhaust smoke was not entirely explained by the measured variables. This implied that these variables were also influenced by factors other than those recorded.

Table 10. Results of the complete statistical analysis showing the range of variation in the dependent variables and the contribution of the independent variables.

Dependent Variable	Minimum	Maximum	Range as a % of Ref.	Range as a % of Max.
= f(Independent variables: 1 to N) R^2 : 1 to N as a %.				
Speed	1700	2000	15%	15%
Cause: No independent variables.				
BMEP	0	818.9	100%	100%
Cause: No independent variables.				
Pmax	4152	10142	64.93%	59.06%
= f(+BMEP, -dEpt, +Delay, -CmDur, -Speed) 94.42 96.22 98.73 98.94 99.13				
TGmax	1081	2488	59.75%	56.55%
= f(+BMEP, +Speed, +Pmax, -CmDur) 96.76 97.83, 98.52, 99.03				
dPdt	1304	23644	140.51%	94.48%
= f(+dEdT, -dEpt) 97.02 98.42				
dEdt	321	4084	139.53%	92.14%
= f(+BMEP, +Speed, +Delay, -InDur) 77.55 80.37 81.49 83.61				

Table 10 continued

Dependent Variable	Minimum	Maximum	Range as a % of Ref.	Range as a % of Max.
= f(Independent variables: 1 to N) R^2 : 1 to N as a %.				
dEpt	351	373.5	6.06%	6.02%
= f(-BMEP, +Delay, +Speed) 68.21 75.26 77.50				
Txst	160.38	709.58	78.46%	77.40%
= f(+TGmax, +Smoke, +Indur) 95.17 97.37 97.64				
Therm	0.0	0.341	102.66%	100.00%
= f(+BMEP, $-BMEP^2$, $+BMEP^3$, -InDur, -TrnsAve) 68.85 97.32 99.28 99.43 99.47				
InDur	7	25.5	86.05%	72.55%
= f($+BMEP^2$, -Smoke, +Speed, $-BMEP^3$) 82.36 88.79 92.78 95.10				
CmDur	25.5	55	53.64%	53.64%
= f(+BMEP, +Smoke, -dEdt, -Delay) 78.66 85.74 88.87 90.15				
TGave	189.78	603.21	70.81%	68.54%
= f(+Txst, +TGmax, -Pmax) 98.93 99.78 99.90				
Delay	5.5	11.5	80%	52.17%
= f(+Indur, $-BMEP^2$, $+BMEP^3$) 41.76 49.28 56.29				
Smoke	0.21	4.69	95.52%	95.52%
= f(+Delay,+CmDur, -InDur, +Txst, -Pmax) 9.50 20.49 51.43 60.77 73.58 (Note: Smoke is a dummy variable.)				

Table 10 continued

Dependent Variable	Minimum	Maximum	Range as a % of Ref.	Range as a % of Max.
= f(Independent variables: 1 to N) R^2 : 1 to N as a %.				
TWave	140.01	353.54	65.42%	60.40%
= f(+Pmax, +InDur, +dEdt, +Speed, -Smoke, +$BMEP^2$) 94.57 98.55 98.92 99.04 99.13 99.33				
MxCoef	1.0459	4.8157	108.36%	78.28%
= f(+Pmax, -Smoke, -$BMEP^3$, -dEdt) 53.04 71.19 79.17 80.51				
TrnsMx	773.43	6256.3	121.77%	87.64%
= f(+BMEP, -Smoke, -$BMEP^3$) 79.14 91.09 96.80				
TrnsPt	358.02	381.54	6.17%	6.16%
= f(+dEpt, +Smoke, -BMEP, +CmDur, +$BMEP^3$) 86.06 92.75 95.30 95.60 95.83				
TrnsAve	71.127	386.21	84.75%	81.58%
= f(+TGmax, +$BMEP^2$, -Smoke) (Combustion variables) 97.50 97.81 98.25 or = f(+TwAve, +TrnsMx, +$BMEP^2$) (Heat transfer variables) 98.71 99.19 99.41				
Strain	98.657	313.55	78.65%	68.54%
= f(+Pmax, +dPdT) 96.05 98.96 or = f(+Pmax, +dPdt) by forcing the constant to zero. 99.49 99.90				
PstTmp	351.3	381.8	8.68%	7.99%
(dummy variable)				
Life	3352.4	8012.8	58.16%	58.16%
(dummy variable)				

It is well known that variables such as ignition delay, exhaust smoke and combustion rate and duration are affected to a large extent by the chemical and physical properties of the fuel. Since the quantification of the chemical and physical properties of the fuel did not fall within the objectives of the research, the incomplete correlations were no cause for concern. The determination of the relationship between fuel properties and combustion behaviour is a separate problem which is already being addressed.

Neither peak combustion rate nor peak rate of pressure rise correlated with peak cylinder pressure. It was found that apart from load and speed, the timing of combustion and the duration of both combustion and ignition delay determined the peak cylinder pressure. Contrary to what was expected, the rate of pressure rise did not correlate at all well with ignition delay. Variations in peak combustion rate and combustion timing did, however, account for the 98,42% of the variation in rate of pressure rise. Ignition delay accounted for a small proportion of the variation in peak rate of heat release.

It is important to note that 99,33% of the variation in measured wall temperature and 98,25% of the variation in calculated heat transfer rate were accounted for by variables determined from other transducers and calculations. These correlations serve to verify the accuracy of the heat flux probes and the related calculations and assumptions. The fact that other measurements from the heat flux probes accounted for 99,41% of the variation in calculated heat transfer rate also served to verify the calculation methods.

The presence of ethanol in some of the fuels tended to increase the injection duration at a particular load due to the reduced calorific value. The result was that injection duration played the role of calorific value and other fuel properties in some of the

regressions. An example of this is illustrated by the role played by injection duration in the regression of exhaust smoke emission. The coefficients of the regression indicate that increased duration of injection reduces smoke emission. This is known to be incorrect and is the result of the injection durations of the ethanol based fuels having an artificial "leverage" on the regressions. It was thus necessary to consider the effect of the presence of ethanol on injection duration and exhaust smoke in the interpretation of the regression results.

The results of the complete statistical analysis were then used to guide the second analysis in which speed and torque had been eliminated. The first analysis provided conclusive evidence as to which variables were interrelated. In the second analysis any variables which had been proved to play a role in the variation in the dependent variable were forced into the regression. In addition to these variables the automatic variable selection function of Statgraphics was allowed to select significant variables. Since the sample size was only 7 points, the resulting regression equations were not always considered to be statistically significant, particularly when the number of independent variables was large. This did not, however, present a problem because the objective of the analysis was merely to identify the relative interactions of the different variables. The results of the analysis are illustrated in table 11. The format used in table 11 is identical to that used in table 10. The name of the fuel which resulted in each extreme value is also listed. These results all apply to a condition of 2000 r/min and 700 kPa.

The elimination of speed and load from the statistical analysis resulted in a significant reduction in the range of variation in the variables. The remaining variation was the result of different fuel properties and test conditions alone. The lower R^2 values of the second analysis indicated that a smaller proportion of the

Table 11. Results of the second statistical analysis showing the range of variation in the dependent variables and the contribution of the independent variables.

Dependent Variable	Maximum Fuel Name	Minimum Fuel name	Range % of Ref.	Range % of Max.
= f(Independent variables: 1 to N) R^2 : 1 to N as a %.				
Pmax	9294.2 ETHN	8217.3 SASL	12.98%	11.59%
= f(-CmDur, +Delay, -dEpt) 94.13 95.50 97.60				
TGmax	2387.4 25ET	2196.6 15ET	8.55%	7.99%
= f(-CmDur, -Pmax) 59.49 74.22				
dPdt	23817. 25ET	10655. ETHN	94.33%	55.26%
= f(+dEdt, -dEpt) 95.00 95.39				
dEdt	4117.3 25ET	2102.4 SASL	86.61%	48.94%
= f(+Delay, -InDur) 8.99 36.09				
dEpt	359.24 ETHN	353.54 TMNG	1.60%	1.59%
= f(+Delay) 5.55				
Txst	640.11 25ET	547.61 ETHN	15.24%	14.45%
= f(+InDur, +TGMax, +Smoke) 58.91 87.65 93.72				
Therm	0.3267 15ET	0.3095 TMNG	5.38%	5.26%
= f(-TrnsAve,+InDur) 27.00 27.78 or = f(-TrnsAve,-CmDur) 27.00 30.70				

Table 11. continued.

Dependent Variable	Maximum Fuel Name	Minimum Fuel name	Range % of Ref.	Range % of Max.
= f(Independent variables: 1 to N) R^2 : 1 to N as a %.				
InDur	25.127 ETHN	19.620 SASL	27.27%	21.92%
= f(-Smoke) 93.73				
CmDur	45.354 NAPT	37.797 ETHN	16.78%	16.66%
= f(-Delay, -Smoke, +dEdt) 80.85 83.11 84.21				
TGave	566.99 25ET	515.50 ETHN	9.71%	9.08%
= f(+Txst, +TGmax, -Pmax) 79.80 95.39 99.23				
Delay	10.166 ETHN	7.3333 SASL	37.78%	27.86%
= f(+InDur) 66.96				
Smoke	4.69 CSTL	0.21 ETHN	95.52%	95.52%
= f(-InDur, +CmDur, +Txst, +Pmax, -Delay) 93.73 95.94 97.57 97.85 98.02				
TWave	348.55 ETHN	294.35 SASL	18.17%	15.55%
= f(+Pmax, +InDur, +dEdt, -Smoke) 94.53 98.90 99.65 99.86				
TrnsMx	6198.8 ETHN	4550.9 CSTL	36.21%	26.58%
= f(-Smoke, -dEdt) 89.11 96.14				
TrnsPt	364.50 25ET	360.12 TMNG	1.20%	1.2%
= f(+dEpt, +Smoke, -CmDur) 45.78 89.95 99.58				

Table 11. continued.

Dependent Variable	Maximum Fuel Name	Minimum Fuel name	Range % of Ref.	Range % of Max.
= f(Independent variables: 1 to N) R^2 : 1 to N as a %.				
TrnsAve	357.17 TMNG	331.99 15ET	7.47%	7.05%
= f(+TGmax, +Smoke) 63.66 63.91 or = f(+Pmax, +Smoke) 61.24 93.18				
PstTmp	381.8 ETHN	351.3 CSTL	8.68%	7.99%
= f(+Pmax, +TGmax, +TWave, +dEdt) 97.27 98.86 99.70 99.97				
StrAmp	1.9360 ETHN	1.6554 CSTL	16.95%	14.49%
= f(+Pmax, +TGmax, +Twave, +TrnsAve) 97.07 98.88 99.65 99.98				
Life	8012.7 CSTL	3352.3 ETHN	58.16%	58.16%
= f(-Pmax, -dEdt, -TGmax,+Smoke) 95.03 98.53 99.47 99.91 or = f(-Pmax, -TGmax) 95.03 97.68				

variation in the variables could be explained by the regressions. The variations were nevertheless well accounted for by the regressions. Due to the reduced range of variation the effects of measurement and calculation errors on the regressions would be more pronounced. It would in fact be unrealistic to expect the R^2 values to exceed 99%, particularly for those variables which had involved extensive modelling.

The independent variables which were found to be significant in the first analysis were not always significant in the second analysis. The second analysis also found some of the variables to be significant which had not been significant in the complete

analysis. This was, however, to be expected due to the fact that the primary causes of variation were different for the two sets of data, the variations in the complete analysis being mainly due to speed and load changes and in the second analysis being mainly due to fuel property and timing changes. All variables found to be significant in either of the analyses are displayed in table 11 in order of decreasing significance.

The variation in peak pressure was well accounted for by the variations in the duration of combustion and the ignition delay as well as the timing of combustion. It is somewhat surprising that neither the rate of pressure rise nor the rate of combustion correlate with peak pressure. The fact that fuel chemical properties play a role in gas temperatures is illustrated by the fact that only 74,22% of the variation in peak gas temperature was accounted for by measured variables. Despite the fact that the variation in both the rates of pressure rise and combustion was large, the variation in the ignition delay could only account for a small proportion of this variation. Other factors such as fuel preparation rate clearly played a significant role in the rate of combustion.

As was the case with the complete analysis, the injection duration, ignition delay and the exhaust smoke tended to represent the physical and chemical properties of the fuel. This is illustrated by their presence in the regression of exhaust temperature. It is possible that they only appear in the regression due to their good correlation with the proportion of ethanol or other fuel properties. It is unlikely that increased injection duration or reduced smoke would directly result in reduced exhaust gas temperature.

The good correlation between injection duration and smoke also indicates that they both correlate with fuel properties. In the

same manner the correlation between injection duration and ignition delay is most likely the result of the low calorific value and poor ignition quality of ethanol. It is interesting to note that the average rate of heat transfer correlated with thermal efficiency. The increased rate of heat transfer which resulted from advancing the timing with coastal diesel thus explained the reduced thermal efficiency.

It was found that the tests which experienced extended ignition delay also experienced reduced combustion duration. This is partly due to the fact that a greater proportion of the fuel is injected prior to ignition in the event of an extended delay. Much of the injected fuel will be prepared before ignition and burn soon after ignition. The duration of injection remaining after ignition would also be reduced by extended ignition delay. This, however, would only explain a small proportion of the variation in combustion duration. The majority of the variation is certainly the result of differing fuel properties which is indicated by the presence of ignition delay and smoke in the regression of combustion duration. The fact that average gas temperature correlated well with exhaust temperature, maximum gas temperature and maximum pressure was to be expected, since it was calculated from the same data as these variables.

The good correlations between heat transfer results and heat release results served as additional verification of the heat transfer results. Peak cylinder pressure was clearly the variable which played a dominant role in the rates of heat transfer and thus controlled component temperatures to a large extent. There was also considerable evidence that the soot deposits in the combustion chamber surfaces influenced the rate of heat transfer. The extent of the effect was, however, small.

The presence of the rates of pressure rise and heat release in the regressions of wall temperatures and heat transfer rates was expected. This was because increased rate of pressure rise was expected to cause rapid flow of hot gas out of the piston bowl into the squish zone. The resulting turbulence was expected to cause an increase in the heat transfer coefficients early in the expansion stroke. The fact it did occur is illustrated by the correlation between the maximum rates of heat release and heat transfer. This phenomenon, however, only occurred during a small portion of the engine cycle and thus, did not have a significant effect on the average rate of heat transfer. Average rate of heat transfer and component temperatures were found to be controlled by gas pressure, gas temperature and soot deposits.

As was the case with the heat transfer results, most of the variation in the finite element results was explained by the heat release results. Due to the limitations of the heat flux probe and the heat transfer calculations, high values of R^2 had not been expected. The accurate determination of heat transfer rates is a difficult process which is vulnerable to numerous errors. Finite element analysis of engine components is also a complex process. Despite these factors good correlations between finite element results and heat release results were achieved. Maximum combustion rate could not have played a significant role in piston life despite the fact that it appeared in the regressions. This is because maximum combustion rate was not found to affect gas temperatures or heat transfer rates significantly. These variables formed the basis of the life prediction.

The life of the piston was reduced by 58,16% as a result of an increase in peak pressure of 13,11% or a piston temperature rise of 8,68%. This fact was significant in that it indicated that component life is extremely sensitive to peak pressure. This in fact correlated well with the observations of Falk (1988),

Wotherspoon (1988) and Myburgh (1989) who noted that small adjustments to the engine timing could have dramatic effects on engine life. It can be seen in the results of Falk (1988) that an increase of less than 7% in peak pressure resulted in a reduction in piston life of at least 50%.

Although the predicted piston life is considered to be realistic, it should be borne in mind that the harsh environmental factors in the engine were not included in the analysis. Nor were effects such as fuel impingement included in the analysis. The predicted component life is thus expected to slightly exceed those observed in practice.

The minimal correlation between ignition delay and important combustion variables was significant. This served to illustrate the inability of the cetane scale to represent the relevant characteristics of the fuel. It is in fact evident that neither the cetane scale nor the ignition delay provide any useful information about the quality of many of the unconventional fuels.

The statistical analysis was successful in that the significance and validity of all the results was indicated. The statistical analysis also successfully proved beyond doubt that thermal stresses and subsequent engine life are controlled by peak cylinder pressure predominantly. Clearly the analysis made a significant contribution to the success of the entire project.

8. CONCLUSIONS

In order to achieve the objectives of the project it was necessary to develop a large amount of equipment as well as computer software. The engine test bed was designed and built for the project and the dynamometer was modified to suit the application. All the conventional transducers were then installed. Specialized transducers which were also installed required considerable development time. A complex data acquisition system was developed to monitor and record all engine variables. Apart from improvements which were carried out on the existing heat release model, heat transfer and finite element models were also developed. The results of the different analyses were then analyzed statistically.

All three of the mathematical analyses used for the research were validated thoroughly. The validation included sensitivity studies. The statistical analysis provided final confirmation that all the relevant variables had been determined with adequate accuracy thus allowing reliable conclusions to be drawn. The entire experimental system was capable of quantifying accurately not only the combustion behavior of different fuels, but also the thermal and mechanical stresses. It was thus concluded that the experimental apparatus and software which were developed for the project, satisfied all the requirements of the research.

Dynamic mechanical loading was investigated with the aid of data recorded from the strain gauge cylinder head displacement transducer. The results of the transient dynamic finite element analysis also contributed to the analysis. The role of rate of pressure rise in the mechanical stresses in the piston was found to be insignificant. These results proved that although stresses

in some components are affected by rate of pressure rise, the stiffness to mass ratios of most of the components are too high for them to be affected significantly. This is particularly true for those components which were known to fail in practice. Peak cylinder pressure is thus the variable which determines mechanical stress in the engine. High rates of pressure rise are in fact responsible for little more than audible noise and vibration.

The effect of high cycle thermal loading on the life of the piston was investigated. It was found that the life of an aluminium piston was unaffected by high cycle thermal loading. The effect was in fact so small that even a cast iron piston which experiences greater temperature swings would be unaffected. This becomes particularly evident when one considers that the thermal expansion coefficient and fatigue strength of cast iron are far more favourable than those of aluminium. It was thus concluded that the average rate of heat transfer determined thermal stresses.

Step changes in engine load were found to cause rapid changes in piston stresses. However, the magnitude of the stresses did not exceed those achieved during equilibrium conditions. These findings contradicted the results of other researchers who reported high transient stresses after step changes in load. There are a number of possible explanations for this contradiction. Firstly, the piston considered in the project was a relatively small aluminium piston, while most researchers reported on large cast iron pistons. Secondly, the conclusion was only reached because a manual iterative method of accounting for plastic deformation was used. Automatic finite element methods would have erroneously predicted transient peak stresses. Equilibrium heat transfer conditions were thus used to determine low cycle thermal strain amplitudes.

The magnitude of pressure induced mechanical stresses in the piston were found to be far smaller than the thermal stresses. Pressure induced mechanical stresses were in fact so small that they would not have affected the fatigue life of the piston crown. It was thus assumed that thermal stresses are the predominant cause of piston failure and not pressure induced mechanical stresses. Failure is thus the result of low cycle thermal fatigue and not high cycle mechanical stresses. This conclusion was well supported by failures observed in practice. The predicted failure locations and mechanisms also agreed well with those observed in practice. The most significant conclusion is, however, that heat transfer to engine components and thus thermal stresses are determined by peak pressure, maximum gas temperature and soot deposits on the surfaces. The life of the engine is in fact almost entirely determined by maximum cylinder pressure.

Despite this fact, numerous researchers have associated increased rates of pressure rise with engine failure. The most logical explanation for this error is that rates of pressure rise can vary by more than 100% while peak pressures vary by less than 15%. Engine failures were thus, most probably associated with the rate of pressure rise because it exhibited the most dramatic increase when the nature of combustion changed.

Even if the finite element analysis had not been successful, the heat release and heat transfer results would have achieved the objectives of the research project. These results prove that heat transfer rates and thus thermal loading are controlled by maximum cylinder pressure. A significant conclusion of the project is that neither rate of heat release nor rate of pressure rise have a significant effect on the average rate of heat transfer. They therefore do not affect thermal loading or the life of the engine significantly. Peak cylinder pressure not only determines the magnitude of thermal loading, but is also the predominant cause of

high cycle mechanical stresses. Maximum cylinder pressure is thus the variable which determines the life of most of the components in the diesel engine. Different fuel properties result in varying maximum gas temperatures for a given peak pressure. Gas temperature is thus not entirely dependent on peak pressure. Therefore maximum temperature also plays a limited role in the determination of component life.

The relative absence of ignition delay in the regressions illustrated the inability of ignition delay and thus the cetane scale to represent the relevant fuel properties. This was possibly the result of the wide variety of different fuels tested. When it is considered that South Africa will in future, rely heavily on fuels based on crude-oil, coal, natural gas, ethanol and methanol, it is evident that the cetane scale will be of little value. It has now become necessary to account for more than just the variations in ignition delay. Fuel properties such as volatility are now playing a role in the variations in combustion behavior. There will thus be a shift away from the cetane scale, particularly for research applications. More relevant variables such as peak pressure and engine noise and roughness will be analyzed. In order to optimize production processes and generate fuels of acceptable quality, it has become necessary to identify the relationships between the fuel chemical and physical properties and the relevant combustion parameters. The author is already engaged in work of this nature.

Apart from the significant results and conclusions which resulted from the project, it was successful in establishing a comprehensive fuel research facility. The facility has already been used for subsequent research projects. The data acquisition system has been duplicated and installed in a second research laboratory. The heat flux probes and related computer programs are contributing to the development of a new heat transfer model. Even the strain gauge

cylinder head displacement transducer may find applications as a low cost means of monitoring cylinder pressure.

The value of the results can be illustrated by considering the range of fuels that was tested. Firstly, it can be seen that there is little difference between coastal diesel and Sasol diesel. This observation is supported by the fact that no differences have been found between engines operating in the field. Secondly, it is apparent that the 15%, 25% and 93.5% ethanol fuels would compromise the durability of the diesel engine. Durability testing of an engine operating on a 15% ethanol-diesel blend conducted by Hansen, Lyne and Meiring (1984) proved that the fuel had detrimental effects on engine life. However, had the results of the project been available at the time, it would have been possible to reduce peak pressures with ignition improvers or by adjusting the engine timing, before commencing testing.

The fact that the 93.5% ethanol fuel had the lowest rate of pressure rise, lowest exhaust temperature and the highest peak pressure of all the fuels would have been confusing were it not for the conclusions of the project. In the past the wrong emphasis has been placed on the role of these variables in engine failure. On the basis of existing knowledge it would have been difficult to predict engine life, and durability testing would have been catastrophic. The ethanol fuel is, however, not necessarily unsuitable. With the aid of the results of the project it will be possible to conduct further laboratory tests on the fuel. The injection timing could be retarded in order to reduce peak pressure and the amount of ignition improver could be optimized. In this manner combustion behavior superior to that of conventional fuels could be achieved before testing the fuel in the field.

It can be stated with certainty that the objectives of the project have been adequately achieved. The real significance of the

results is that the relevant engine and fuel parameters have been identified in order of their importance. It is now possible to interpret the results of both engine and fuel tests. The implications of both engine modifications and alternative fuels can now be determined with a high level of confidence after a short test. This will obviate much of the expensive durability testing which has been required in the past. With the aid of the results of the project it will be possible to optimize the engine modifications or fuel properties before verification by durability testing.

9. REFERENCES

ADAMS, D.R., REVELLO, P.L., VAN RUITEN, P. and TRAVAILLI, J., 1986. Enhancement of crown and ring groove durability. Proceedings of the Associated Engineering (AE) Technical Symposium. Hepworth and Grandage, Neville Road, Bradford, UK.

AMANN, C.A., 1985. Cylinder-pressure measurement and its use in engine research. SAE paper 852067.

ASSANIS, D.N. and BADILLO, E., 1988. Transient analysis of piston-linear heat transfer in low-heat-rejection diesel engines. SAE paper 880189.

BACON, D.M., BACON, N., MONCRIEFF, I.D. and WALKER, K.L., 1980. The effects of biomass fuels on diesel engine combustion performance. Proceedings of the Fourth International Symposium on Alcohol Fuels Technology, Guaruja, Brazil.

BENSON, R.S. and WHITEHOUSE, N.D., 1983. Internal combustion engines. Pergamon Press, Oxford, UK, 70-93.

BLECH, J.J., 1982. Heat transfer and stress analysis of engine heads and evaluation of methods of preventing head cracks. SAE paper 820504.

BROWNE, K.R., PARTRIDGE, I.M. and GREEVES, G., 1986. Fuel property effects on fuel/air mixing in an experimental diesel engine. SAE paper 860223.

BUCHTA, R., 1981. Piston strength calculations. Karl Schmidt GmbH, Neckarsulm, Federal Republic of Germany.

BUCHTA, R., 1989. Personal communication. Karl Schmidt GmbH, Neckarsulm, Federal Republic of Germany.

CALLAHAN, T.J., YOST, D.M. and RYAN, T.W., 1985. Acquisition and interpretation of diesel engine heat release data. SAE paper 852068.

CHAN, C.M.P., MONCRIEFF, I.D. and PETTITT, R.A., 1982. Diesel engine combustion noise with alternative fuels. SAE paper 820236.

DOWLING, N.E., 1982. A discussion of methods for estimating fatigue life. SAE paper 820691.

EDWARDS, J.B., 1977. Combustion: The formation and emission of trace species. Ann Arbor Science Publishers Inc., Ann Arbor, Michigan, USA, 21-78.

FALETTI, J.J., 1981. Energy release rates of hybrid fuels in a diesel engine. M.Sc. Eng. Thesis, University of Illinois, Urbana, Illinois, USA.

FALETTI, J.J., SORENSON, S.C. and GOERING, C.E., 1982. Energy release rates from hybrid fuels. ASAE paper 82-1548.

FALK, R.S., 1988. Operation of an ADE 236 diesel engine on light diesel fuels. SAE paper 881646.

FRANCIS, B., GRIFFITHS, W.J., GAZZARD, S.T. and AVEZOU, J.C., 1986. Piston developments for medium speed diesel engines. Proceedings of the 1986 Associated Engineering (AE) Technical Symposium. Hepworth and Grandage, Neville Road, Bradford, UK.

GATOWSKI, J.A., BALLES, E.N., CHUN, K.M., NELSON, F.E., EKCHIAN, J.A. and HEYWOOD, J.B., 1984. Heat release analysis of engine pressure data. SAE paper 841359.

HADDAD, S.D. and WATSON, N., 1984. Design and applications in diesel engineering. Ellis Horwood Limited, Chichester, UK, 125-150.

HANSEN, A.C., LYNE, P.W.L. and MEIRING, P., 1984. Evaluation of ethanol-diesel fuel blends for tractors. Unpublished report, Department of Agricultural Engineering, University of Natal, Pietermaritzburg, RSA.

HANSEN, A.C., TAYLOR, A.B., LYNE, P.W.L. and MEIRING, P., 1987. Heat release in the compression-ignition combustion of ethanol. ASAE paper 87-1506.

HARDENBERG, H.O., 1986. Personal communication. Daimler Benz, Stuttgart, Federal Republic of Germany.

HARDENBERG, H.O. and DAUDEL, H., 1981. Ermittlung der luftbewegung im quetschspalt von dieselmotoren aus dem warmeubergang an den zylinderkopf. Daimler Benz, Stuttgart, Federal Republic of Germany.

HARDENBERG, H.O. and EHNERT, E.R., 1981. Ignition quality determination problems with alternative fuels for compression ignition engines. SAE paper 811212.

HARDENBERG, H.O. and HASE, F.W., 1979. An empirical formula for computing the pressure rise delay of a fuel from its cetane number and from the relevant parameters of direct-injection diesel engines. SAE paper 790493.

HOHENBERG, G.F., 1979. Advanced approaches for heat transfer calculations. SAE paper 790825.

KACH, R.A. and ADAMCZYK, A.A., 1985. Effects of thermal loading on pressure measurement in a combustion bomb. Ford Motor Company, Dearborn, Michigan, USA.

KOEBERL, K. and WURZINGER, A., 1986. Personal communication. AV List, Graz, Austria.

KRIEGER, R.B. and BORMAN, G.L., 1966. The computation of apparent heat release for internal combustion engines. ASME paper 66-WA/DBP-4.

LAWTON, B., 1987. Effect of compression and expansion on instantaneous heat transfer in reciprocating internal combustion engines. Proceedings of the Institute of Mechanical Engineers, Volume 201, No A3, 175-186.

LEONE, G., DANIELI, G.A. and CANONACO, M., 1979. Modelling the performance of a prechamber diesel engine. Proceedings of the International Symposium on Automotive Technology and Automation, Graz, Austria.

MEIRING, P., HAESTIER, I.R. and NORTH, R.P., 1972. A photoelectric recording fuel flowmeter. Agr. Eng. in RSA, 6, 50-55.

MIYAMOTO, N., MURAYAMA, T. and GOTOH, S., 1980. Unique measuring method of indicator diagrams using strain history of head bolts. SAE paper 800983.

MOREL, T., KERIBAR, R. and BLUMBERG, P.N., 1988. A new approach to integrating engine performance and component design analysis through simulation. SAE paper 880131.

MOREL, T., WAHIDUZZAMAN, S. and FORT, E.F., 1988. Heat transfer experiments in an insulated diesel. SAE paper 880186.

MOREL, T., WAHIDUZZAMAN, S., TREE, D.R. and DEWITT, D.P., 1987. Effect of speed, load, and location on heat transfer in a diesel engine - measurements and predictions. SAE paper 870154.

MUNRO, R., 1979. Some diesel piston features in design analysis and experiment. SAE paper 790858.

MUNRO, R., GRIFFITHS, W.J., ALLEN, G.L., TRAVAILLI, J. and BOLTON, A.E., 1986. Improved piston designs for heavy duty diesel applications. Proceedings of the 1986 Associated Engineering (AE) Technical Symposium. Hepworth and Grandage, Neville Road, Bradford, England.

MYBURGH, I., 1989. Personal communication. Council for Scientific and Industrial Research. Pretoria, RSA.

RAO, V.K. and BARDON, M.F., 1985. Convective heat transfer in reciprocating engines. Proceedings of the Institute of Mechanical Engineers, Volume 199, No D3, 221-226.

REIPERT, P. and BUCHTA, R., 1981. New design methods for pistons. SAE paper 810933.

REIPERT, P., MOEBUS, H. and SCHELLMANN, K., 1983. Computer design of a steel-nodular cast iron piston capable of withstanding high loads for application in mid-speed diesel engines. Karl Schmidt GmbH, Neckarsulm, Federal Republic of Germany.

ROEHRLE, M.D., 1978. Thermal effects on diesel engine pistons. SAE paper 780781.

RYAN, T.W., 1985. Correlation of physical and chemical ignition delay to cetane number. SAE paper 852103.

SAEED, M.N. and HENEIN, N.A., 1984. Ignition delay correlations for neat ethanol and ethanol-DF2 blends in a D.I. diesel engine. SAE paper 841343.

SANDER, W. and SCHOECKLE, S., 1979. Design and fatigue life evaluation of pistons for high BMEP diesel engines. SAE paper 790857.

SARSTEN, A., 1979. Survey of theoretical and experimental evaluation of thermal loading of diesel engines in Norway. SAE paper 790819.

SAUGERUD, O.T., 1981. Methods for material response calculation and life prediction of thermally loaded engine components. Division of Combustion Engines and Marine Engineering. University of Trondheim, Norway.

SAUGERUD, O.T. and SANDSMARK, N., 1979. Strength analysis of thermally loaded engine components by two-dimensional and three dimensional finite element models. SAE paper 790820.

SCHOCKLE, S., 1981. Piston strength calculations. Karl Schmidt GmbH, Neckarsulm, Federal Republic of Germany.

SEALE, W.J. and TAYLOR, D.H.C., 1971. Spatial variation of heat transfer to pistons and liners of some medium speed diesel engines. Proceedings of the Institute of Mechanical Engineers, Volume 185, No 17/71, 203-218.

SAVAGE, L.D., 1982. Cited by Faletti, Sorenson and Goering (1982). University of Illinois, Urbana, Illinois, USA.

SIHLING, K. and WOSCHNI, G., 1977. Experimental investigation of the instantaneous heat transfer in the cylinder of a high speed diesel engine. University of Munich, Federal Republic of Germany.

SMITH, L.W.L., ANGUS, H.T. and LAMB, A.D., 1971. Cracking in cast iron diesel engine cylinder heads. Proceedings of the Institute of Mechanical Engineers, Volume 185, No.58/71, 807-823.

STREHLOW, R.A., 1982. Cited by Faletti, Sorenson and Goering (1982). University of Illinois, Urbana, Illinois, USA.

TAYLOR, A.B., 1984. Knock reduction measures for application on dual-injected methanol-diesel engines. Unpublished B.Eng. (Mech) Thesis, Dept. of Mech. Eng., University of Stellenbosch, Stellenbosch, RSA.

TAYLOR, A.B., 1987. Combustion quality of selected compression-ignition fuels. Unpublished M.Sc. Eng Thesis, Dept. of Agric. Eng., University of Natal, Pietermaritzburg, RSA.

TAYLOR, C.F., 1979. The internal combustion engine in theory and practice. The MIT Press, Cambridge, Massachusetts, USA, 187-204.

TIMONEY, D.J., 1987a. Problems with heat release analysis in D.I. diesels. SAE paper 870270.

TIMONEY, D.J., 1987b. Effects of important variables on measured heat release rates in a D.I. diesel. SAE paper 870271.

WACKER, E. and COELINGH, W., 1984. Aluminum pistons for diesel engines, Karl Schmidt GmbH, Federal Republic of Germany.

WACKER, E. and SANDER, W., 1982. Piston design for high combustion pressures and reduced heat rejection to coolant. SAE paper 820505.

WHITEHOUSE, N.D. and WAY, R., 1971. A simple method for the calculation of heat release rates in diesel engines based on the fuel injection rate. SAE paper 710134.

WOSCHNI, G., 1967. A universally applicable equation for the instantaneous heat transfer coefficient in the internal combustion engine. SAE paper 670931.

WOSCHNI, G., 1979. Prediction of thermal loading of supercharged diesel engines. SAE paper 790821.

WOSCHNI, G. and FIEGER, J., 1979. Determination of local heat transfer coefficients at the piston of a high speed diesel engine by evaluation of measured temperature distribution. SAE paper 790834.

WOTHERSPOON, D., 1988. Personal communication. Atlantis Diesel Engines. Atlantis, RSA.

WU, H. and CHIU, C., 1986. A study of temperature distribution in a diesel piston - comparison of analytical and experimental results. SAE paper 861276.